VIBRATION BASED FAULT DETECTION FOR SOLENOID VALVES

CHRISTIAN ELLWEIN

A thesis submitted in partial fulfilment
of the requirements of the
University of Northumbria at Newcastle
for the degree of Doctor of Philosophy

In collaboration with:
University of Applied Sciences at Heilbronn, Germany
Fraunhofer-Institute for Nondestructive Testing, Dresden, Germany
Bürkert Fluid Control Systems, Ingelfingen, Germany

FEBRUARY 2002

Abstract

Solenoid valves play a vital role in many machines and systems. If one of these devices breaks down the whole system can be affected. Because of this importance of valves, it is desirable to observe these parts to detect faults, both when they are occurring and before they can cause serious damage. Among several possible methods of observation (monitoring actuation time, electrical current, fluidic parameters and others) the observation of mechanical vibrations is a well known method of observing mechanical systems which is commonly used for observation of rotating machinery, but which includes several challenges for diagnosis of solenoid valves.

This thesis investigates the possibilities and advantages of vibration analysis of fault detection for solenoid valves. New algorithms are developed to automatically segment the overall non-stationary raw data to smaller sections with a higher degree of stationarity. These new segments are interpretable in a mechanical sense and they separate different sources of vibration. Furthermore a new method to detect regions of interest in a spectrum for classification without "a priori knowledge" about the process has been developed.

The experiments presented in this thesis give the evidence that these new methods of pre-processing and feature extraction enable reliable classification results for transient signals as they occur in the vibration of a switching valve.

Contents

List of Tables

List of Figures

Glossary

ACF	autocorrelation function
ADC	analog-digital converter
AE	acoustic emission
AIC	Akaike's information criterion
AR	autoregressive
EMI	electromagnetic interference
FFT	fast Fourier transform
FIR	finite impulse response
FT	Fourier transform
MEMS	microelectromechanical system
MLP	multi-layer-perceptron
NN	neural network
PCA	principal component analysis
PDF	probability density function
QA	quality assurance
RMS	root mean square
SAM	spectral analysis matrix
SBS	Source Based Segmentation
SNR	signal-to-noise ratio
SOV	solenoid operated valve
STFT	short-time Fourier transform
SVD	singular value decomposition
TFD	time-frequency distribution
TSD	time-scale distribution
WT	wavelet-transform

List of Main Notation

ψ	number of flux linkages	Tm^2
ϕ	magnetic flux	Wb
$\delta(\cdot)$	dirac impulse	
ε_l	overlapping threshold for the Spectral Analysis Matrix (SAM)	
λ_c	number of classes in a classification	
λ_f	dimension of the feature space	
λ_m	dimension of the measurement space	
κ_m	magnetic coefficient of efficiency	
τ_i	duration of the impact (time when a force is acting between the impact partners)	s
τ_S	contact time of body and movable mass in a model of the switching process	s
ϖ_{res}	resonance angular frequency	rad
Δx	stroke of the valve	m
A	time point of the impact	m
c	force constant of the spring	s
c_{MODEL}	stiffness	N/m
c_{SAM}	number of columns in the Spectral Analysis Matrix (SAM)	
E_{el}	electrical energy	J
E_{kin}	kinetic energy	J
E_{mag}	magnetic energy	J
E_{th}	thermal energy	J
F(t)	force	N
F_{spring}	force of a spring	N
f_{res}	resonance frequency	Hz
i(t)	electrical current	A
L	inductance of the coil	H

m	mass	kg
m_1	mass of the movable part in the valve	kg
m_2	mass of the valve body	kg
n_w	number of effective turns in the winding	
o	order of a model	
$\mathbf{O}$	measurement matrix	
q	vector with the discriminative power of certain frequencies in the Spectral Analysis Matrix (SAM)	
R	ohmic resistance of the coil	Ω
r_{SAM}	number of rows in the Spectral Analysis Matrix (SAM)	
$\mathbf{S}$	Spectral Analysis Matrix (SAM)	
s_{ij}	a distinct element of the Spectral Analysis Matrix (SAM)	
s_{max}	maximum value in the Spectral Analysis Matrix (SAM)	
s_{min}	minimum value in the Spectral Analysis Matrix (SAM)	
t	time	s
t_1	threshold for the Spectral Analysis Matrix (SAM)	
t_2	threshold for the Spectral Analysis Matrix (SAM)	
T_{res}	inverse of resonance frequency f_{res}	s
t_{switch}	switching time (time between switching on or off the voltage and ceasing of all bouncing in the valve	s
$u(t)$	electrical voltage	V
$v(t)$	velocity	ms^{-1}
v_0	initial velocity	ms^{-1}
v'_1	velocity of the movable part in the valve after the impact	ms^{-1}
v'_2	velocity of the valve body after the impact	ms^{-1}
v_1	velocity of the movable part in the valve before the impact	ms^{-1}
v_2	velocity of the valve body before the impact	ms^{-1}
$x(t)$	displacement of the movable part of a valve	m
x_{max}	maximal displacement of the movable part of a valve	m
x_{min}	minimal displacement of the movable part of a valve	m

Acknowledgements

I would like to thank all the people who were involved in this project for their support and their help to complete this research.

First of all, I am very grateful to my supervisor Dr. Sean Danaher for all his excellent advice and for sharing all his knowledge and experience in digital signal processing with me. I really learned a lot during this project from him. I also appreciate very much his patience in the way he explained some algorithms of digital signal processing that were new to me.

I'm also greatly indebted to Prof. Dr. Uwe Jäger for his uncomplicated support and advice. His feedback to my lectures and his recommendations for problems in the field of signal processing were a valuable help for me.

Special thanks are dedicated to my wife Doris. By her patience and love she was a great help during the project.

Last, but not least I would like to give thanks to Dr. Dieter Hentschel, Dr. Lothar Haupt, Bernd Frankenstein, Klaus-Jochen Fröhlich (all Fraunhofer-Institute for Nondestructive Testing, Dresden, Germany), Mathias Mannhardt and Petre Sora (both University of Applied Science, Heilbronn, Germany) and Dr. Egon Hüfner and Dr. Gunter Kabisch (Bürkert Fluid Control Systems, Ingelfingen, Germany) with whom I have had several collaborations during my PhD-research in different projects.

Declaration of originality

The contents of this thesis are original except where reference is made to the work of other researchers. This works has not been submitted in whole or part for a degree at any other university.

University of Northumbria

at Newcastle upon Tyne

Christian Ellwein

1 Introduction

1.1 Motivations and Research Objectives

Condition based maintenance and tool monitoring are techniques which have been used in many systems and machines. It became necessary with a rising demand on the availability of industrial systems to detect faults before they can cause serious damage. Vibration analysis is a common way to supervise the state of mechanical systems and devices. Nevertheless, there is a need for observation systems for rather small and cheap valves. These devices have not been monitored until now because the expense of these parts is rather low. Today solenoid valves are used in the field of biotechnology, in fuel cells, in medical applications like dialysis and so on. This usage increases the need for higher reliability and supervision. Thus it was the objective of this research work to develop a vibration based condition monitoring system for small and cheap solenoid valves.

1.2 Overview of vibration analysis

Vibration analysis is used for quality control and condition based maintenance in a large variety of tasks and situations. The vibration of a machine, device or product will often give very valuable information about the state or the quality of the monitored system. A well-established approach for many problems is to use human expert knowledge for the observed sound. If a worker has gained enough experience he/she can often hear if a machine or a product is non-faulty or getting out of order. This method is still popular but there are several drawbacks: first, the work is tedious and misinterpretation will happen more probably with the working time. Another problem is that the knowledge

about the classification is bound to the worker. If he/she leaves the company the ability to monitor the process is lost. Consequently it has been an important aim since the fifties of the last century to develop artificial systems with the ability to monitor the sound of a system, or process, and to perform a classification between different states or classes [Pohl56]. A large body of work has been done in the field of rotating machines [Alguindigue93; McCormick96]. These systems are very suitable for vibration analysis because the resulting signals are periodic. Another reason for monitoring rotating machinery, such as generators and large engines, is the high cost of this equipment. They are rather expensive, thus there is a great need for maintenance and observation. Another application of vibration analysis is monitoring artificial heart valves. If an artificial heart valve is implanted in a human body it is necessary to observe the valve at periodic intervals to recognise faults and deterioration before serious damage happens. X-ray imaging is a non-invasive method but has the drawback of radiation exposure. Thus the sound of the heart valve is a commonly used signal for this monitoring task [Candy95; Plemons95]. Circuit Breakers in power transmission systems are also often monitored non-invasively. Vibration analysis is a common means for this observation [Park90; Aurud91; Runde96]. Another field for vibration analysis and failure detection is the observation of combustion engines [Cann92; Azzoni95]. Here also reciprocating events are measured and one important challenge of this task is to separate the different sources of vibration in an engine. Geological vibrations and seismic waves are also monitored with accelerometers and analysed to predict earthquakes and tidal waves like tsunamis [Basseville93; Conte96; Gupta00].

1.3 Condition monitoring for valves

Current plants and machines include many valves. These devices are often rather cheap and small but play a vital role in the overall system. If one of these devices breaks down the whole system can be affected. Because of this importance of valves it is desirable to observe these parts to detect faults both when they are occurring and before they can cause serious damage. In [Casada96] it was shown that no appreciable differences are apparent in relative failure rates of check valves used in nuclear power stations according to component age. Hence, straightforward approaches like measuring the life-time of a valve are not guaranteed to give reliable results. Due to this several more sophisticated methods for monitoring valves have been developed within the last few decades.

One approach is to analyse the coil current and voltage and to find features in the current shape which give the ability to classify between faulty and non-faulty valves [Kryter90; Blakeman97]. These systems make use of the typical shape of the current which has two changes in the sign of its derivative (see Figure 6-3, page 88). The vibration of valves is also used to observe the state of the devices. These approaches combine the signals of two [Uhrig93] or up to four [Gallier97] accelerometers at different positions of the valve body and use the different signals to detect failures in the device. The observed valves in these research works were used in power plants and they were much larger than valves used for the research of this PhD-project. Another parameter of the devices which can be used for the supervision task is the actuation time of the device. Different operating times and root-mean-square values (RMS) of the vibrations signal are used to monitor artificial induced faults in servo valves [Yamashina90]. Active systems, which use an ultrasonic transmitter-receiver

transducer, are also used to determine the position, angle, velocity or flutter of the movable part in a check-valve and to detect failures by this means [Au-Yang91]. Sometimes flow induced vibrations are also used for the observation task. This is especially of interest if only leakage needs to be detected [Dimmick86; Thompson 97].

There are two important limitations of the known techniques: first, some of them need many expensive sensors or/and substantial computational power. This is an important drawback if rather cheap valves in the fields of automation and control should be monitored. The second limitation is that some of the current approaches seem not to be able to monitor common faults such as some shown in Table 2-1 (page 15). For example, it seems to be impossible to monitor fault 3 (indentation in the seal) by observing the shape of the electrical current. But all the faults in Table 2-1 have been stated to be very important and serious by the quality assurance (QA) and service departments of Bürkert company [Bürkert00]. Thus, an approach based on vibration analysis with an accelerometer is used in this research work, because all important parts of the valve which should be observed are affected by the movement in the valve and thus may also influence the vibration pattern.

Important properties for a monitoring system are: the method of testing (intrusive or nonintrusive), the need for hardware equipment (sensors etc.) and computational power. All these factors have to be suitable for the particular supervision task. If the demand of reliability is very high and the effect of valve breakdown without earlier warning is very serious then one will accept higher expense of the monitoring system. This situation can occur for example to some valves in a nuclear power station. In a power station it is necessary to implement a nonintrusive test because it is not possible to shut down the plant very often. Nonintrusive testing is necessary also for artificial heart valves because

they have to be observed in vivo in a human body. A different situation is given for industrial plants and systems with lower safety requirements than e.g. a nuclear power station. It is often desirable to implement some diagnostic operation in the system, but the needs are much lower than in systems with a high dependability. A further application of monitoring is the final test after production. There is no need for a nonintrusive test because the devices are not yet assembled in a final circuit or system.

The project is a collaboration between the University of Northumbria at Newcastle, the University of Applied Sciences at Heilbronn, Germany, the Fraunhofer Institute for Non-Destructive Testing at Dresden, Germany and Bürkert Fluid Control Inc. at Ingelfingen, Germany. The aim of the project is to develop algorithms for monitoring the vibration signals of small solenoid valves for failure detection. One of the requirements of such algorithms is self-adaptation both to different valves and different environments. This research aims to integrate an accelerometer and some pre-processing electronics together with the valves to enable an online observation of the devices over their whole lifetime. It is possible to sense different process quantities, such as flow and pressure, for valves to observe the devices but the costs of the necessary equipment begin to outweigh the savings made by a condition based maintenance. Thus the aim of the project is to monitor the device with only one low-cost accelerometer and to gather all necessary information from this sensor.

An accelerometer was used, because the failures mentioned in Table 2-1 (page 15), which are the most important ones for valves, are of mechanical nature. The vibration of a device or a system was seen in many recent research projects to be a good indicator of mechanical failures [Cann92; Park90]. The devices which are to be monitored in this work are rather small compared with devices monitored in previous work. Also there is

only a single closing mechanism inside the devices which is different from the devices investigated in previous work. Thus a single accelerometer was seen to be a suitable sensor for data gathering.

1.4 Overview of the Thesis

1.4.1 Organisation of the Thesis

This thesis is divided into four parts:

I. Background (Chapter 2)

II. Theory (Chapter 3 - 4)

III. Experiments & Results (Chapter 5 - 9)

IV. Conclusions & Recommendations (Chapter 10)

In the first part of the thesis brief introductions to vibration analysis and solenoid valves are given. Both topics are not explained in full detail but mainly in their relevance for the research project. In the second part a model of the switching process is developed which covers the energy conversions during the switching process and an asymptotic estimation of the resulting spectra. Also some theoretical background about classification is presented. Results and the classification algorithm developed in this project and the contributions to knowledge of this research are presented in detail in the third part of the thesis. Emphasis is given to new techniques for pre-processing of the measured raw data developed during this PhD project. Finally, in the last part conclusions and recommendations for further work are given.

1.4.2 Involved persons and their projects

The following summary shows all other persons with their projects who where involved in the PhD project (ordered by date). These projects were proposed and supervised by the author or they were a collaboration with an external partner, respectively, as means of developing the ideas and results presented in this thesis.

Table 1-1 Involved persons and their projects

Name	Date	Type of Project	Contents	Reference
M. Mannhardt	**2000**	**MSc project**	**Model Based Feature Extraction**	**[Mannhardt00]**
Dr. D. Hentschel **Dr. L. Haupt** **K.-J. Fröhlich** **B. Frankenstein**	**1999 – 2002**	**Research project granted by the Federal Ministry of Education and Research (BMBF) (Förderkennzeichen: 16 SV 1107/8)**	**Condition Monitoring for Valves by Means of the Short Time Fourier Transformation**	**[Ellwein01c, Ellwein01d]**
P. Sora	**2001-2002**	**MSc project**	**Condition Monitoring for Solenoid Valves Using Wavelet-Transform**	

2 Background

2.1 General

This chapter provides some background information about solenoid valves and vibration analysis. The chapter is organised as follows: firstly, different types of solenoid valves are described briefly. Next the safety demands of valves in different applications are presented. The second topic, vibration analysis, is introduced first by describing an accelerometer used to measure vibration patterns and after this more information about the random character of several vibration signals and an organisation of vibration signals into distinct families are given. The chapter ends with a summary of important failures which are to be detected by the monitoring system developed in this research project.

2.2 Solenoid Valves

Solenoid valves are used in the fields of automation and control to perform a on-off-operation for fluid and gas flow. In contrast to this, a process valve operates continuously. On-off-valves are important and are very commonly used because of their low price, high operation speed and the low need of controlling intelligence.

2.2.1 Different valve types

Many different types of solenoid valves are used in industry. A very important kind of solenoid valves is the plunger-type system. These valves have a cylindrical plunger which is moved by the solenoid. The geometry of the movable part is an important advantage for machining the device and thus the plunger-type devices are the most

important valves (the quantity of sold plunger-type valves is higher than the quantities of all other principles). Other basic principles for solenoid valves are the rocker-principle and the pivot-principle. These different techniques are especially used when a separation between fluid and solenoid-circuitry is necessary. In Figure 2-1 a technical drawing of the plunger-type valve 6011 of Bürkert Company is shown. A detailed Figure of the plunger and the spring is also shown in Figure 6-4 (page 88). This type is typical for small size valves. Many devices of different manufactories and companies have a similar structure and thus this valve is representative of a large class of mechanical devices.

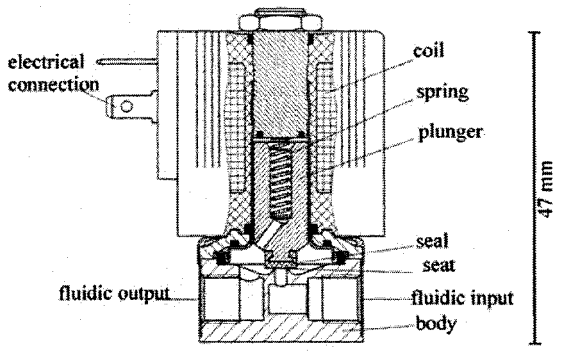

Figure 2-1 Technical drawing of valve type 6011

Figure 2-2 Valve type 6011

In Figure 2-2 the valve type 6011 is shown. The material of the body is brass and the housing of the coil and the cable plug is polyamide. The height of the device is 47mm and the weight is 125g. The nominal voltage is 24V DC and the power is 4W. The opening time is typically between 8 and 12 ms and the closing time between 14 and 16 ms. The dimensions of this valve are relatively small compared with many other valves used in power stations for example. Due to this, valves of these dimensions are often called *miniature solenoid valves*. This valve is used to control the flow of fluids and gases such as water, air, hydraulic fluid or technical vacuum. A large family of similar valves (scaled in the housing dimensions and the nominal diameter) is available from Bürkert and also from other suppliers, and they are implemented in many applications and systems. They often play a very important role in the overall system and thus there is a need for automatic supervision of these devices. This research work is validated with this type of valve but it is anticipated that the results can be generalised to a large number of different devices.

2.2.2 Typical applications and safety demands

Valves like the 6011 are used for example in electro-peneumatical machines such as packaging machines or assembling lines. These applications have normally no

extremely high safety demands. The risk for the environment or humans if one of these devices breaks down is not very severe. Nevertheless the economic costs caused by an unexpected break down of a single valve can be serious. These are the reasons, why condition based maintenance and failure detection for these valves was developed.

2.3 Vibration analysis

2.3.1 Introduction

Mechanical movement of systems, machines or devices usually causes vibration. This vibration signal differs considerably for each application and system. There are also often significant differences in the vibration pattern for different conditions of the same device or machine. If the air-connected surface of a system is vibrating than the vibration becomes audible and the condition of the system can be assessed by a human expert. The vibration can also be monitored by a sensor like an accelerometer, microphone or laser-vibrometer.

2.3.2 The accelerometer

To measure the vibration of mechanical systems an accelerometer is a frequently used sensor. An accelerometer is a damped mass-spring-system where the acceleration of the internal movable mass is causing an electrical measurable physical effect like the change of a capacity or the transfer of an electrical charge. The accelerometer is affected mainly by structure-borne sound and not by airborne sound. Thus a firm connection between the sensor and the measured object is necessary and the measurement is barely disturbed by other sources without a direct connection. Accelerometers are available for a wide range of frequency bandwidths, measurements ranges and sensitivities. Due to this it is possible to select a suitable transducer for

different types and sizes of valves. The selection of the sensor and the criteria which led to the decision to use an accelerometer in this research work are presented in detail in chapter 5. More background information about accelerometers can be found in the literature, for example [Lyon87, Wowk91, Wilson99 or Shieh01].

2.3.3 Random character of vibration signals

The vibration of a complex system like a valve (containing a spring, a moving mass, an elastomer seal, an armature guide tube, a coil and some screwed connections) is not a fully deterministic signal. The vibrations of a train of switching events of the same device do not coincide exactly. Because of mechanical tolerances in the measured valve and perturbations in the measurement chain, there is a stochastic part in each vibration pattern. Due to this it is necessary to work with a set of valves for each signal processing task and to implement algorithms which can deal with this random character of the patterns. It is also extremely difficult to develop an exact and reliable mathematical or physical model (white box model) of the vibrations.

2.4 Applied vibration analysis

2.4.1 Different sources

It is a common situation that vibration signals of a system, device or machine are recorded and classified to set of distinct classes which represent different conditions of the monitored object. Depending on the character of the vibration signals some steps of pre-processing are necessary which are determined by the kind of vibration and the type and influence of distortion. There are three main families of vibration signals which cover most of the signals interesting for condition monitoring: first, vibration signals can be gathered from rotating machinery like gears, electric motors, shafts and similar

systems. These vibration signals have periodicities and depend on the revolutions per minute of the system. This family is not a topic of this thesis. The second class of vibration signals is a kind of noise. These vibrations are caused by friction or they can be flow induced, for example. The difference to the first mentioned class is that these vibrations have no inherent periodicity because the process causing the vibrations is not periodic. Finally, the third important family of vibrations signals are transient signals. They occur in the cylinders of a combustion engine, they are generated by an impact hammer which is often used to excite an object during tests and they also can be recorded from switching devices like valves, relays or pneumatic cylinders where a linear motion is stopped rapidly. A typical vibration signal of this transient class is shown in Figure 2-3. It was recorded from a valve type 6011 from Bürkert company. The transient character of the process can be found in the observed pattern: the vibration signal is vanishing at the beginning and the end and it is highly non-stationary. Real world signals can often be a combination of more than one vibration family.

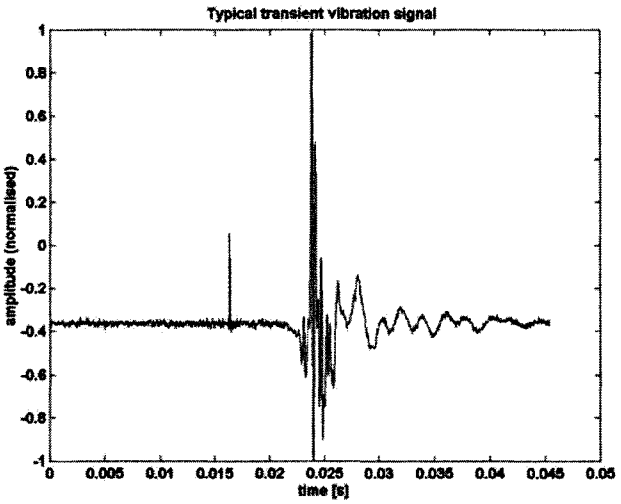

Figure 2-3 Typical transient vibration signal

Very often measurements are influenced by distortion and the signal of interest is not the only measured data. Vibration signals are often influenced by other external sources of vibration. In the case of solenoid valves common sources of distortion are for example pumps, other valves, motors and similar equipment often used in plants or systems. This effect was taken into account in this research project by adding "real-world" distortion to the vibration signals (see section 5.4.3). Another source of distortion in this project was the influence of electromagnetic interference (EMI) on the accelerometer when the solenoid was switched on or off. More details regarding this problem were presented later on in section 6.1.2.

2.4.2 Applications

Vibration analysis is used in many distinct areas due to the fact that many technical processes cause mechanical vibrations during their operation. These vibration pattern often alter with changes in the condition of the process or system. Hence, observing and classifying vibration patterns is a commonly performed task. Important applications are:

- Observation of movement caused vibration (for example reciprocating systems, rotating machinery, grinding processes, geological processes like earthquakes and many other applications) [McCormick96, Kocur00].
- Active monitoring systems with a vibration source and a transducer. These systems generate a determined vibration in the device under test and measure the response of the monitored system. Changes in the condition of the system which alter the transfer function of the transmission path for the vibration signals can be detected. A typical application is the final test of roof tiles which were striked with a wooden stick and the subsequent sound pattern is analysed to detect faulty products

[Jonuscheit98], or condition monitoring for valves with an active ultrasonic system [Au-Yang91].

- Supervision of the environment of a device or machine to detect external sources or situations which may affect the monitored object. This is done, for example, with data loggers to record shocks during transport [Hascher96].

2.5 Important failures of solenoid valves

There are several different failures which can occur in a miniature solenoid valves as described in section 2.2. A summary of possible failures is presented by Kryter in [Kryter90]. After discussion with the service engineers and the quality assurance (QA) department, both at Bürkert, the following failure classes were chosen for the classification:

Table 2-1: Failure classes detected in this research project

	Failure class	Effect	(Artificial) creation
1	**Hardening of the seal**	**Valve will become leaky**	**Age the seal and the movable part in the oven (150° - 200°C), some hours to some days**
2	**Swelling seal**	**The flow through the open valve is reduced**	- **Put seal and closing member in boiling water** - **Acetone, coffee, oil and shampoo can also cause this failure**
3	**Indentation in the seal**	**Valve will become leaky**	**Switch the valve without fluidic medium several million times to intend the seat in the seal**
4	**Waste in the valve**	**Valve will become leaky**	**Insert small pieces (chips) of metal or plastic in the valve which will be found within the valve.**
5	**Calcification of the valve**	**The internal friction is increased and the valve will stuck to open or close finally**	**Put the valve into hard water and vaporise the water by boiling.**

All the artificially induced faulty were beginning faults. This means that the deteriorated valves were still working and the classifier was trained to detect occurring faults before they can cause serious damage. Miniature solenoid valves are usually not repaired but replaced in case of a failure because this is cheaper in most cases. Thus failure *detection* is much more important than failure *identification.* For a replacement of a faulty valve it is enough to know that a failure has occurred. Details about the type of failure are only important if the valve should be repaired. If the different failures are not distinguished and only one decision boundary is trained between unfaulty and all the faulty classes the classifier will become smaller and the computational burden is reduced. This is the reason why all the different failures are mapped to one common cluster in this classification. In Figure 2-4 an idealised graphical representation of this classifier is given. Of course, the classifier developed in this project is not a naïve one such as the linear classifier in Figure 2-4 and the classes will not separate as perfectly as shown in Figure 2-4. This Figure only highlights the combination of all failures to one single cluster in opposition to the unfaulty patterns.

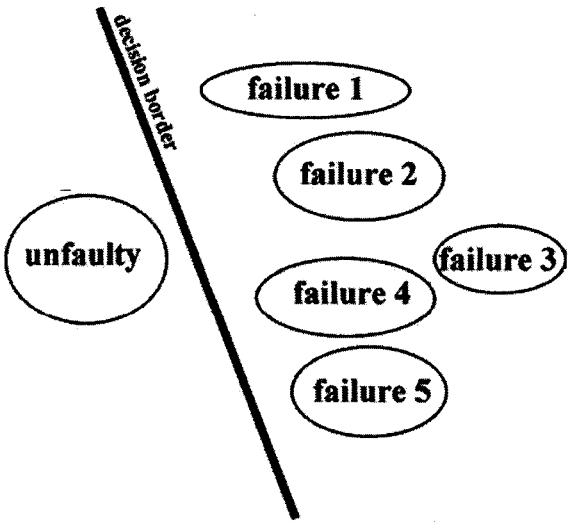

Figure 2-4: Idealised decision border

2.6 Conclusions

This chapter gave brief background information about the project. Solenoid valves were described and differences were shown between the family of small valves investigated in this project and devices observed in earlier work. After that an introduction to vibration analysis was presented and typical signals and applications were mentioned. Finally, important details about the supervised failures and the mapping of classes were given. In the next two chapters deeper theoretical information is presented: first a model of the switching operation is developed and after this an introduction to classification is given. The different steps to classify the failures mentioned in Table 2-1 were presented afterwards in chapters 5 to 9.

3 Model of the switching processes

3.1 Introduction

Modelling of physical or technical processes means finding an abstract description of the observed process. A model is a representation of a "real-world" signal or system which should cover the properties of interest with a suitable accuracy. Modelling is extremely useful for gathering deeper information about the process or to improve algorithms in fields such as classification, system identification, control or data transmission, to mention only some very important ones [Lindner99].

Several kinds of models have been developed and are used in a large variety of applications. Models can be arranged into three main classes [Isermann92]:

- *White-box models* are mathematical or physical models which are based for example on conservation laws (energy, impulse and so on) or chemical or physical equations of state. They can be generated without measurements, only by identifying physical laws which govern the process of interest.
- *Grey-box models* are differential equations where the elementary and internal structure of the process is lost and only the input-output-relation is represented for model-order $o > 1$. This can be seen also by the fact that it is not possible to give a unique block diagram for a differential equation of order $o > 1$.
- *Black-box models*, finally, are non-parametric models which were derived only from measurements with neither knowledge of the internal structure of the observed

process nor knowledge of physical or chemical laws which govern the process. A well-known example for this kind of model are Neural Networks.

The above cited organisation of different models is not consistent in literature: in [Hellendoorn97], for example, differential equations are denoted as white-box models.

To gather deeper information about the switching process of solenoid valves a model based of the energy conversions during the switching process was developed which is presented in the next sections. Additionally an asymptotic estimation of the excited frequencies due to the impact of the valve is presented in section 3.3. These theoretical results are validated by experimental measurements at the end of this chapter and also later on in section 5.2.2. Finally, a Simulink model is presented in section 3.4.

3.2 Energy conversions during valve switching

The vibration caused by switching a solenoid valve is caused by the movement and the impact of the movable part inside the valve. Several energy conversions are performed during the switching process. These steps are different for energising and de-energising of the solenoid and they are performed at different locations in the valve. A model of the different conversions of energy is shown in Figure 3-1 as a block diagram:

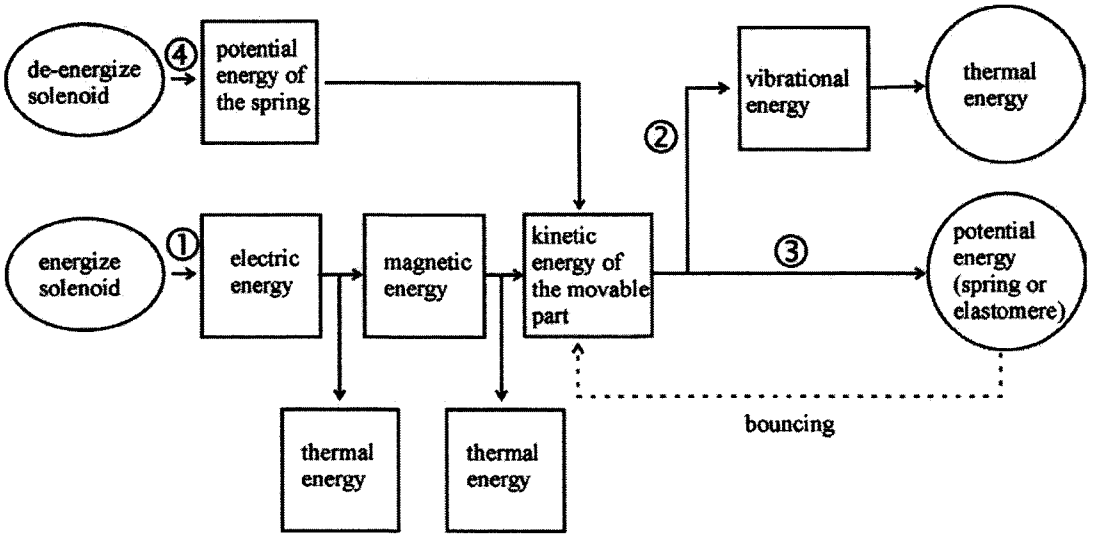

Figure 3-1 Energy conversion during switching

Both switching processes (energising and de-energising) start at the left side of Figure 3-1. The rectangular boxes represent different kinds of energy and the arrows indicate the paths of energy conversion. If two arrows go out of a single box then the energy represented by this box is converted into two different kinds of energy. The circles at the right side of Figure 3-1 indicate the final states of the conversion process which are accomplished during valve switching. In the following the different conversions are explained in more detail.

Electric energy is the initial energy in the valve-energising-process (① in Figure 3-1). It is converted by the solenoid into magnetic energy and thermal energy. Because of the ohmic resistance of the coil some electrical energy is converted into thermal energy and lost for the further process of switching the valve. Magnetic energy is acting on the movable part in the valve against the force of the spring. If the state of the solenoid is changed from unpowered to powered then magnetic energy is converted into kinetic energy of the movable part. This conversion is lossy because of eddy currents and

leakage flux and thermal energy is increased again. Friction is converting kinetic energy via vibrational energy into thermal energy during movement in the valve (path ② in Figure 3-1). Potential energy is increased by strain of the spring and deformation of the elastomer of the seal. This is different for switching-on and –off (③ in Figure 3-1). The movable part in the valve may bounce one or more times. This means that potential energy of the spring or the elastomer is re-converted to kinetic energy and the movable part lifts again. This situation is indicated in Figure 3-1 by the dashed line. Vibrational energy is also caused by the impact of the valve. This energy is converted to thermal energy by internal friction in the device and the surrounding air. This conversion is also shown in path ② of Figure 3-1. When the solenoid is de-energised and the valve switches off the potential energy of the compressed spring is converted into kinetic energy (path ④). This kinetic energy is converted mainly into vibrational energy and thermal energy because the potential energy of the elastomer will be almost zero after bouncing when the valve has closed finally. Thus the de-energisation is mainly from ④ over path ② to thermal energy.

Until this point the switching processes were described in a qualitative way. The following sections give more quantitative information about the different states during switching.

The electric energy applied to the solenoid during the switching time t_{switch} is defined by Equation (3-1).

$$E_{el} = \int_0^{t_{switch}} u(t)i(t)dt \tag{3-1}$$

with

$u(t)$ is the voltage and

$i(t)$ is the electrical current through the coil

t_{switch} is the time between switching on or off the electrical voltage and all bouncing in the valve has ceased

A certain part of this energy is converted to magnetic energy E_{mag} the other part is converted into thermal energy E_{th} which is lost during the switching process [Dobrinski93, Kallenbach00].

$$E_{el} = E_{mag} + E_{th}$$
$$E_{el} = u_1(t) + u_2(t) + \int_0^{t_{switch}} Ri^2(t)dt \tag{3-2}$$
$$E_{el} = \int_0^{t_{switch}} i(t)\left(\frac{\psi(x,i)}{i}\frac{di}{dt} + \frac{\psi(x,i)}{x}\frac{dx}{dt}\right)dt + \int_0^{t_{switch}} Ri^2(t)dt$$

with

u_1 is the reverse voltage due to deviation of the electrical current and

u_2 is the reverse voltage due to deviation of the position of the plunger

R is the coil's ohmic resistance

Ψ is the number of flux linkages [Lowther85] with

$$\Psi = n\phi \tag{3-3}$$

where

n is the number of effective number of turns in the winding

ϕ is the magnetic flux

The kinetic energy which is converted from the magnetic energy and which is stored in the movable part is defined by:

$$E_{kin} = \kappa_m \cdot E_{mag} \tag{3-4}$$

κ_m is the magnetic coefficient of efficiency which depends on the stroke of the valve, the construction of the magnetic circuitry, parasitic air gaps, the materials used in the magnetic circuitry and the electrical excitation of the solenoid. The typical range is rather wide: $0{,}1 < \kappa_m < 0{,}75$ [Kallenbach00].

For these conversion steps the following equation holds for small changes:

$$dE_{el} = dE_{th} + dE_{mag} + dE_{kin} \tag{3-5}$$

The kinetic energy is limited because the velocity of the movable part is decreased to zero after switching. Thus also measured vibration caused by vibrational energy are bound in amplitude and temporal duration. A typical vibration signal of a switching valve is shown in Figure 2-3 (page 13).

During the impact kinetic energy of the movable is converted to vibrational, thermal and potential energy. Equation (3-6) holds for this process [Biegner99]:

$$\frac{1}{2}m_1 v_1^2 + \frac{1}{2}m_2 v_2^2 = \frac{1}{2}m_1 v_1^{\bullet 2} + \frac{1}{2}m_2 v_2^{\bullet 2} + \Delta E_{th} + \Delta E_{pot} \tag{3-6}$$

v_1 and v_2 are the velocities of the movable part and the valve body before the impact and $v_1^{\bullet}$ and $v_2^{\bullet}$ are the velocities after the impact. m_1 and m_2 are the masses of the movable part and the valve body, respectively. ΔE_{th} is increase of thermal energy after the impact and ΔE_{pot} is the change in potential energy of the spring. The work done on the spring is the integral over the force F_{spring} given in Equation (3-7).

$$W_{spring} = \int_{x_{min}}^{x_{max}} F_{spring} dx = -\int_{x_{min}}^{x_{max}} c\,x\,dx = -\left[\frac{1}{2}c\,x^2\right]_{x_{min}}^{x_{max}} = \frac{1}{2}c\,x_{min}^2 - \frac{1}{2}c\,x_{max}^2 \tag{3-7}$$

Thus the change in potential energy of the spring is [Riley96]:

$$\Delta E_{pot} = \frac{c\cdot\left(x_1^2 - x_2^2\right)}{2} = \frac{c\Delta x^2}{2} \tag{3-8}$$

where

c is the force constant of the spring and

Δx is the stroke of valve

v_2 (the velocity of the valve body before the impact) can be assumed to be zero and also $v_1^{\bullet}$ and $v_2^{\bullet}$ are zero after decaying of the vibration. Thus Equation (3-6) can be reduced to

$$\frac{1}{2}m_1 v_1^2 = \Delta E_{th} + \Delta E_{pot} \tag{3-9}$$

3.3 Frequency excitation caused by the impact

Vibration at the housing of the valve is caused by the movement in the valve (friction) and the impact of the movable part (excitation of natural frequencies and bouncing). An idealised model of the impact is the Dirac-impulse $\delta(t)$ with an infinite short duration in time. The spectral representation of a Dirac-impulse is infinite, flat and continuous. One important property of the Dirac-impulse is that it is highly localised in time or space:

$$\delta(t) = \begin{cases} \infty & \text{if} \quad t = 0 \\ 0 & \text{else} \end{cases} \tag{3-10}$$

In Figure 3-2 $\delta(t)$ is shown in the time- and frequency domain. A real-world impact differs from this idealised model in Equation (3-10) because the duration τ_i of impact is finite.

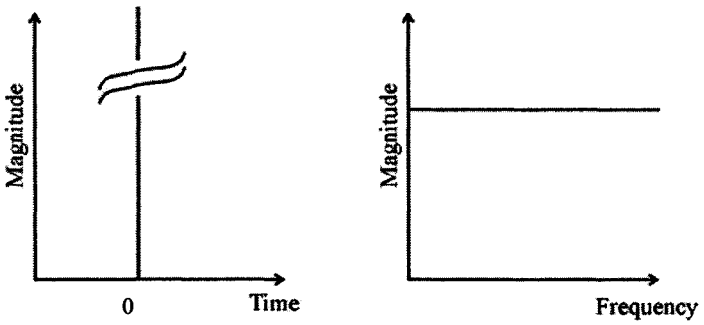

Figure 3-2 Dirac impulse

A model of the mechanical impact in valve is presented in [Lyon87; Biegner99]. The process can be modelled by an elastic body of mass *m* striking a rigid surface. This idealised model is related to the closing of the valve (when the elastomer seal gets in contact with the metal seat). For the opening process of the valve, the solid back end of the movable part hits the second stable position in the valve and the force onset it very abrupt (metal to metal impact). This second case is discussed later. In Figure 3-3 different stages of the modelled switching process are shown:

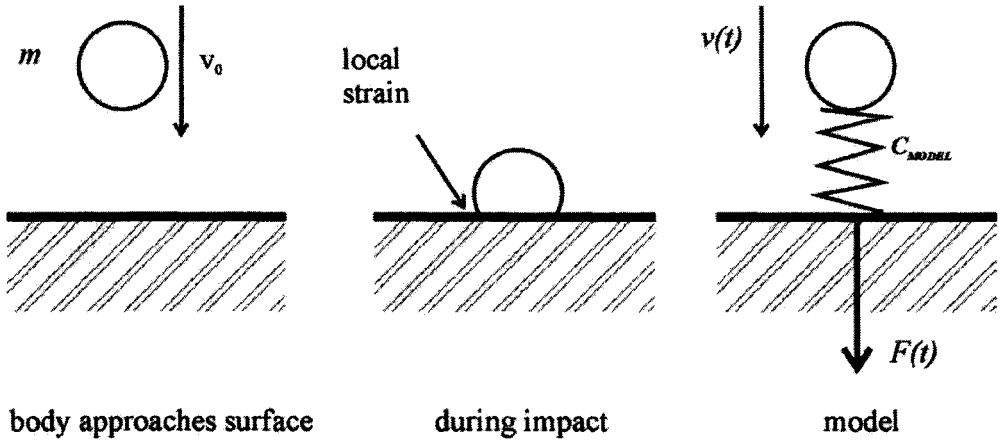

Figure 3-3 Model of the impact

An elastic body with mass m is considered to move with velocity v_0 and to strike the rigid surface at time t=0. The local strain of the body can be modelled by stiffness c_{MODEL} (right hand in Figure 3-3). $v(t)$ is the velocity of the body of mass m and $x(t)$ in Figure 3-4 is the displacement of the body with $v(t) = \dot{x}(t)$.

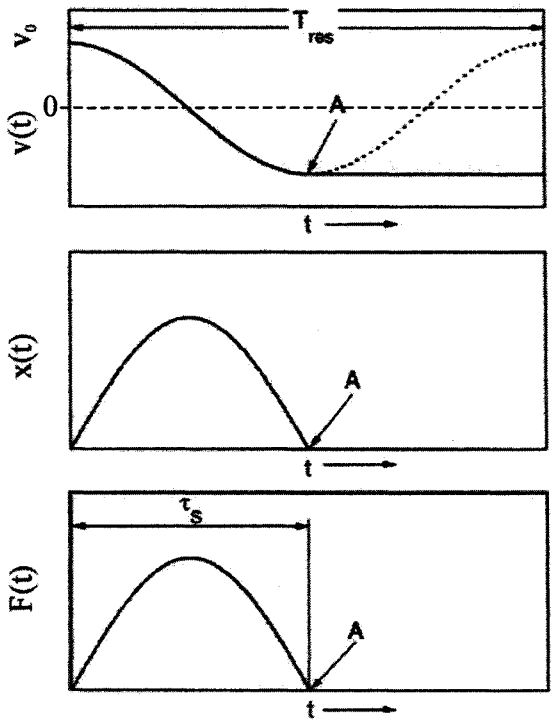

Figure 3-4 Model of velocity *v(t)*, displacement *x(t)* and force *F(t)* for body impact at a rigid surface. Body leaves surface at *A*.

In Figure 3-4 the force $F(t)$ during the impact process is shown. The body hits a rigid surface at time t=0 and leaves the surface at time $t = A$. τ_S is the contact time of body and surface. When the spring-mass-system is in contact with the surface it begins to oscillate with a period determined from the resonance frequency

$$f_{res} = \frac{\varpi_{res}}{2\pi} = \frac{1}{2\pi}\sqrt{\frac{C_{MODEL}}{m}} \tag{3-11}$$

The resonance period is the reciprocal of the resonance frequency:

$$T_{res} = \frac{1}{f_{res}} = 2\pi\sqrt{\frac{m}{C_{MODELL}}} \tag{3-12}$$

The displacement *x(t)* is the integral of the velocity *v(t)* and will have the sinoidal shape shown in the middle curve in Figure 3-4 over the half period in which the body stays in contact with the surface. The displacement times the contact stiffness equals the applied force which is shown in the bottom curve in Figure 3-4.

In [Lyon87], where the above presented model is proposed, the velocity v_0 is assumed to be constant for $t < 0$. This is not true for the closing process of a solenoid where the movable part is accelerated by the spring. Thus the model has to be expanded. The closing process starts when the voltage over the coil is switched off and the movable part is accelerated by the spring. The force of the spring depends on the position of the movable part:

$$F_{spring}(x) = -cx \tag{3-13}$$

The electrical current and the magnetic field are decay more slowly than the electrical voltage because the solenoid acts as a first order delay element for the electrical current (due to the inductance). The delay time of the coil depends on the external circuitry such as a freewheeling diode, varistor or similar approaches. Higher frequencies are excited in the valve for the higher velocity v_0 which is reached for the boundary condition with only the spring acting (see Equation (3-16). Also friction during the

switching process which is reducing the velocity is ignored for this investigation of the boundary condition in the following equations.

The acceleration of the movable part is given by

$$a(x)=\frac{F(x)}{m}=\frac{cx}{m} \tag{3-14}$$

The velocity of the movable part is the integral of the acceleration:

$$v(x)=\int a(x)dx=\int\frac{cx}{m}dx=\frac{cx^2}{m\cdot 2} \tag{3-15}$$

v_0 is the integral of Equation (3-15) taken from x_{min} to x_{max}, where x_{max}-x_{min} is the stroke of the valve. With $v(x_{min})$=0 the final velocity v_0 is $\frac{c(x_{max}-x_{min})^2}{2m}$.

The spectrum of the force $F(t)$ is important for the excited frequencies in the valve. It is determined by Equation (3-16) and shown in Figure 3-5.

$$F(\varpi)=\int_0^{t_{switch}} F_{max}\sin\left(\frac{\pi t}{\tau_S}\right)e^{j\varpi t}dt=-\frac{2mv_0}{1-\Omega^2}\cdot e^{\frac{j\Omega}{2}}\cdot\cos\left(\frac{\Omega}{2}\right) \tag{3-16}$$

with $\Omega=\frac{\varpi}{\varpi_{res}}$

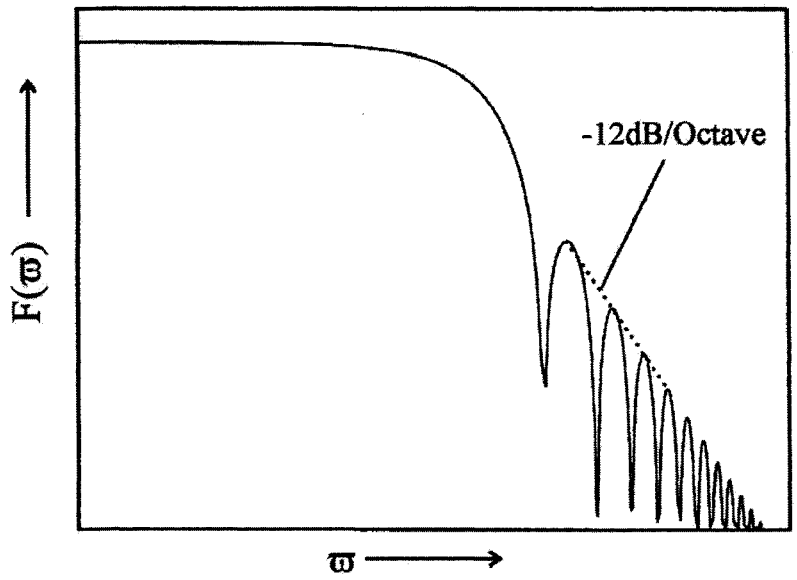

Figure 3-5 Spectrum of the impact force

When the valve is opened the movable part is accelerated by the magnetic force against the force of the spring. The magnetic force is known in [Kallenbach00] to be

$$F_{mag} = -\frac{\partial}{\partial x}\int_0^{\psi_0} i(\psi, x)\, d\psi \tag{3-17}$$

which is highly non-linear.

A qualitative diagram of the magnetic force and the elastic force of the spring is given in Figure 3-6.

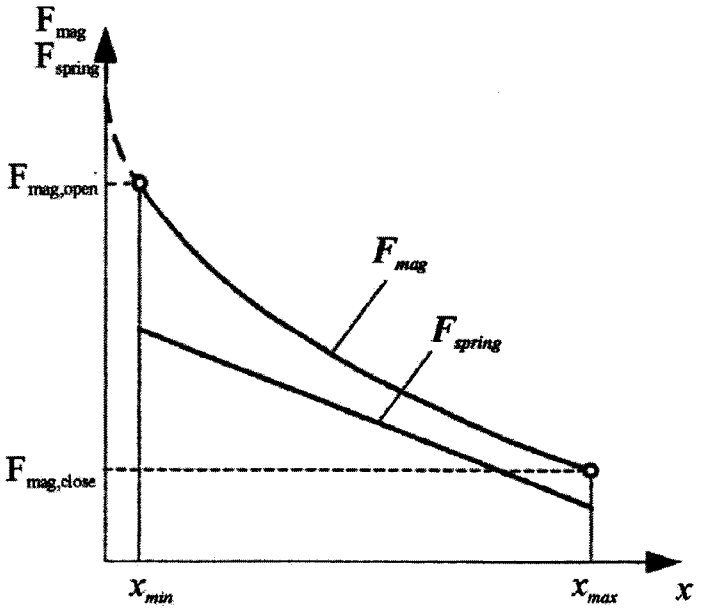

Figure 3-6 Forces of solenoid and spring - after [Kallenbach00]

For this switching on event the impact is much more abrupt than for the switching off process because when the plunger in the valve moves up and opens the fluid channel the impact will happen between the metal backside of the plunger and the metal end of the armature guide tube. On the other hand, in the above explained case of a switching off valve, when the fluid channel is closed, the elastomer seal hits the metal seat of the valve. Thus the shape of the switching-on-force can not be modelled by a sinoidal shape as done in Figure 3-4. The shape of the force *F(t)* which is exciting vibrations in the valve is a square wave in this case of metal to metal contact [Bigner99]. The spectrum of a square wave decays more slowly than a spectrum of a sinoidal half wave (shown in Figure 3-5). The decaying rate is reduced to –6dB/octave for this process. Thus higher frequencies are excited for the switching-on event than for the switching-off process. In Figure 3-7 the result of the above presented model description (bold line) and the data-

derived spectrum (dashed line) of a switching-off event are shown. The power spectral density was estimated using Walsh's averaged modified periodogram method with a window width of 128. The peak at the end of the spectrum (①) is due to the resonance frequency of the transducer.

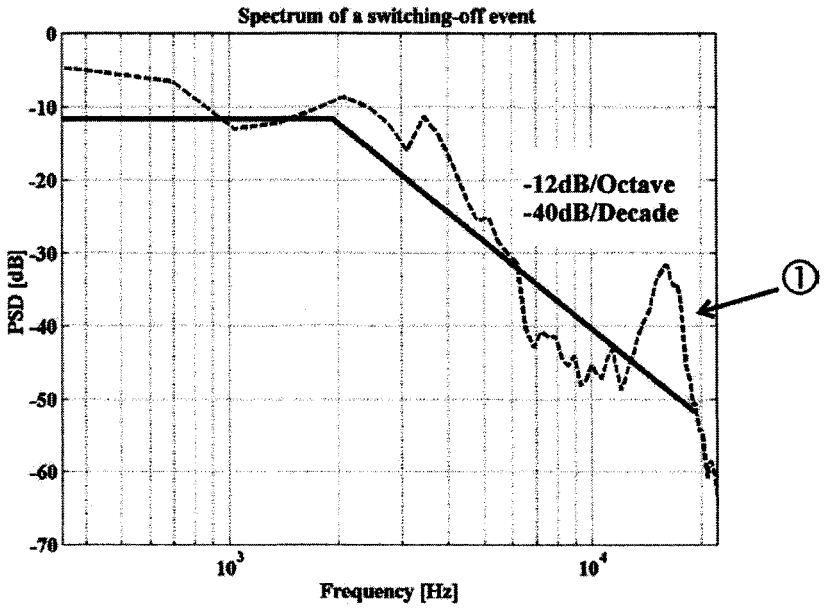

Figure 3-7 Spectrum and model for a switching-off event

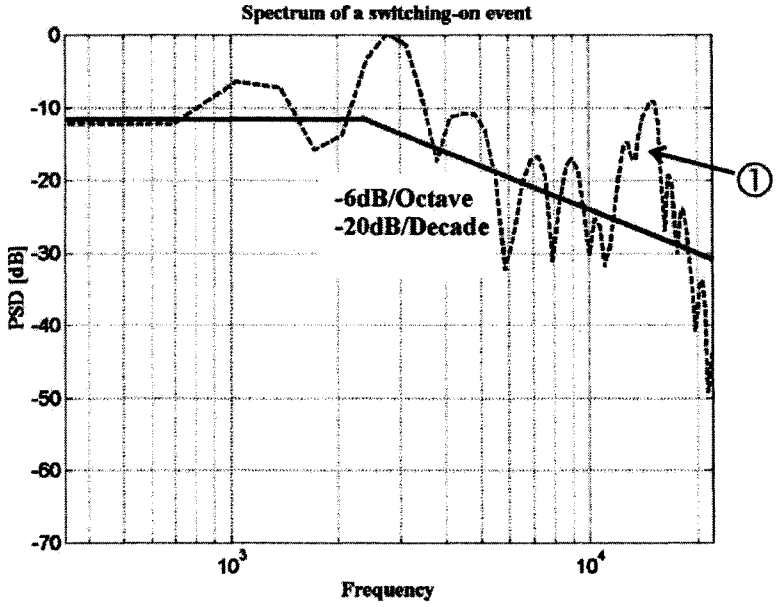

Figure 3-8 Spectrum and model for a switching-on event

In Figure 3-8 the corresponding diagram is shown for the switching-on event. The influence of the materials in these switching processes (elastomer → metal or metal → metal) is significant: the switching off event with the elastomer seal is a 2nd order lowpass and the switching on event with two metals included is a 1st order lowpass. It can be seen that the model fits quite well, and a piecewise linear trend of the frequency distribution is predicted.

3.4 Simulink model

Additional to the above presented model a simulink model of a solenoid valve is shown in Figure 3-9 which was developed at Bürkert some years ago [Beck94]. Because the model was already developed before this PhD-project it is only presented as "state of the art".

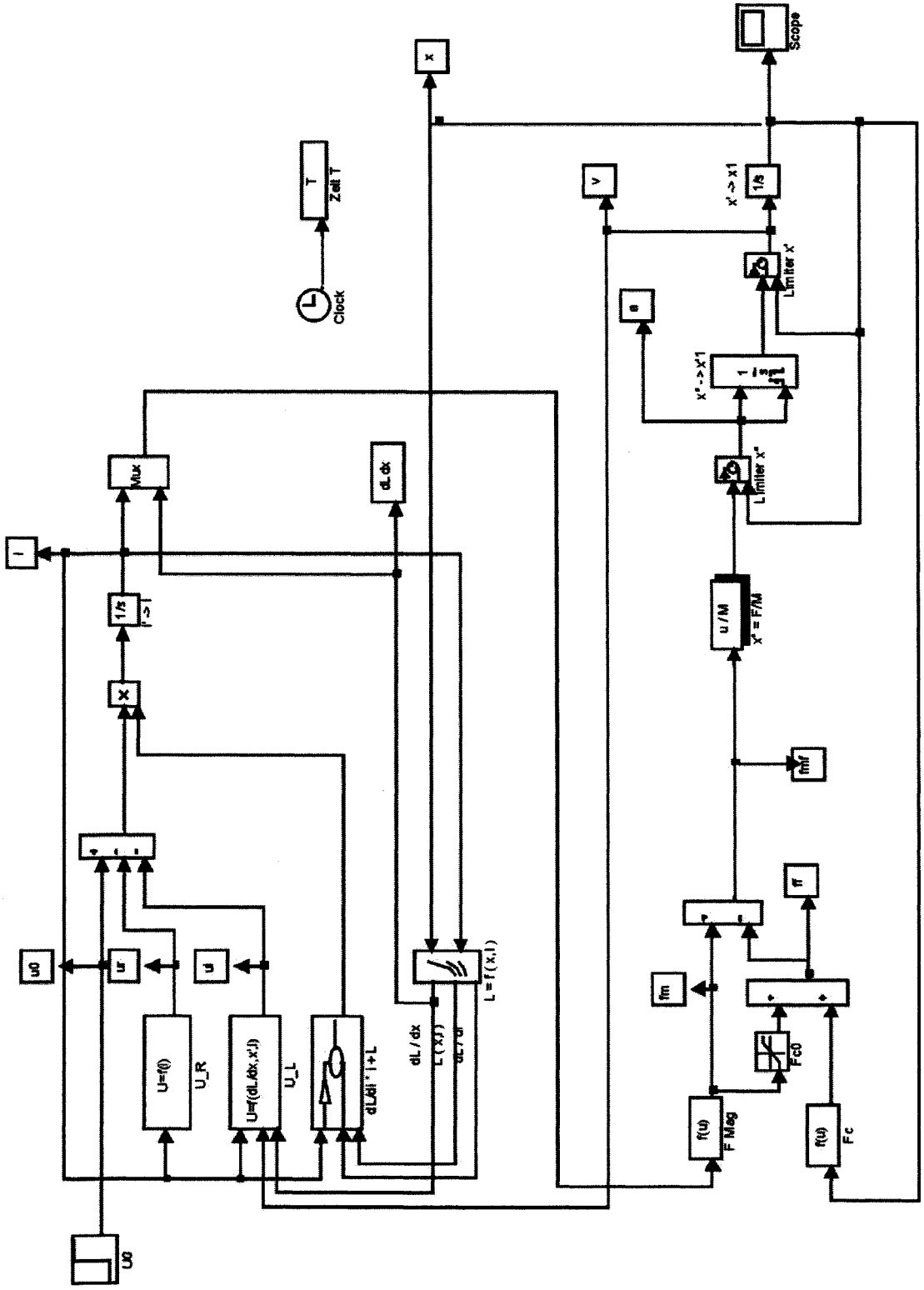

Figure 3-9 Simulink model of a switching valve – after [Beck94]

The inductance L of the solenoid circuitry depends on the displacement of the plunger and the electrical current. This non-linear relation was estimated with a FEM computation with ANSYS. The result is shown in Figure 3-10.

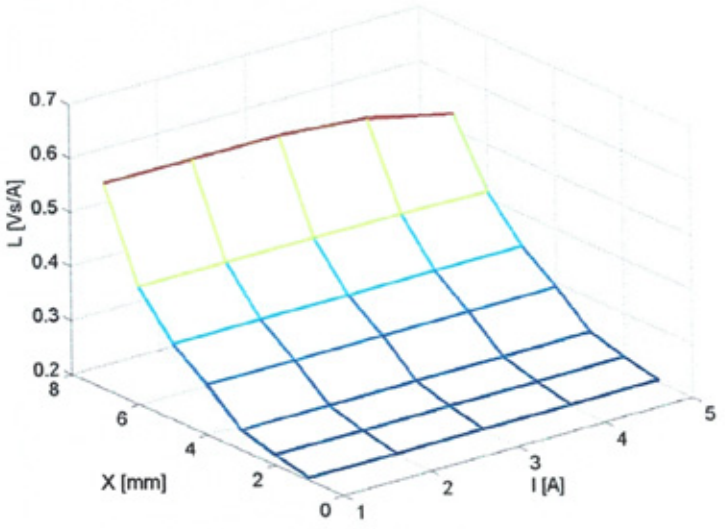

Figure 3-10 FEM computation of *L*

The output of the model is shown in Figure 3-11. It can be seen that different times and operations occur during valve switching (response time, travelling time). More details about the operation are also given in chapter 7.

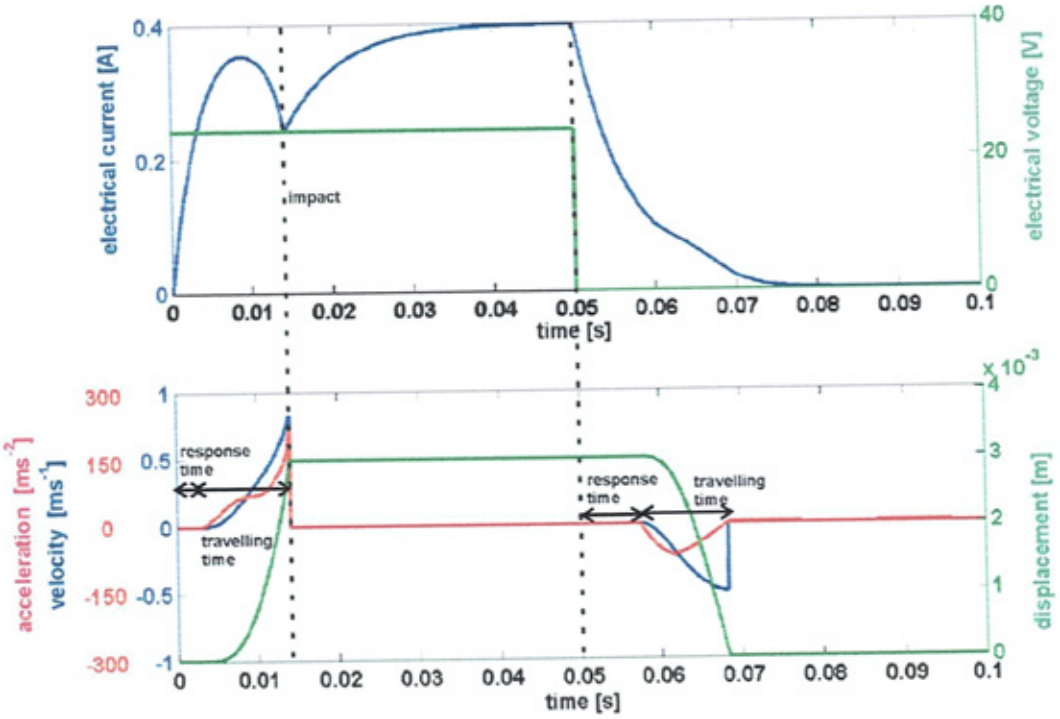

Figure 3-11 Results of the simulink model

3.5 Conclusions

The above presented models give deeper insight in the switching processes of a solenoid valve. The different steps of energy conversion led to a new technique of segmenting the overall vibration signal in the time-frequency plane. This new algorithm is presented later on in chapter 7. Important advantages of this new technique are that the resulting time-frequency segments are interpretable in a mechanical or physical sense and that they correspond to distinct physical processes which generate different parts of the overall vibration signal. The spectra of the excited vibration signals were investigated in more detail in section 5.2 to select a suitable sensor for the data acquisition process. Before these practical results and experiments first theoretical background information is given about classification within the next chapter. This topic was of high relevance

because the main goal of the project was to separate faulty and unfaulty valves by means of classifying the generated vibration patterns of solenoid valves.

4 Classification

4.1 Introduction

In this chapter the most important principles and essentials about 'classification' are summarised. Classification has been topic of scientific research for many decades and is still a very active field of research. Many textbooks have been published in this area and for further information it is referred to literature which is cited within the following sections. The rest of this chapter is organised as follows: first, general information about classification is summarised and then the classification scheme is presented in section 4.3 which shows the representation of the objects to be classified in different vector spaces. More details about preprocessing and feature extraction are given in sections 4.4 and 4.5, respectively. A survey on different classifiers follows in section 4.6 where the main focus is set on Neural Networks which are used as classifier in this project. The chapter ends with some conclusions and results in section 4.7 which were important for the experimental work presented in the next chapters.

4.2 General information

Classification is the task of mapping a set of objects which are each represented by several variables (features) to a smaller number of predefined distinct groups (or classes, or clusters) in a way that the structure within the set of objects is preserved in the new mapping. That is the within-group-scatter should be smaller for similar objects than the between-group-scatter [Gordon81; Li95]. There are many applications for classification in a large number of different fields, for example recognition of hand-

written or printed characters, speech recognition or crash detection in the airbag system of a car. Also many tasks in the field of digital image processing are concerned with classification. Different terms for this operation are 'discriminant analysis', 'pattern recognition' or 'supervised learning'. The mapping of measured data to distinct classes is performed by a so called 'classifier'. A classifier is an operator which works with numerical or symbolic data and can be related to as different fields as function approximation, statistics, vector analysis or set theory. It is usually a parameterisable operator which has to be adapted to a certain problem. This step of adaptation is called training or learning. Training of a classifier may be supervised or unsupervised. Unsupervised training (also called 'clustering') is based on the ability of the data to self-organise into a number of groups. Supervised training is performed if a labelled set of training data is used for the learning process. Further objects from the test data set are assigned to the class with the highest similarity [Darrell98]. The details of the learning process differ significantly for each family of classifiers but a common feature for all classes is that a training data subset of the objects to be classified is used for the training. This subset has to be representative of the relevant statistical properties of the overall classification set.

Sometimes it is difficult to get training-data which cover all uncertainties and differences within one class or group in an experimental programme. It is also often not known if examples of every possible class can be simulated with a reasonable level of accuracy, either numerically or experimentally. These are the reasons to sometimes choose an unsupervised classification strategy [Skitt93]. Unsupervised classification (mostly called 'clustering') is a task were the number of classes is not known before

classification and there are no labelled training data available. Thus the classifier itself has to be capable of exploring the number of classes which is optimal in a certain sense.

After training the classifier it is necessary to validate the accuracy of classification and measure the misclassification rate. This is done by applying a new and different set of test data to the classifier. These data should not have been used during the training process because the trained data are usually identified with higher accuracy than new data. The ability of a classifier to deal with unseen data which were not used during the training is called 'generalisation'. A lack of generalisability is called 'overfitting'. An overfitted classifier is able to classify the training data very well but the test data cannot be identified with suitable degree of accuracy. The degree of generalisation of a classifier is determined among other factors by the 'size' and the architecture of the classifier. 'Size' is the number of trainable basis-units in this context. A basis-unit is, for example, a single neuron in a Neural Network.

4.3 Classification scheme

Classification of patterns to distinct classes can be seen as a process of three steps:

1) Data acquisition and preprocessing

2) Feature extraction or feature selection

3) Classification

In Figure 4-1 a rough flowchart of this typical classification process is shown. These three steps represent the information about the objects in different vector-spaces. With one or more sensors, and suitable data acquisition tools, measurements are taken from an object to be classified. When the data are gathered from a set of sensors, the dimensionality is determined by the sampling rate, the number of channels (that is

usually the number of transducers) and the sampling time. The dimension of this raw data vector is λ_m. Because λ_m is often very large (some hundred to many thousand data points are not unusual) and because interesting features may be hidden in the overall noisy raw signal the measured data are preprocessed and transformed to the feature space [Lai88]. The term "preprocessing" can include many different algorithms and techniques like filtering, quantisation, normalisation etc. A feature-vector of dimension λ_f is a representation of the measured pattern in a lower dimensional space which contains and emphasises information of the original data with a high discriminative power. There are two common families of techniques to generate a feature vector [Niemann90, Fukunaga90, Webb99]:

- *feature selection* is the process when a smaller subset of set original data was used as features
- *feature extraction* is the process when the feature vector is gathered from a transformed (linear or non-linear) version of the original variables [Basak98].

The feature vector itself is used as input vector for a classifier which assigns the vector to one of λ_c distinct classes or clusters. The higher the discriminative power of the features, the more easily the classifier can be realised.

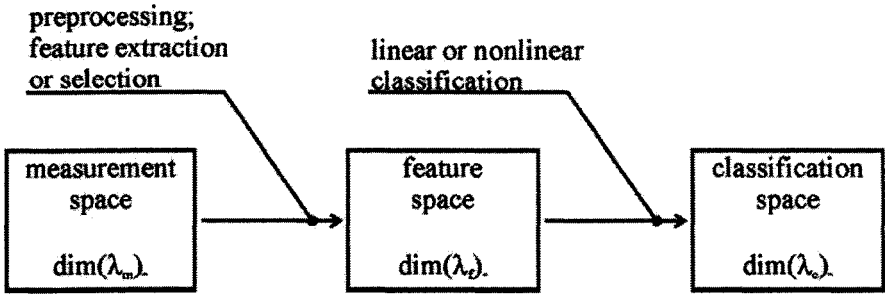

Figure 4-1 Classification process

For the dimensionality of the three spaces the following inequality holds:

$$\lambda_m > \lambda_f > \lambda_c \tag{4-1}$$

The aim of classification is to partition the measurement domain into λ_c disjoint classes Ω_λ (λ=1,2,...,λ_c), i.e. $\Omega_\mu \cap \Omega_\nu = \varnothing$ for $\mu \neq \nu$ [Paulus01]. Because the dimension of the spaces is reduced in both transformations as shown in Equation (4-1) the transformations are singular and some information is lost.

The careful and sophisticated selection of preprocessing steps and feature extraction or selection techniques is very important for the classification performance. The different steps in Figure 4-1 are explained in more detail in the following sections.

4.4 Preprocessing

Preprocessing is often one of the first operations performed on the measured data, which increases the ability of the measurements to be classified. The operations used for preprocessing depend on the type of data which should be classified, the measurement chain and the desired result of classification. Usually, preprocessing algorithms are type-sustaining which means the type of the preprocessed object is not altered (an image is still an image or a speech signal is still a speech signal after preprocessing) [Paulus01]. Some important aims of preprocessing are mentioned in the following points.

- *To reduce noise or deterioration in the signal*: common techniques to reduce noise are to limit the bandwidth of the signal by filtering or to substitute the raw data by locally bound statistical properties like the mean or median value.

- *To compress the signal by different coding or quantisation*: this step is, for example the reduction of a colour image to a grey-scale or black-and-white representation. In many situations this step is very valuable for a classification of images and the differences between distinct classes appear much more clearly in the reduced image than in the coloured one.

- *To eliminate effects of different amplification or different sources by normalisation*: often the source or the measurement chain is altered by effects which are not correlated with the different classes. So there might be a variability in the measured data which has no discriminative power for the classification process. One important example is speech recognition. The distance of the speaker to the microphone or the loudness of his speech may alter and possibly even the identity of the speaks are not constant. Thus it is necessary for automatic speech recognition (especially for speaker independent recognition) to normalise certain parameters of the measurements. It is possible to normalise the range of the signal (typically to [0;1] or [-1;1]), the energy of the signal or the mean and standard deviation ($\mu=0;\sigma=1$) [Niemann90]. Dynamic Time Warping: the time-axis of a time-sequence is also often normalised to deal with faster or slower signals (for example faster or slower speaking).

In many applications it is extremely important to preprocess the measured raw data in a suitable way because all ongoing steps in the classification will often not only be solved with less computational burden but also with higher accuracy after these steps.

4.5 Feature extraction or selection

The preprocessed signals are usually not suitable for direct classification because the dimensionality of the data vector is too high. The aim of feature selection or extraction is to find a smaller subset of variables in the preprocessed data which covers most of the discriminative power of the original data but reduces the dimensionality of the data vector by ignoring aspects of the measured sequence which do not contribute to classification. Features to be extracted can be, for example, statistical or geometrical parameters or the coefficients of a model based representation of the signal [Alguindigue93, Jossa99, Bissessur99]. Feature extraction is mostly driven by human experience because there are a vast amount of possible features which can be computed. It is also possible and very common to transform the measured data into a new domain (for example frequency-domain or time-scale-domain). This new description of the data is often very important in the extraction or selection of features. These transformations are sometimes seen as a preprocessing step [Niemann93] and sometimes attributed to feature extraction [Paulus01] in the literature. In this thesis they are used as one step of the feature extraction process because a new technique of feature extraction from spectra was developed during this research project and hence the relation of both tasks is very close in this work.

Very often some variables in a multivariate data set of features are correlated. Such a linear dependency is prejudicial for classification because linear dependent variables do not contribute further discriminative power but they enlarge the size of the classifier which increases the computational burden. To reduce redundant information within the feature set linear transformations to a lower dimensional spaces like the Singular Value Decomposition (SVD) or Principal Component Analysis (PCA) are used. These

techniques are often termed "feature selection in the transformed space" in pattern recognition literature [Webb99]. The basic principles of the SVD are presented in the following. For details it is referred to literature.

A *m*-by-*n* matrix **A** of measurements is considered to contain the preprocessed data. The SVD is an algorithm to decompose a matrix **A** into three new orthogonal matrices:

$$\begin{aligned}&\mathbf{U}^T\mathbf{A}\mathbf{V}=\mathbf{\Sigma}\\&[u_1,\ldots,u_m]^T\,\mathbf{A}[v_1,\ldots,v_n]=diag(\sigma_1,\ldots,\sigma_p)\quad p=\min\{m,n\}\\&\text{where}\\&\sigma_1\geq\sigma_2\geq\ldots\geq\sigma_P\geq 0\end{aligned}\tag{4–2}$$

A trimmed down version of the SVD is shown in Equation (4-3):

$$\begin{aligned}&\mathbf{A}=\sum_{i=1}^{r}\sigma_i u_i v_i^T\\&\text{with}\\&\sigma_1\geq\ldots\geq\sigma_r>\sigma_{r+1}=\ldots=\sigma_P=0\end{aligned}\tag{4-3}$$

This expansion of **A** is in a lower dimensional space if $r < p$ covers the most important information of the original measurements. All new variables are linearly independent and thus very useful for classification [Golub96].

4.6 Survey of different classifiers

4.6.1 Introduction

Nowadays there is a vast number of different classifiers available [Gordon81, Niemann90, Webb99]. Due to this the focus of this survey is to emphasise the main differences and properties of the different classifiers. One of the main differences between the classifier families is the use of the class-conditional probability density function $p(\mathbf{x}|\omega_i)$ for their operation [Ellwein02a]. This is the probability of the

occurrence of feature vector **x** when the class is ω_i. The first group is based on an estimation of this density. The Bayes' classifier in Equation (4-4) is one example for this group and the classifier with the optimal misclassification rate at all:

$$p(\omega_i|\mathbf{x}) = \frac{p(\mathbf{x}|\omega_i)p(\omega_i)}{p(\mathbf{x})} \tag{4-4}$$

Because the probability densities are often not known many classifiers based on the class-conditional density function use estimates of the probability density function. Usually the normal distribution is assumed in this case. The algorithm used for this estimation is one important difference between the classifiers of the first group. This estimation can be parametric by assuming a certain model for the probability distribution (for example the normal distribution) or nonparametric like kernel density estimation.

The second important family of classifiers is based on decision rules which are derived directly from the data without explicit estimation of the class-conditional density function. An important linear classifier based on this approach is the singular value decomposition (SVD) [Danaher92] and frequently used non-linear classifiers of this family are neural networks [Webb99].

In this research work only the second family was used because it is not possible to define or estimate the probability of the different classes $p(\omega_i)$. This probability depends very much on the final application where the valve is used (temperature, kind of fluid which is switched by the valve, pressure of the medium...). Thus it is not possible to give a general value for this distribution and all classifiers based on this distribution can not be used.

Different classifiers can be compared by considering the probability of misclassification and the cost of making the classification (for example the computational effort which has to be taken) [Young74].

4.6.2 Neural Networks

4.6.2.1 Introduction

Neural Networks (NN) are a technical simulation of parts of the human brain[1] and they are used for non-linear function approximation, classification, control and other applications. Neural Networks have several interesting properties: they are parallel systems which consist of an interconnected mesh of simple processing elements, the neurons. Neural Networks are trainable and adaptable to different situations and tasks and they have the ability of generalisation which means they can cope with unseen data which are only similar to the trained patterns. They are often able to process vague, uncertain or incomplete information and data. Nevertheless, Neural Networks are no "deus ex machina" which can solve all classification problems. There are several drawbacks which are described in more detail in the following sections. On difficulty is the lack of interpretability of the trained net. The internal parameters can usually not be related to physical, technical or other empirical effects. Also there are no clear and universally valid rules for the selection of architecture and size of a Neural Net for a certain problem or task.

---

[1] Neural Networks are sometimes considered as a simulation or a model of the human brain. Actually, this is misleading and not correct. The human brain is not well understood in many parts and operations. Neural Networks are much simpler and less sophisticated than the brain. Thus we can say that Neural Networks are inspired by results of neurology and there are several basic similarities between NNs and the human brain but the brain is many times more complex (the human brain is assumed to have about 10^{12} neurons each with an averaged number of $2*10^4$ connections to other neurons). Artificial Neural Networks are far away from these dimensions.

Still experience of the researcher and expert knowledge are very important for the design process. In any event, Neural Networks are often very successfully used as classifiers and also in this research project a NN was implemented. Hence Neural Networks were described in more detail in the following sections. Because of the very large amount of knowledge and experience which has been contributed by vast number of researchers this introduction is far from being complete. Further details and additional information can be found in literature, for example [Cichocki93, Kinnebrock94, Webb99].

4.6.2.2 Inspiration by human brain

The human brain work significantly different from a man-made computer: while most computers are based on the von-Neumann- or the Harvard-architecture which are both sequential structures the human brain, on the other hand, is a massively parallel system with an estimated number of 10^{12} basic processing units, the neurons and each neuron around $2*10^4$ connections to other neurons [Smith99; Trepel99]. In Figure 4-2 a simplified sketch of a neuron is shown:

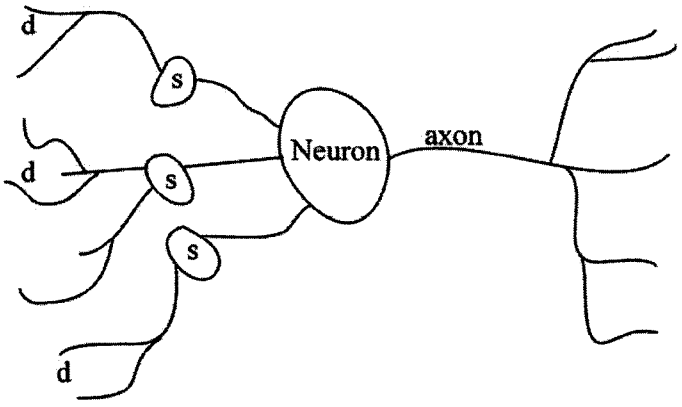

Figure 4-2 Sketch of a human neuron - after [Kinnebrock94]

The inputs of the neuron are shown on the left side of Figure 4-2. Receptors of the human body like haptic, optic, acoustic or thermal excitable cells generate signals which are transmitted to the brain and received by neurons. These signals and the outputs of other neurons can be the input for a certain neuron. Cells called *synapses*, *s*, are a kind of interface between different neurons and they can amplify or attenuate the input value. In the *neuron* itself the logical function is realised. The output of the neuron (*axon*) is a function of the input values and is determined in the neuron. If the sum of input signals exceeds a certain threshold the neuron becomes active and "fires". A short electrical pulse is sent through the output (axon). The *dendrites*, *d*, are a highly branching tree of fibres which connect the neuron to other neurons and connect the output of one to the inputs of a large number (up to 10^4) of other neurons [Kinnebrock94, Cichocki93].

4.6.2.3 The artificial neuron

As mentioned before the neuron is the basic processing unit in a neural network. Though there is a large number of Neural Network architectures and training algorithms all Neural Networks are based on a connection of similar neurons. In Figure 4-3 a block diagram of an artificial neuron is shown. The neuron has n inputs $i(\cdot)$ which are each multiplied with an individual factor, the so called weights, $w_i(\cdot)$. These weighted inputs are summed up in the left block together with another factor, the bias. The bias is static for the trained net but adjusted during training. The output of this sum-operator is applied to a second block with a threshold function. The threshold function can be linear or non-linear, continuous or discontinuous. For several training algorithms the threshold function has to be differentiable.

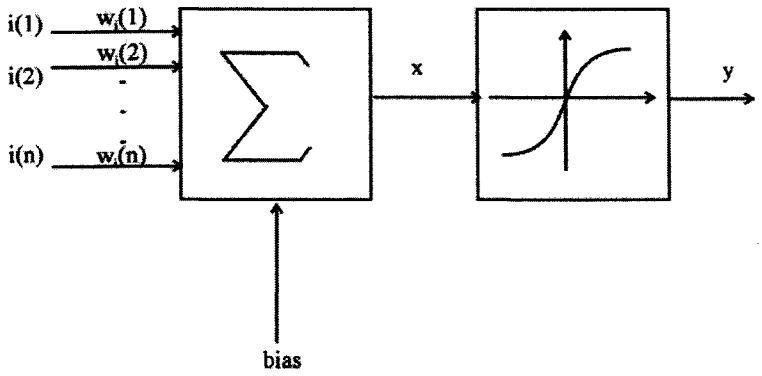

Figure 4-3 A single artificial neuron

The equation of a single neuron is:

$$y = f\left(bias + \sum_{j=1}^{n} i(j) \cdot w_i(j) \right) \tag{4-5}$$

where $f(\cdot)$ represents the threshold function. The term *neuron* was used first by McCulloch an Pitts [McCulloch43] in the forties of the 20th century for a very similar neuron.

Two very common threshold functions are the symmetrical sigmoid-function:

$$y(x) = \tanh(\gamma x) = \frac{1 - e^{-2\gamma x}}{1 + e^{-2\gamma x}} \tag{4-6}$$

and the unsymmetrical sigmoid function:

$$y(x) = \frac{1}{1 + e^{-\gamma x}} \tag{4-7}$$

where γ is a positive constant or variable which controls the "steepness" (slope) of the sigmoid function and x is the output of the summing unit in the neuron.

4.6.2.4 Learning of the neuron

One of the most important properties of a neuron is that it is trainable. The weights and the bias can be adjusted to fit a certain function between input and output. The aim of this training process is that desired output signals are produced for appropriate inputs. Unfortunately, there is no analytical algorithm to compute the coefficients of a neuron. In contrast, a neuron is trained in a sequence of learning steps by applying input (and often also appropriate output) patterns to the system. *Supervised learning* means that both, input and output patterns are presented to the neuron or the neural network and the system is learning to approximate a transfer function between in- and output. *Unsupervised learning* is the case when only input patterns are presented and the system is self-organising in a way that groups or clusters within the applied patterns are represented. There is a large number of training algorithms today available but one of the very first steps in this field was done by the psychologist Donald Hebb in 1949 by developing the so-called Hebbian learning rule [Hebb49]. His rule stated that information can be stored in the weights of neurons and a certain weight would be increased during learning by the repeated activation of one neuron by the other one across that weight [Pandya96]:

$$\Delta w_{ij} = \varepsilon x_i y_j \tag{4-8}$$

with

ε is a learning rate

4.6.2.5 The Multi-Layer-Perceptron

Neural Networks with one or more neurons in a single layer have one important drawback that many functions which are not linearly separable can not approximated (the so-called XOR-dilemma which was published 1969 by Minski and Papert [Minski69]). A 10 year lasting lack of interest in Neural Networks was the result of this

publication until the eighties of the last century. By inserting one or more so called "hidden" layers between the neurons connected to the inputs and the output neurons a new and very powerful architecture was developed, the Multi-Layer-Perceptron (MLP). It was shown that a MLP with one hidden layer is able to approximate any continuous function and a MLP with two or more hidden layers is theoretically capable of approximating any non-linear function to any arbitrary accuracy [McCormick96, Cichocki93]. In Figure 4-4 a MLP with one hidden layer is shown.

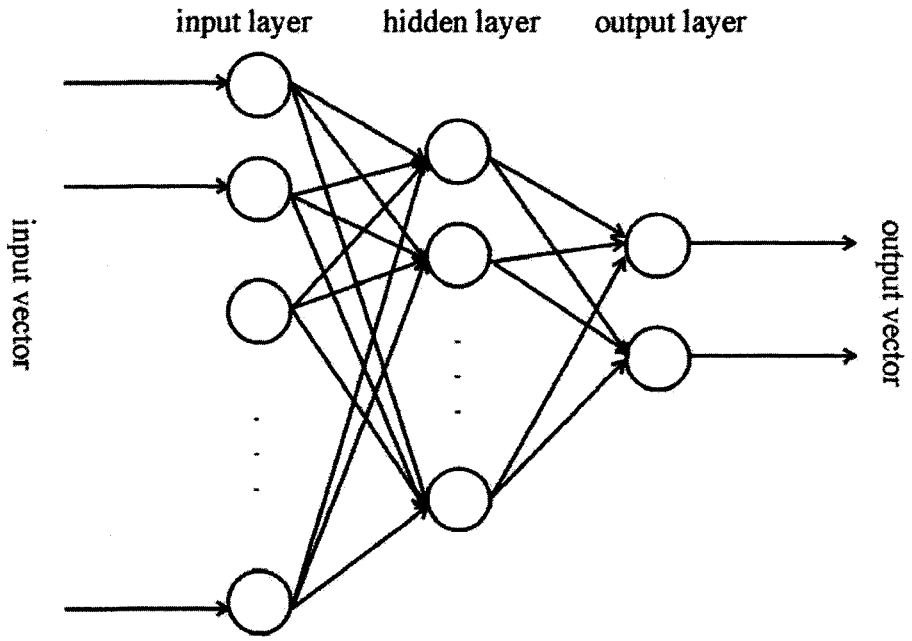

Figure 4-4 Multi-Layer-Perceptron

There are a large number of different and further architectures which are also often used. In this introduction only the Feed-Forward MLP was presented because it was used as classifier for the features extracted from the vibration pattern.

4.6.2.6 Backpropagation

Backpropagation is a very commonly used technique to train multilayer nets. It is a gradient descent method which makes it necessary that the transfer functions of the

neurons are differentiable. The most important paper which proposed the backpropagation algorithm was published 1986 by Hinton, Rummelhart and Williams [Hinton86]. The backpropagation algorithm is used to adjust the weights of the neural net [Pham01].

Each neuron in a hidden layer or output layer in a MLP has a output signal

$$y_j = f\left(\sum w_{ij} x_i\right) \tag{4-9}$$

where $f(\cdot)$ is the transfer function. The aim of most training algorithms is to minimise the sum squared error E between the outputs of the neurons y_j and the desired outputs y_{dj} (targets).

$$E = \frac{1}{2}\sum\left(y_{dj} - y_i\right)^2 \tag{4-10}$$

To adjust the weights w_{ij} increments Δw_{ij} are computed. The backpropagation algorithm to perform this operation for the k^{th} iteration of training is:

$$\Delta w_{ij}(k) = -\alpha \frac{\partial E}{\partial w_{ij}(k)} + \mu \Delta w_{ij}\left(k-1\right) \tag{4-11}$$

with

α is the learning coefficient and

μ is the momentum coefficient

4.7 Conclusions

In this research project a Neural Network was used as classifier because Neural Networks are not based on the estimation of the probability of the different classes $p(\omega_i)$. The different faults mentioned in Table 2-1 (page 15) have an individual probability which depends on the final application of the valve. It is not possible to

predict the probability that a certain valve will, for example, break down because of calcification (fault 5 in Table 2-1). This probability depends very much on the medium which is controlled by the valve (water, oil or compressed air) and the temperature of the fluid. These parameters are not known before mounting the valve into the final system or application. Thus it is not possible to give a general value for this distribution and all classifiers based on this distribution can not be used. Neural Networks do not need this probability information and it is possible to train them with a set of sample valves. This is also very suitable because all important environmental parameters and conditions like ambient temperature, pressure of the medium, switching frequency or the voltage over the coil (see also section 5.4) can be taken into account during training. Thus it is not necessary to develop one large model which covers all these parameters, because this would not be feasible with the necessary accuracy. The training data were acquired during this research project. More details about the data acquisition and the test bench were given later on in chapter 5.

5 Data acquisition

5.1 Introduction

Data acquisition is the task of measuring and storing data of interest. There are two main challenges in performing this step:

- The interesting signal is often of non-electric nature. Later processing steps are usually performed on a computer or by using an analog circuitry, which require a voltage or current input. Hence a suitable transducer has to be used which is capable of transforming the quantity of interest into an electric value (electrical voltage, current, resistance, charge or similar).
- Today most applications in the field of signal processing are designed as digital circuits or digital algorithms, respectively. To work with a measured time-signal in a digital processor it is necessary to sample the continuous signal at discrete time-steps. This is usually performed by a analog-to-digital converter (ADC). Several aspects have to be taken into account if an ADC is used.

These challenges are discussed in detail in the following sections and results and solutions are presented. The rest of this chapter is organised as follows: first, the selection of a suitable sensor is discussed. Several basic sensor principles were investigated to find a suitable transducer for fault detection. After this the selected sensor is presented in more detail in section 5.2.3 and especially the aspect of being a low-cost transducer is discussed in section 5.2.3.1. In section 5.2.4 different positions at the valve are analysed for their suitability for mounting the sensor. Sampling of the

analog values is discussed in section 5.3 and detailed information about the experimental setup is given in the following section 5.4. The chapter ends with conclusions regarding the data acquisition process in section 5.5.

5.2 The sensor

5.2.1 Selection of the sensor principle

The sensor is used to acquire data from the valve with the purpose of condition monitoring in this research work. There are several possible parameters and quantities proposed in literature which can be measured to observe a valve. In Figure 5-1 an overview is given. The chosen path through this tree is indicated with bold lines. The reasons for this decision are explained in detail in the following paragraphs. In the following the selection of the sensor is shown for one case study investigated in this research project. However it is anticipated that this selection criteria can be generalised to many other similar valves.

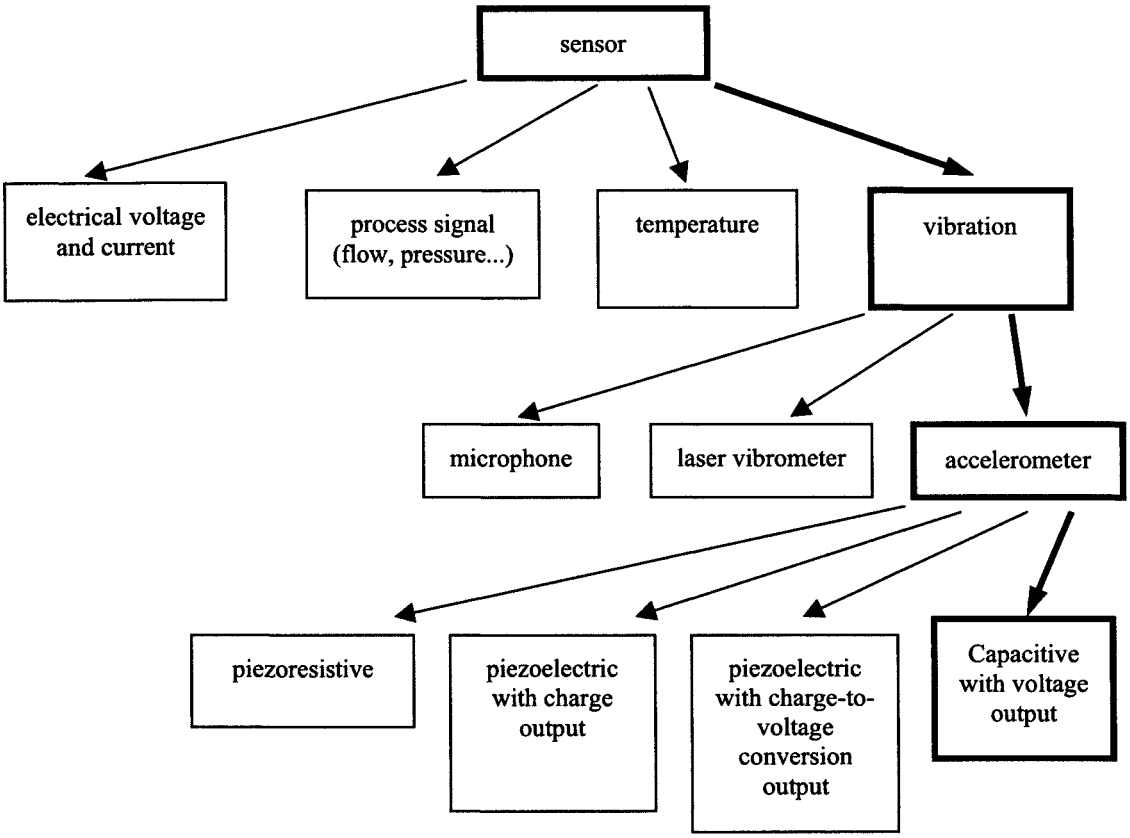

Figure 5-1 Possible sensors

The *electrical voltage and current* are used in a work of [Kryter90] and [Blakeman97]. This principle has the drawback that mechanical faults are sometimes difficult or impossible to detect because the influence of deterioration of the seal, the seat or the valve body have minimal influence on the electrical parameters. These parts of the valves were not observed in both papers mentioned above.

Process signals like the flow though the valve or (differential) pressures give important information about the fluidic part of the valve. These sensors are implemented for example in [Gallier97]. The drawback of these approach is the effort which has to be taken is very high. If the leakage, which can be measured very easily with a flowmeter,

is not the only interesting fault then a set of sensors has to be assembled to the valve. Each sensor has to be connected electrically and fluidic. This effort often many times outweighs the expense of the valve itself many times and thus this strategy is not feasible in many applications.

The *temperature of the coil* is an indicator for possible reduced coil life [Kryter90].The temperature has a linear relationship with the resistance of the coil which can be computed from the electrical voltage and current. Though this parameter can be acquired with little effort, it is not that interesting because the coil itself is seldom the reason for a breakdown of the valve according to information of the service department and the quality assurance department of Bürkert Fluid Control Systems.

The *mechanical vibration* of a device is a signal very often used for quality assurance and condition based maintenance. During the switching operation a valve generates significant vibrations and thus the vibration is a possible parameter for observation in this work. During the experiments the vibration was seen to be very interesting, because changes in many different parts of the valve influence the pattern (seat, seal, plunger, waste in the valve). The influencing parts also correspond perfectly with the main reasons for breakdown of the device. To select a suitable transducer a survey of important kind of vibration sensors was performed. There are three different main kinds of vibration sensors available:

- microphones gather airborne sound. Usually a membrane in the sensor gathers sounds waves from the air and the vibration of the membrane is altering an internal capacitor, resistor or an internal inductance [Putnam96]. These sensors are influenced rather strongly by other sources in vicinity to the measured object. This was the reason not to use a microphone, because valves are often assembled in a

environment with many sources of sound and vibration like engines, cylinders, gears and so on.

- Laser vibrometers are very accurate noncontact sensors. The surface of the device under test is scanned with a laser beam and vibration of the monitored device causes a dislocation of the reflected laser spot. But unfortunately, the assembly of a laser vibrometer in combination with a valve is to difficult and expensive to be used in real world applications.
- Accelerometers, finally, measure the structure borne vibration and are thus less affected by other vibration sources. They can be mounted easily by screwing or gluing. Accelerometers are available in a large variety of technical parameters like frequency range, sensitivity or housing. Different principles of operation are explained in the following for certain accelerometers.

There are three main groups of accelerometers: capacitive, piezoresistive and piezoelectric sensors. *Capacitive sensors* make use of the vibration changing the electrodes distance of an internal differential capacitor. Two of these electrodes are fixed and a third one between them is movable as shown in Figure 5-2 [Putnam96].

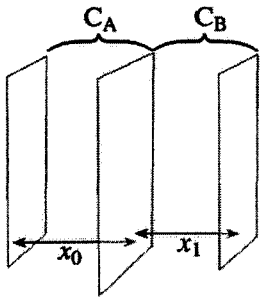

Figure 5-2 Principle of a capacitive accelerometer

If the sensor is accelerated the distance of the internal electrodes is dynamically altered. The differential capacitiy of the condenser for a displacement x of the middle plate is [Putnam96]:

$$\Delta C = C_A - C_B = C \quad x_0 \left[\frac{1}{x_0 + x} - \frac{1}{x_0 - x} \right] = \frac{2x}{x^2 - x_0^2} \tag{5-1}$$

where

$C = C_A = C_B$ for $x_1 = x_2$

The piezoelectric effect which is used for *piezoelectric sensors* was discovered in the 1880's by the Curie brothers: it converts mechanical energy into electrical energy. If a pressure (piesein ($\pi\iota\acute{\varepsilon}\zeta\varepsilon\iota\nu$) means "to press" in greek) is applied to a polarised crystal, the resulting mechanical deformation results in an electrical charge [Putnam96] which is typically converted into an electrical voltage by a charge amplifier.

Piezoresistive sensors are built from piezoresistive material which has the ability to change its resistance under physical pressure or mechanical work. Piezoresistive accelerometer designs use typically the sensors pendulous arm, connected to the proof mass, as a strain gauge. One important drawback of piezoresistive materials is their temperature-sensitivity (they are used as thermistors [Verplaetse95, Schubert95] and the sensitivity drift is often very high (+2000 ppm $°C^{-1}$) as mentioned in [Zimmermann95]. This sensitivity was the reason not to use a piezoresistive accelerometer as sensor in this project because the temperature of the observed valves may alter significantly when the coil is heating up (see Figures 5-21 and 5-22).

These different accelerometers are compared shortly in Table 5-1and in detail in the following sections.

Table 5-1: Different accelerometers

	capacitive	piezoresistive	piezoelectric (charge output)	piezoelectric (voltage output)
Frequency range	+	-	-	-
Temperature	O	-	+	-
Sensitivity	+	O	O	O
Measurement range	O	+	+	+
self-test	+	-	-	-

+ : perfect, ideal

O : suitable, but not perfect

- : not appropriate or not available

5.2.2 The frequency bandwidth of the sensor

A very important criterion for the conclusive decision for a certain sensor was frequency bandwidth of the occurring vibration signals. To evaluate this range the air-borne sound of switching events of different valves (type 6011 and 6013; an image of these devices is shown in Figure 7-13 at page 107) was recorded. A microphone was used because its coverage of the low frequency range from 50Hz up to 20kHz is suitable for this process. Additionally measurements with a piezoelectric accelerometer were taken to investigate the higher frequencies up to 230 kHz. On the other hand, the accelerometer was not suitable to measure low frequencies below approximately 2kHz. All obtained time sequences were transformed to the time-frequency-domain by Short Time Fast Fourier Transformation (STFFT). This algorithms gives the ability to get a first impression of the frequency distribution over time. Figure 5-3 and Figure 5-4 show the air-borne sound of a valve type 6011 of both, switching on and off events. Figure 5-5 and Figure 5-6 give the same data for a valve type 6013. The valve 6013 has nearly

1.5 times the size of the valve type 6011 and thus more low-frequency parts occur in the spectrograms of the 6013 valves. It can also be seen that the switching on events generate the higher frequencies which corresponds with the results of the model developed in chapter 3.3.

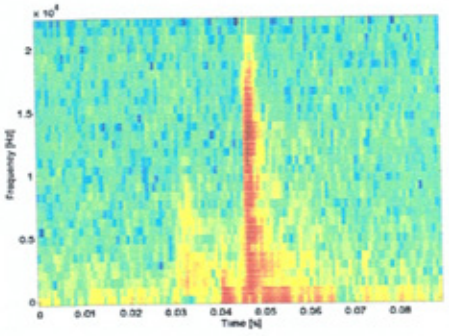

Figure 5-3 STFFT of air-borne sound of a switching on event of valve 6011

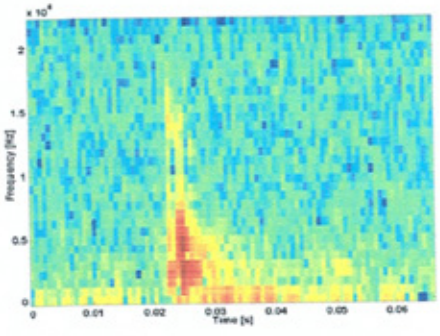

Figure 5-4 STFFT of air-borne sound of a switching off event of valve 6011

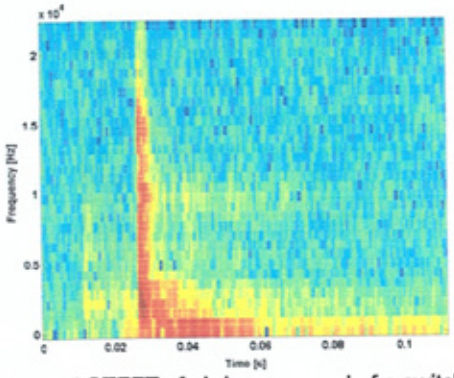

Figure 5-5 STFFT of air-borne sound of a switching on event of valve 6013

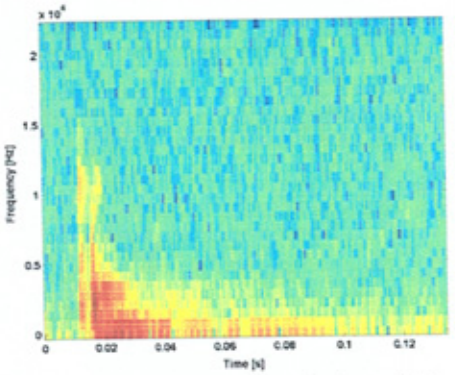

Figure 5-6 STFFT of air-borne sound of a switching off event of valve 6013

All these Figures show that there are peaks in the spectrum in the frequency range below 2kHz. In Figure 5-7 the measurement of a switching off event of a valve type 6011 was shown. This measurement was performed with a piezoelectric accelerometer (Metra KD 91).

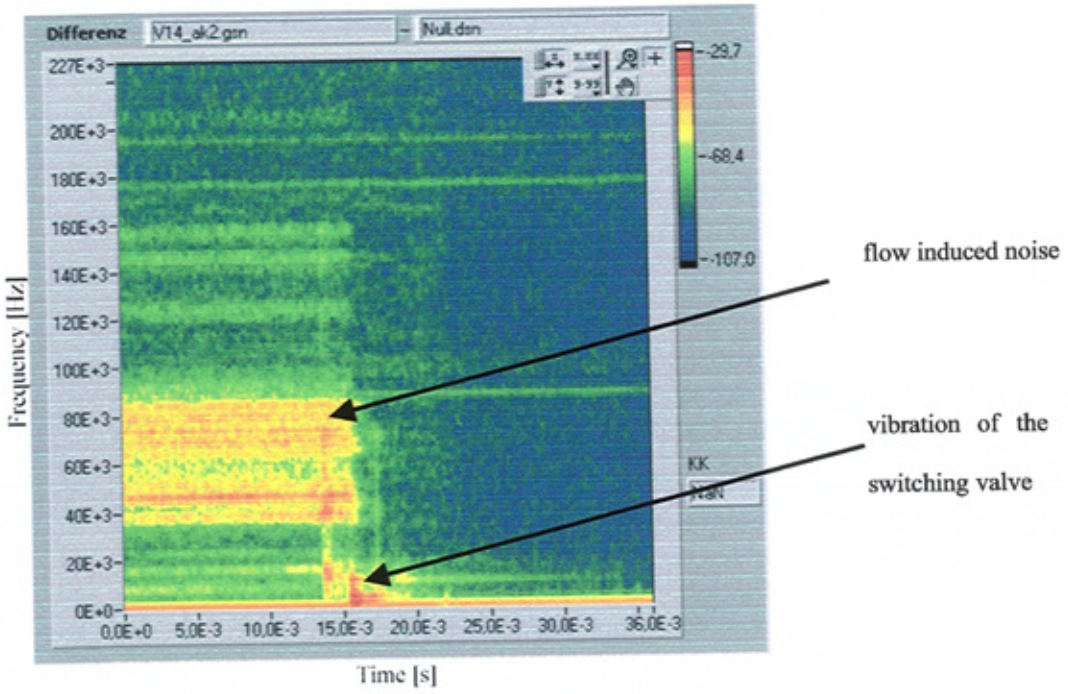

Figure 5-7 Switching off event of valve 6011, measured with a piezoelectric sensor

It can be seen, that flow induced noise is mainly in the frequency band between 35kHz and 85 kHz. The vibration of the valve itself is focused to the frequency range up to 20kHz. These results were verified by a FEM-Simulation of the natural frequencies of the valve. A CAD-model of a valve type 6013 was used to compute the eigenmodes with the DesignSpace Software Tool. DesignSpace is based on the ANSYS-kernel and can do several FEM computations. This model predicted natural frequencies between 388 Hz and 2038 Hz for the first six eigenmodes. In Figure to 5-8 to 5-10 the first three eigenmodes were shown. These images show the relative translation of the oscillating body.

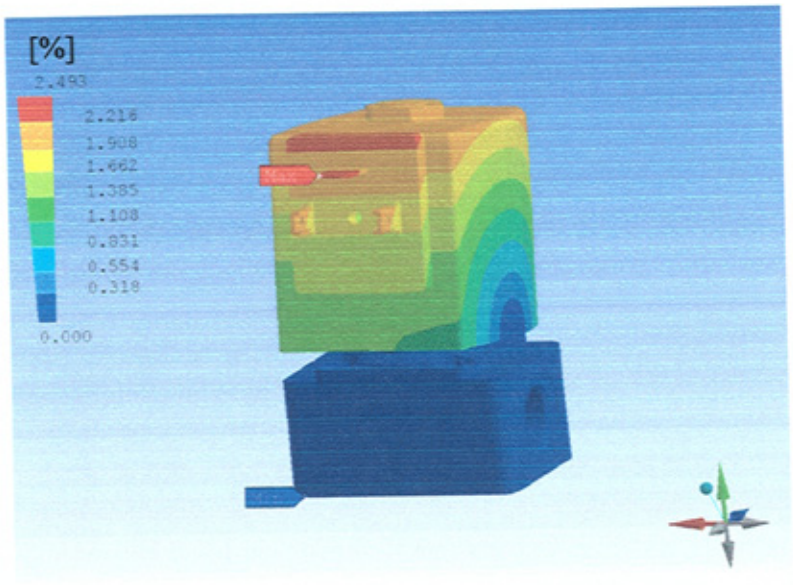

Figure 5-8 First eigenmode

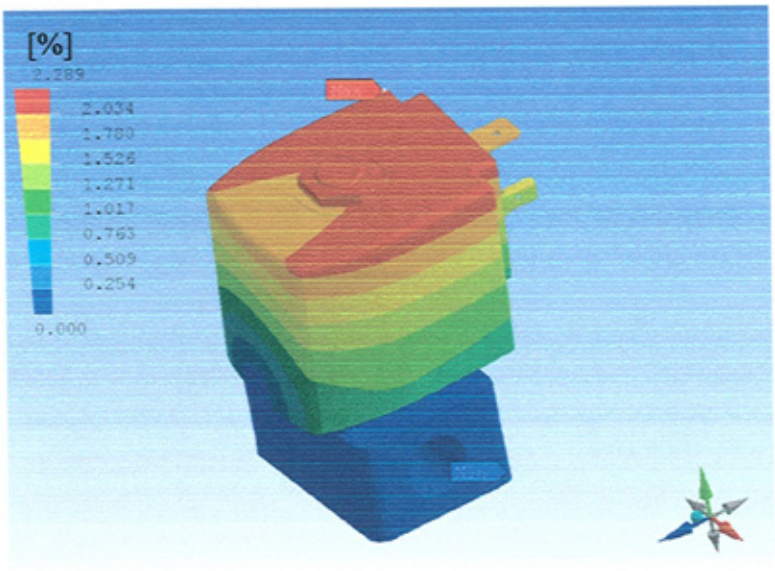

Figure 5-9 Second eigenmode

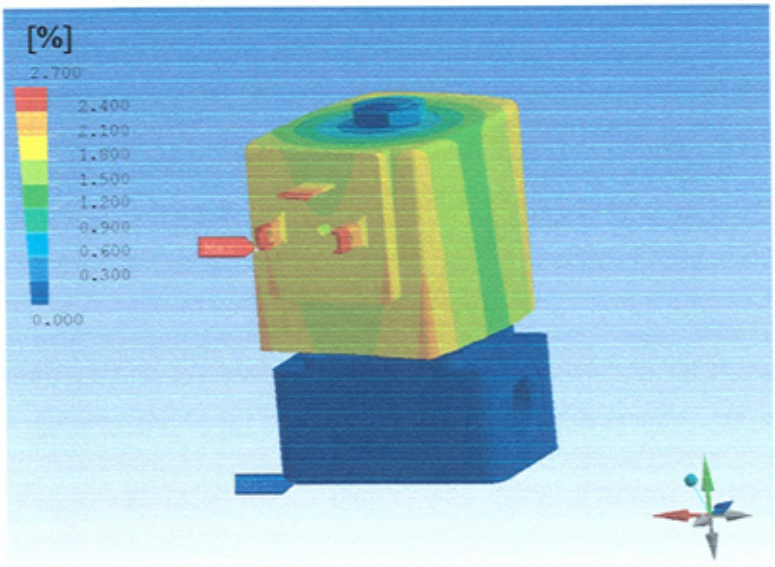

Figure 5-10 Third eigenmode

The natural frequencies of this model were found to be:

$f_1 = 388$ Hz

$f_2 = 408$ Hz

$f_3 = 692$ Hz

$f_4 = 1833$ Hz

$f_5 = 2026$ Hz

$f_6 = 2038$ Hz

The interesting frequency band of the switching events of different valves is between DC and 20kHz and the first natural frequencies were found to be between some hundred Hertz and a few kilohertz. The frequency bandwidth of most piezoelectric accelerometers usually has a lower bandwidth limit of about 2kHz. Only capacitive and piezoresistive sensors can measure frequencies down to DC signals [Schubert95]. Piezoresistive accelerometers have the drawback of higher temperature-sensitivity than capacitive sensors [Verplaetse95, Schubert95]. Hence a capacitive accelerometer was chosen for this research project. The investigated valves were rather small sized devices. It was seen in different experiments that larger valves tend to generate lower frequency vibrations as would be expected. Thus this investigation with the valve 6011 from Bürkert is a kind of border consideration: most valves available are larger, the emitted frequencies are lower and there is no limit in data acquisition depending on the sensor down to lower frequencies. Thus, if it is possible to classify the condition of the 6011 with this monitoring equipment it also should be suitable for a large set of alternative valves.

5.2.3 The ADXL105 accelerometer

5.2.3.1 Using a low-cost sensor

A large variety of possible sensors are available which suit to the criteria defined in sections 5.2.1 and 5.2.2. After taking all the important technical and physical boundary conditions into account finally also the price may be a criterion for the selection of a certain sensor. Because the condition monitoring system in this research work was evolved for small sized solenoid valves which are not extremely expensive the advantages of the supervision system should not outweigh by its expense. This situation led to a new scientific challenge for this research project: it was decided to use a low-cost MEMS accelerometer and to investigate and develop signal processing algorithms which are still able to perform at a suitable misclassification rate. The savings made with the sensor made it necessary to develop more sophisticated algorithms of digital signal processing. This is shown in Figure 5-11: the pre-processing of the raw data is accomplished in steps 2 (segmentation in the time-domain) to 4 (detection of regions of interest). More effort is spent to this part of the condition monitoring system than it is done in comparable projects found in the literature [Kryter90, Kalix93, Uhrig93, Blakeman97, Thompson97, Kiesbauer00].

Important differences between the mentioned papers and this PhD project are for example that in previous projects no effort was taken to improve the degree of stationarity of the vibration signal and to find data derived regions of interest (ROI) in the spectra. Both topics were seen to be important for the classification result in this PhD project using the low cost MEMS sensor [Ellwein00b, Ellwein01a, Ellwein01b].

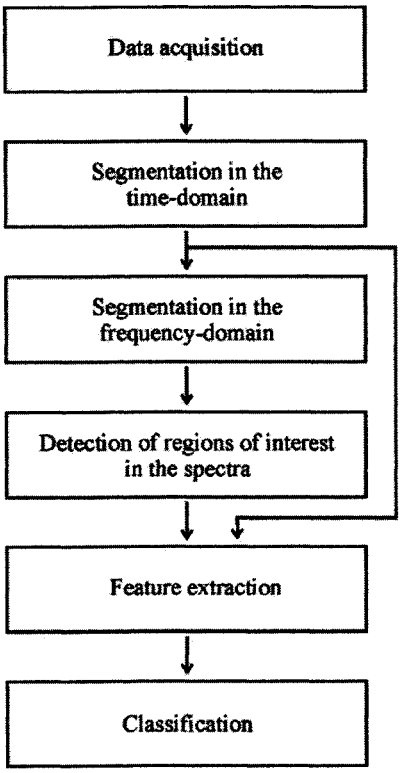

Figure 5-11 The overall classification scheme

The classification results of the monitoring system developed in this PhD project presented in chapters 9 and 10 give confidence that it is possible to use a low-cost sensor in combination with improved signal processing algorithms.

5.2.3.2 Technical data of the ADXL105

The ADXL105 is a single-axis accelerometer with a bandwidth of 10kHz and a resolution of 2mg and measurement range of $\pm 7g$ [Analog99]. Other, similar MEMS-accelerometers from Analog Devices are tested and presented in [Patel92 and Béliveau99] and were found to be very suitable for different applications like airbag control in the automotive sector or shock measurement. The following diagrams (Figure 5-12 to Figure 5-16) were all taken from the ADXL105 Datasheet [Analog99]. In Figure 5-12 the frequency response of the ADXL105-sensor is shown.

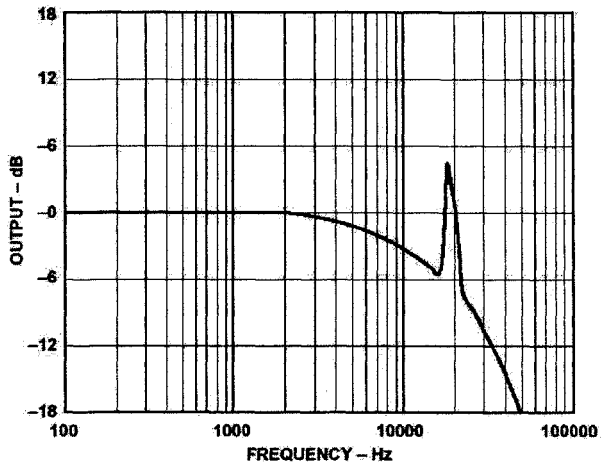

Figure 5-12 Frequency response of the ADXL105 sensor

The disturbance of the sensor output due to noise is not negligible for this sensor. In Figure 5-13 the noise distribution of this sensor is shown.

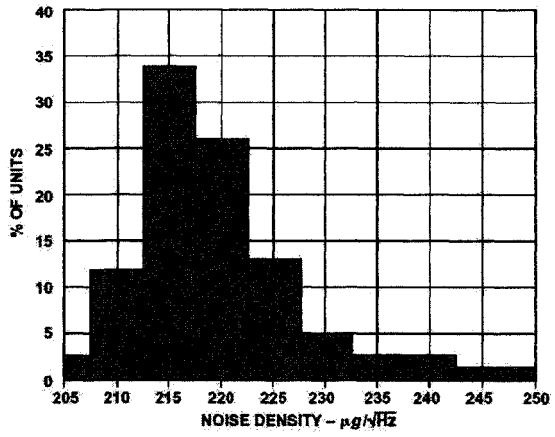

Figure 5-13 Noise distribution

The overall statistical error of the device is indicated in Figure 5-14. This Figure shows the distribution of the output signal for a 0*g* input signal. The determined output signal would be 2.5V for this input signal. Figure 5-15 is a graph of the sensitivity distribution of the transducer. The data for these three Figures (noise distribution, output distribution

and sensitivity distribution) are derived from several characterisation sets and give an overview over the dispersion of important parameters between different sensors. This is a very important aspect to take into account because variations of the sensor parameters within a production lot will influence the measurements. Do deal with these variations a set of ten sensors was used to gather the data for training the classifier.

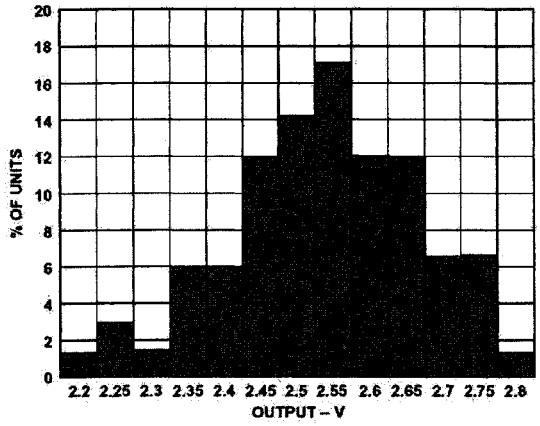

Figure 5-14 Output distribution of the ADXL105

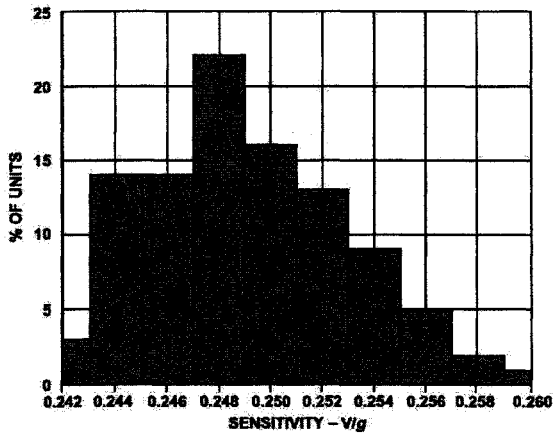

Figure 5-15 Sensitivity distribution of the ADXL105

The noise is also influenced by the supply voltage of the sensor. In the typical noise density versus the supply voltage is shown and it is significant that attention has to be paid to this topic if the sensor is connected to the same supply as the coil of the valve

because the solenoid is a heavy load when it is switched. There are many recommendations and ideas about the design of a suitable supply with voltage regulators and additional circuitry well known and it is referred to literature for this topic [Tietze93].

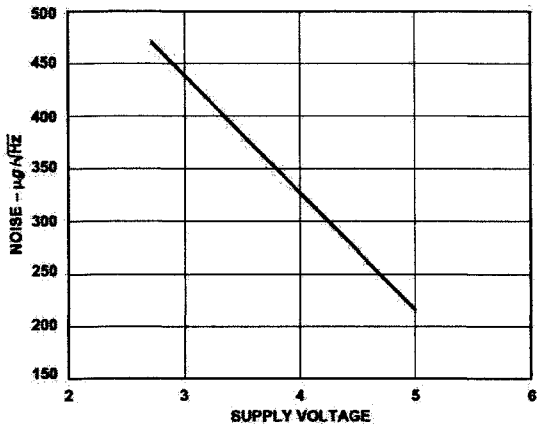

Figure 5-16 Noise density versus supply voltage

Summarising it can be seen that the frequency range of the sensor fits almost perfectly to the vibration signals of the switching valves. The weak point of this sensor is the disturbance of the vibration signal due to dispersion of parameters between sensors. This problem was solved because a set of ten accelerometers was used to gather the raw data for training and testing the classifier. Hence, the distribution of sensitivity, noise and bias are taken into account during training of the classifier.

5.2.3.3 Self-test

The ADXL105 is a micromachined capacitive sensor with an internal differential capacity. The plates of the capacitor can be accelerated by an electrostatic force which is activated by applying a logic high on the self-test pin of the IC. The acting force is approximately 20% of full-scale acceleration input [Analog99] and thus a proportional voltage change appears at the output pin. The self-test function can be used to test both

the mechanical structure and the electrical circuitry. This feature is very important for a condition monitoring system for solenoid valves because it is necessary to assure that the sensor is working correctly over the lifetime of the device under test (valve).

5.2.4 Mounting of the sensor

It is important generally for each measurement to mount the transducer in a suitable way. In Figure 5-17 a typical on-off-valve was shown. The material of the valve body is usually brass or stainless steel. The housing of the coil and the cable plug are made of polyamide or epoxy. The cable plug is connected with a screw firmly to the valve. This valve can be seen to represent a large class of devices, both from the Bürkert company and also from other suppliers. These small sized solenoid valves are always constructed in a similar way (housing of the coil, the coil itself, the cable plug for electrical connection and the valve body for fluidic connection). Thus the results gained from the investigation of these certain valves are anticipated to be representative and generalisable to many other similar devices.

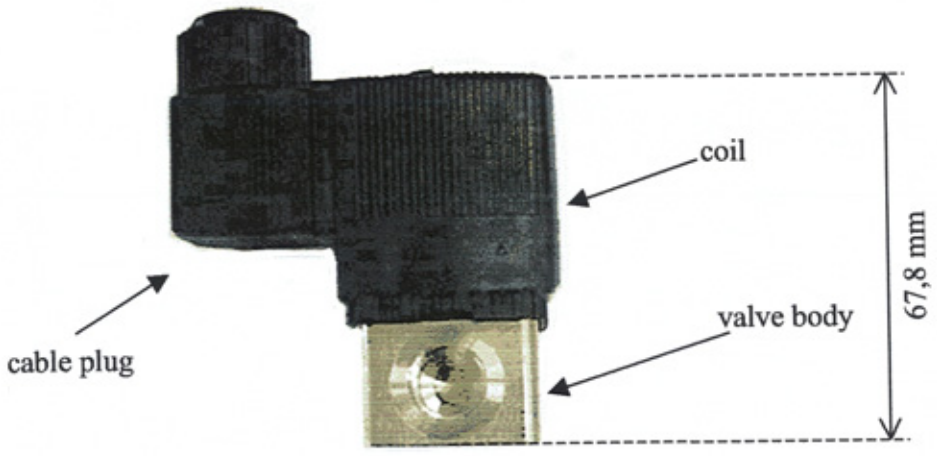

Figure 5-17 A typical on-off solenoid valve

The position of the sensor is very important for data acquisition. The highest accuracy could be reached if the accelerometer was mounted on the valve body, because the seat where the impact happens is part of the body and the vibration signals are least damped. On the other hand, all sides of the body are not suitable, because of mounting the valve itself can reduce the available space at these sides dramatically. The bottom of the valve is usually used to fix the valve in a machine or a plant (Figure 5-18). Thus the accelerometer could not be fixed on this side.

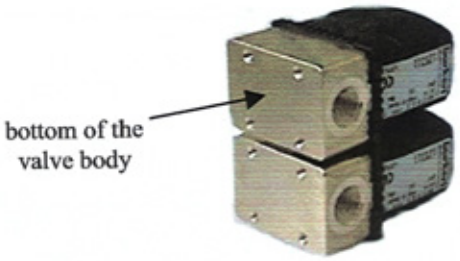

Figure 5-18 Bottom of the valve

Both sides of the valve are also not suitable, because valves can be mounted close together as shown in Figure 5-18 and Figure 5-19.

Figure 5-19 Three valves assembled together

The top of the valve has the drawback, that the coil is mounted with a nut (Figure 5-20) which will limit the available space and also increases the risk of damaging the sensor during assembling and mounting of the valve.

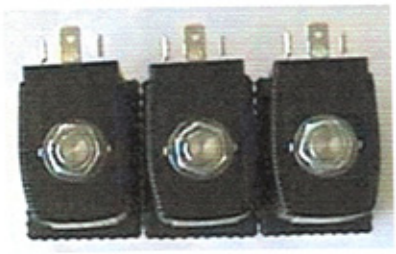

Figure 5-20 Top view of the valves

The cable plug was chosen to mount the sensor, because the available space is sufficient and also the electrical connection is easy and reliable. If a cable is clamped or mounted on the surface of the valve there will always be the risk of damaging the cable. This is avoided by implementing the sensor in the plug. Also the thermal situation is best in the cable plug. The valve body can heat up to 180°C because this is the highest allowed temperature of the medium. The temperature distribution of the coil surface is shown in Figure 5-21 and Figure 5-22. The images were taken at ambient temperature of 25°C and the coil voltage was 27V.

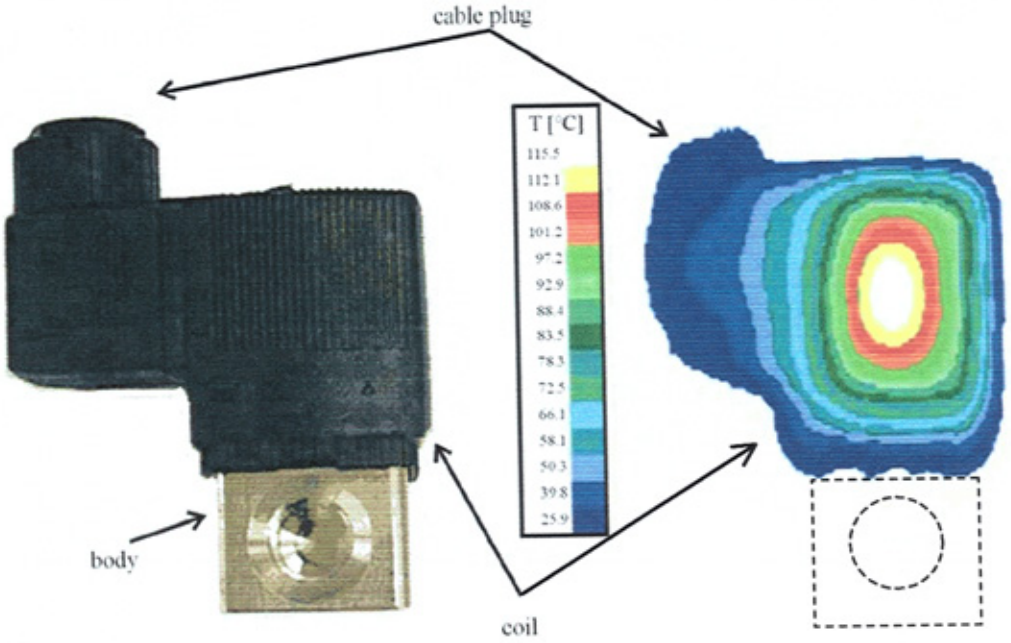

Figure 5-21 Heat image of the coil and the cable plug

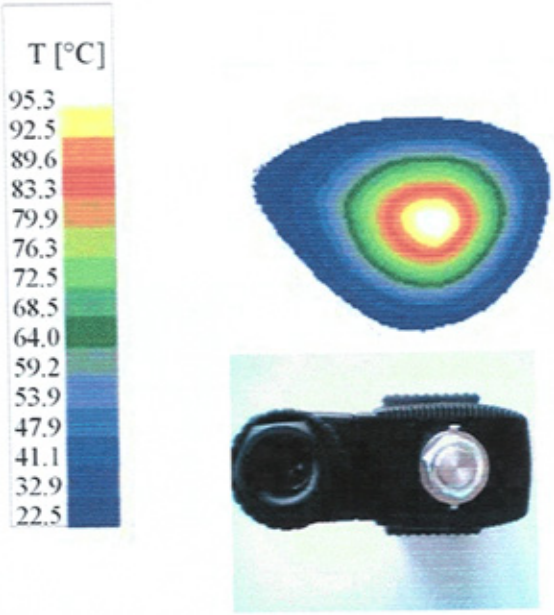

Figure 5-22 Heat image (top view)

The spot temperature was 115°C. The cable plug, on the other hand was below 40°C. The temperature is very important for the operation of electronic devices in order to pre-process and amplify the output signals of the sensor.

Another advantage of the cable plug as mounting position for the sensor is its distance to the vibration source (seat-seal-contact position). All important parts of the valve (armature guide tube, the hinge, the spring, the coil and others) are in the transmission path between the source and the sensor at the cable plug. Due to this all these parts which affect the reliability and condition of the overall valve can influence the vibration pattern. This is important because it is not the aim of this research project to gather or reconstruct the original vibration signal at the source. The main aim is to detect serious changes in the whole device and to accomplish this it is necessary that deterioration at different positions of the valve can impinge on the observed pattern.

All these reasons (available space, temperature conditions and the transmission path) were basis for the decision to assemble the sensor at housing of the cable plug. This approach is new for vibration measurement and analysis and has several important advantages. Due to this it was applied for a patent for this approach (application number DE 101 47 326.5).

5.3 Sampling of the measurements

The sensor was fixed with double sided sticky tape as recommended in literature [PCB Piezotronics99]. To damp the vibration for the measurement range of the sensor a piece of rubber (Acrylonitrile-butadine = NBR) with 5mm thickness was mounted between the transducer and the cable head. The signal is limited to a frequency range about 20kHz. This gives the possibility to sample the vibration pattern with a sound

card (Soundblaster 16pnp). A sampling frequency of 44,1kHz and an accuracy of 16bit were use to gather the analog data. The analog sensor output was amplified with an electronic circuit before sampling. The development of the necessary equipment for data acquisition (hardware and software) was part of the diploma project of Christian Ellwein [Ellwein99, Ellwein00a]. After recording the data were stored on the hard disk as WAVE-files which are readable by MatLab. In total 576 WAVE-files with an average length of 20 seconds were recorded. The size of these raw data was 977.2 MByte. Both events, switching on and off were recorded but for the following steps in signal processing and classification only the switching off events when the elastomer seal gets in contact with the metal seat were used. Both vibration patterns were used for classification but the results for the signals generated by de-energising the solenoid led to significant lower misclassification rates and thus these patterns were used. This is also reasonable because the seal is intensively affected by many faults and due to this the switching event contacting the seal is expected to contain more discriminative power.

5.4 Experimental setup

5.4.1 Environmental conditions

The applications and different environmental conditions where observed solenoid valves are used to vary in many parameters. Depending on the final application temperature, pressure of the medium applied to the valve, switching frequency, supply voltage and orientation of the valve (mounting position and direction) can be different. All these parameters influence the vibration patterns of switching valves. Hence, all important working conditions were changed during the different measurements of the

vibration signal to train the classifier with patterns covering all important statistical variations.

Table 5-2: Experimental setup

Parameter	Range	Comments
Temperature	**25°C / 40°C / 60°C**	**max. ambient temperature: 55°C (Bürkert data sheet)**
Supply voltage	**21V / 24V / 27V**	**nominal voltage was 24V**
Applied pressure (compressed air)	**0bar / 5bar / 10bar**	**max. pressure: 12bar (Bürkert data sheet)**
Switching frequency	**Swept from 0.2Hz to 10Hz and back to 0.2Hz**	**max. switching frequency: 16Hz (Bürkert data sheet)**
Orientation of the valve	**The vibrations were recorded in all typical mounting directions of the valve.**	**There are three typical orientations: bottom up and down and horizontal (90° angle)**

Each measured vibration pattern p of a switching valve can be seen as a function of different parameters:

$$p=\mathrm{f}(V,T,f,p,o,c)$$

with

V: voltage applied to the coil

T: ambient temperature

f: switching frequency

p: pressure of the medium

o: orientation of the valve

c: condition of the valve (unfaulty or one or more faults)

It is necessary to suppress the suppress the influence of all other parameters on the classification except of *c*, the condition of the valve. This is done by varying all other parameters in the typical range during the measurements.

In this project 10 unfaulty valves and 64 faulty valves were used. Two independent sets were build for training and testing the classification system, respectively. The valves applied in the test set were not used in the training set. Hence, the classification system was tested with completely new data. In Table 5-3 the numbers of switching events recorded for each set are shown.

Table 5-3: Number of recorded switching events

	unfaulty	faulty
training set	**480**	**848**
test set	**156**	**1969**

In Figure 5-23 a set of six switching-off events were shown. All the vibration patterns in this Figure belong to the same class – they are all gathered from unfaulty valves. Nevertheless, it can be seen easily by visual inspection that there are important differences between the signals. They are recorded from six different valves and under different environmental conditions as mentioned above. This Figure shows the need of sophisticated signal processing techniques which take the within-class scatter into account. This is accomplished by the new Spectral Analysis Matrix presented later in chapter 8. In Figure 5-24 similar graphs of faulty valves are shown. In both Figures the abscissa of the graphs of unit *time* and scaled in seconds. The ordinate is the measured acceleration at the cable plug and the data are normalised to range [-1;1]. The graphs are unlabeled in both Figures to reduce redundant text in the Figures.

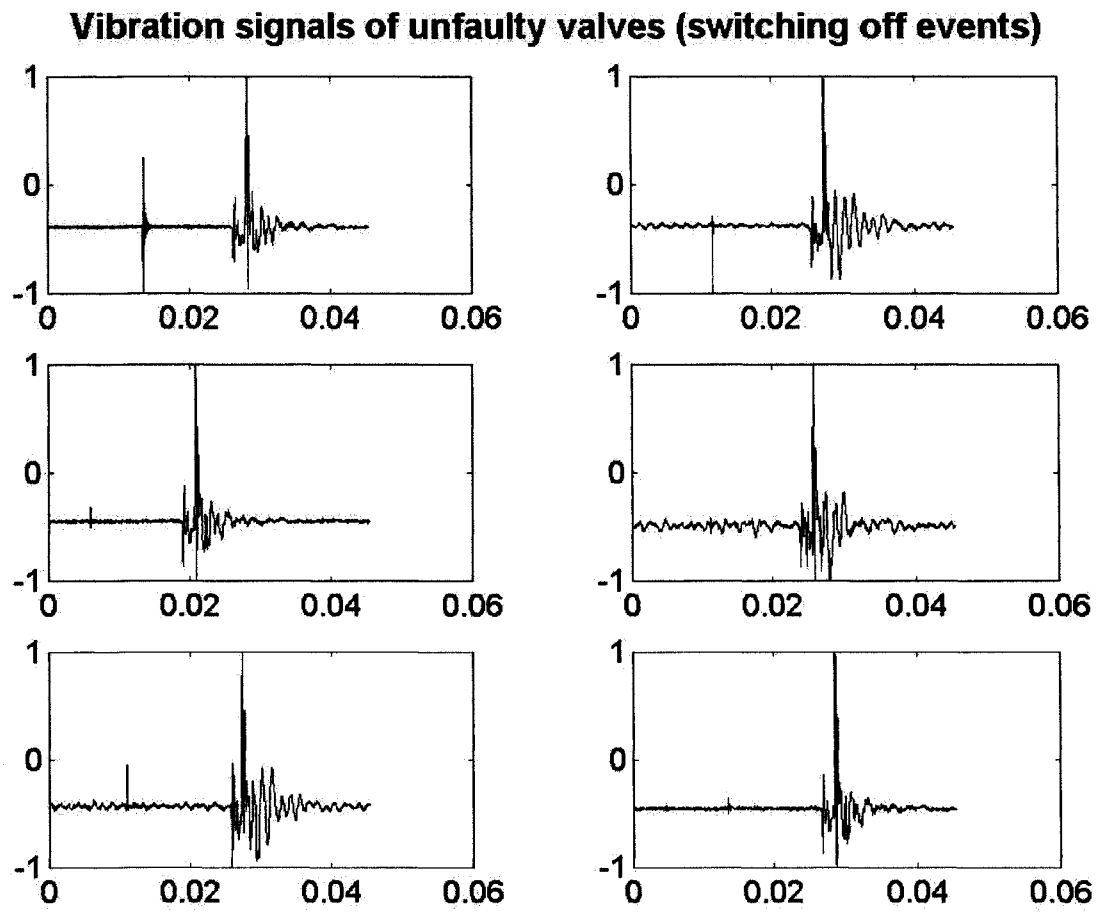

Figure 5-23 Vibration patterns of different unfaulty valves

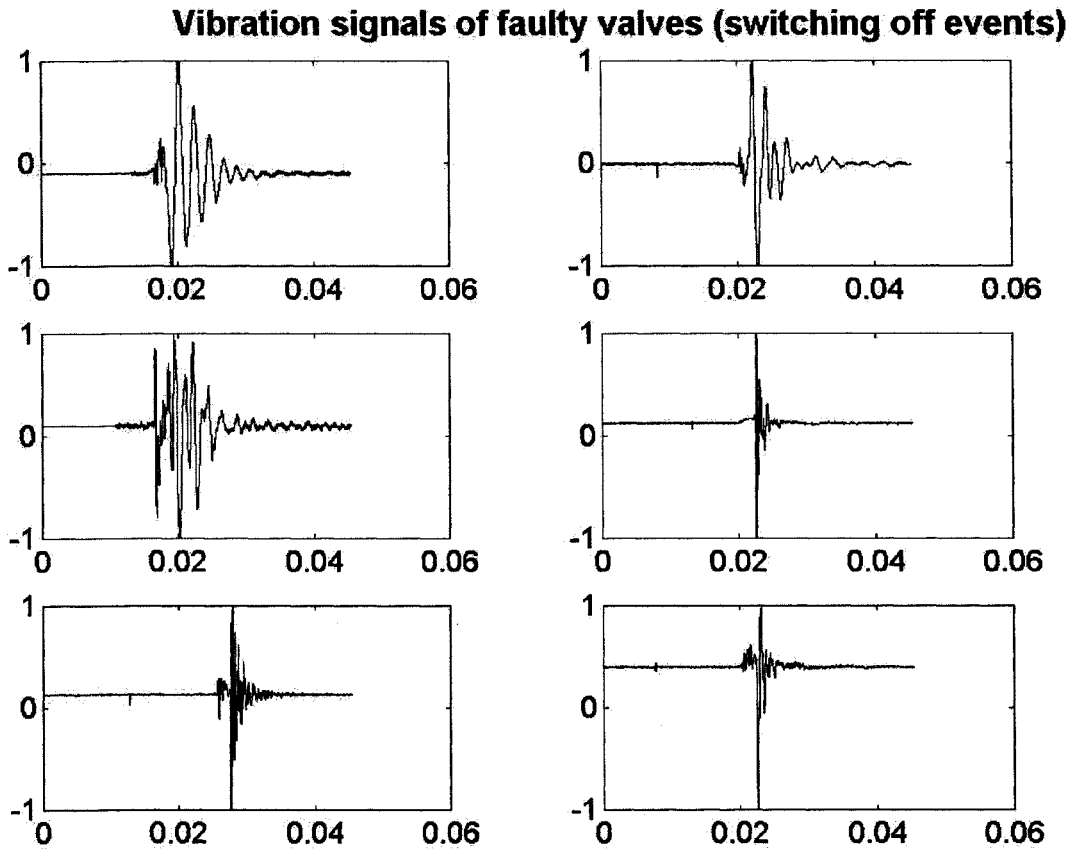

Figure 5-24 Vibration patterns of different faulty valves

5.4.2 Multiple faulty devices

In the test set the faults mentioned in Table 2-1 were not only implemented as single faults but also as devices with multiple faults. Fault 5 (waste in the valve) was combined with fault 1 (harden of the seal) and with fault 4 (indentation in the seal). The results of classifying these devices with multiple failures are presented in chapter 9 and give confidence that a combination of more than one fault in a device is not increasing the misclassification rate.

5.4.3 Deterioration of the measurements

In "real-world" applications usually some other sources of vibration will be near the monitored valves. To estimate the influence of typical deterioration an additional noise-signal was recorded in the endurance test room of Bürkert. In this room many valves and cylinders are switching permanently to test the lifetime and reliability of devices. Hence in this room many vibration sources are grouped together which can affect the classification (Figure 5-25). The same sensor was used to measure both, the vibration pattern of the monitored switching valves and also the background noise in the endurance test room. In this room the sensor was mounted at the compressed air pipe which was supplying the endurance tests. This situation is expected to be similar to many applications of solenoid valves were the valves are connected to a fluidic system together with other devices.

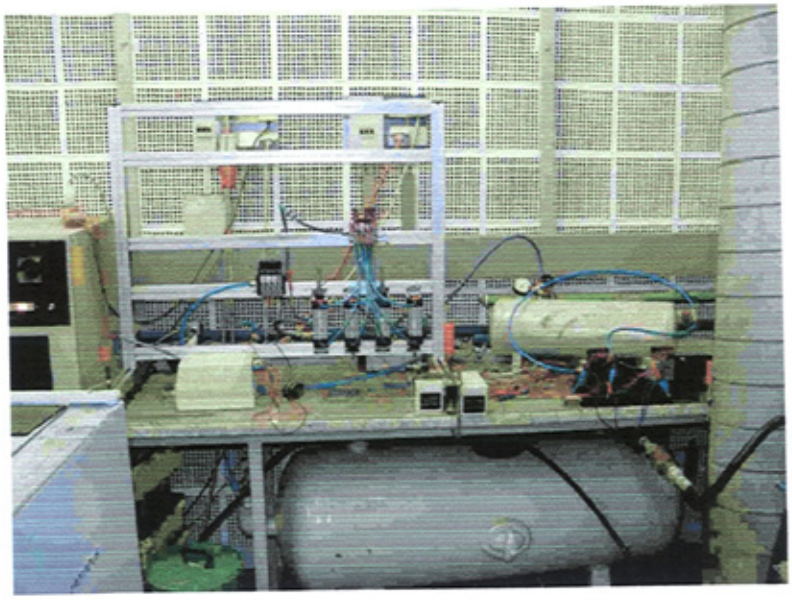

Figure 5-25 Endurance test room of Bürkert

When an observed vibration pattern from the device under test is processed and classified a randomly chosen part of the noise signal was added to the signal of interest (see Figure 5-26).

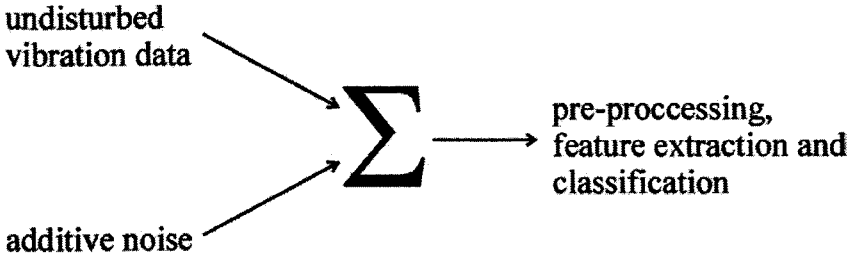

Figure 5-26 Vibration pattern and additive noise

Adding both sources is only reliable and correct if the sensor is a linear system which obeys the principle of superposition. The ADXL105 sensor is linear up to approximately 7kHz if the transducer was soldered and glued. It was seen in first estimations of the vibration signals spectrum with the periodogram-algorithm (Welsh's method) that most of the signals spectral power (about 87%) were bound in a frequency band up to 7kHz. Thus this superposition technique of both sources was expected to give a reasonable estimation of the effect of deterioration.

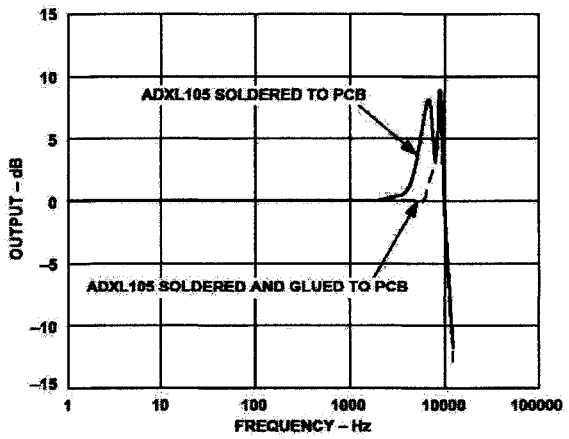

Figure 5-27 Frequency response of the ADXL105

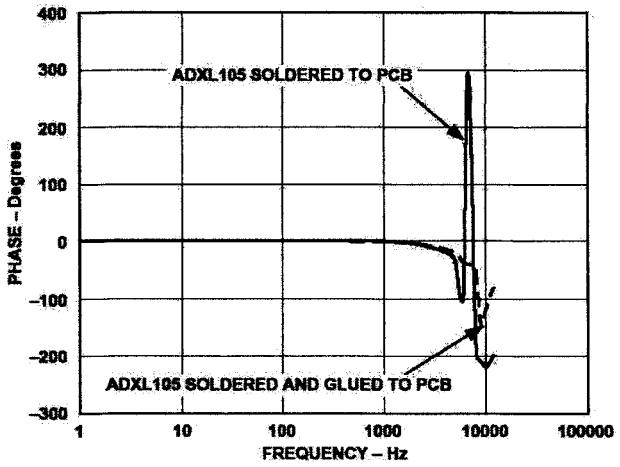

Figure 5-28 Phase response of the ADXL105

This approach of recording the vibration pattern of the device under test without significant ambient sources and to combine this undisturbed signal with separately recorded noise has one important advantage: for the assessment if a certain environment or application is affecting the classification too much or not it is possible to gather some data from the final application or location and to combine this signal with the test data set. It is possible by this means to re-evaluate rather easily whether the classification result still satisfies the needs of each individual final application.

5.5 Conclusions

The selection of an appropriate sensor is very important for the classification result. It was seen that an accelerometer is a suitable transducer gathering data with the ability to discriminate between faulty and unfaulty valves. Discussion of several parameters of the sensor led to the conclusion that the MEMS-accelerometer ADXL105 is appropriate within the most important properties. The mounting position of the sensor was also discussed in detail and the cable plug was found to be the best place. Finally, also the

experimental setup and the sampling of the measurement was presented. Much attention was given to cover the most important environmental conditions like ambient temperature, pressure and so on within the recorded data. After recording and storing the data the next steps were related to the field of digital signal processing and, as mentioned in section 4.3, the first step was to pre-process the raw data. This task is described in detail in the next chapter.

6 Preprocessing

6.1 Important properties of the vibration patterns

A typical vibration pattern of a switching solenoid valve is shown in Figure 6-1. There are two important properties of these signals which determine necessary preprocessing steps and which are discussed in this section. The rest of this chapter is organised as follows to explain these preprocessing steps: first, the stationarity of the signal is taken into account in section 6.1.1 and the second property of the signals which has to be processed is the influence of the electromagnetic interference (EMI) which is described in section 6.1.2. The chapter ends with some conclusions in section 6.2.

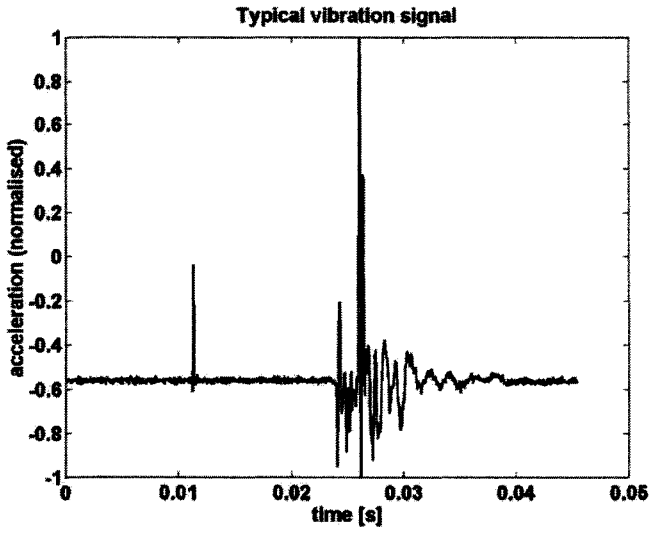

Figure 6-1 Typical vibration pattern

6.1.1 Stationarity

First of all, the stationarity is to be tested. Stationarity is an important property of signals which is necessary for many algorithms in the field of digital signal processing. A random process is called stationary if its statistical properties are time-invariant [Hänsler97]. If only the first and second order moments of a random process are time-invariant the process is called to be *weakly stationary*. If the higher order moments are also time-invariant the process is *strongly stationary* [Hänsler97]. The importance of stationarity is due to the fact that many algorithms and techniques used in the field of digital signal processing are restricted largely to the measurement and analysis of stationary (random) data [Bendat86, Lehmann97, Ellwein01a]. To increase the degree of stationarity it is a common approach to segment a signal into smaller sub-sequences with more stationary than the overall signal. Each of these segments can now be processed individually [Appel83, Niemann90]. A new segmentation approach to isolate more stationary segments in the signal was developed in this project and is presented in chapter 7. This technique segments the signal in the time-domain and the frequency-domain and derives the borders of the segments from the signal itself without a-priori knowledge or assumptions about the process.

6.1.2 Electromagnetic Interference (EMI)

A typical coil of a miniature solenoid valve has an inductance of some ten millihenry. In some applications a reverse voltage protection such as a freewheeling diode or a varistor reduces the distortion produced by the switched inductive load. The protection cannot be guaranteed and thus the worst case of a switching valve without any protection has to be taken into account when the influence of EMI is measured. This is especially important because a capacitive sensor was used which are known to be sensitive to EMI

[Zimmermann95]. To investigate the influence of EMI a modified valve without the movable part (plunger) and the spring was assembled. This valve could not generate any mechanical vibration during operation and thus the output of the accelerometer was gained only be the electromagnetic impulse. In the output signal of the sensor is shown in Figure 6-2. It can be seen that the sensor is reasonable influenced and this disturbance has to be taken into account.

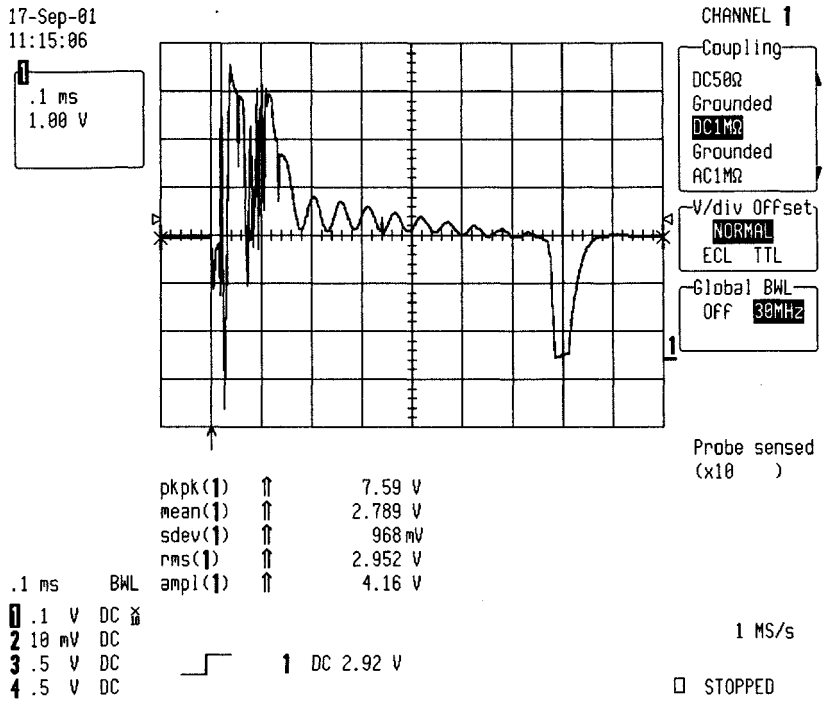

Figure 6-2: EMI response of the ADXL105

In Figure 6-3 the electromagnetic impulses are shown in combination with the electrical current and the mechanical vibration. These switching events are recorded with a varistor parallel to the coil, thus the impulses are different to Figure 6-2. It can be seen that the excitation of the sensor due to the EMI is earlier than the mechanical vibration. This is reasonable because the electrical and magnetical processes in the valve are much faster than the mechanical operation (accelerating the plunger, the movement and the

impact). This time gap between both impulses led to the decision to separate both patterns by a rectangular window as shown in Figure 6-5 [Ellwein01c]. The different operations inside the valve during a switching process are explained in more detail with Figure 6-4 and the corresponding text below.

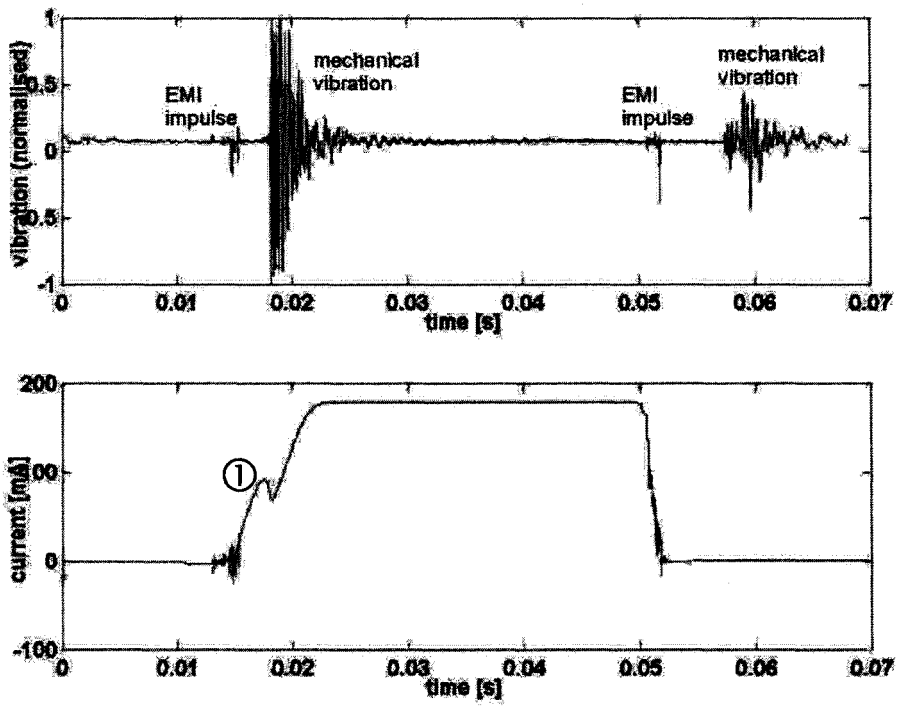

Figure 6-3: EMI with electrical current

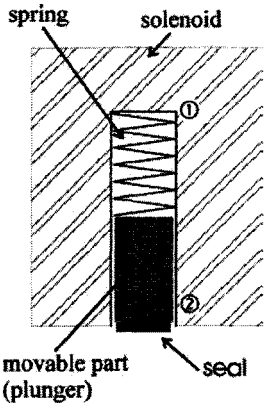

Figure 6-4 Technical drawing of plunger, spring and solenoid

In Figure 6-4 a technical drawing of the interior of a solenoid valve is shown: the solenoid surrounds the spring and the plunger. In Figure 6-4 the switched off valve is shown: the plunger is moved down to the second stable position (②) and the elastomer seal is closing the seat and the fluid channel in the valve. If the voltage is switched on and a current begins to flow through the coil and it has a exponential shape (see also section 7.3.2). When the plunger starts to move upwards driven by the magnetic force the inductance L of the solenoid circuitry is increased because the plunger is made of ferromagnetic material and its permeability μ_R is many times higher than the μ_0 of the air in the gap. Because of this the impedance Z of the coil is also rising and the current through the coil is reduced. When the movements of the plunger ends and the first stable position in the valve is reached (① in Figure 6-4) the inductance is again time-independent and the electrical current is rising again in an exponential shape to a finite value. These effects cause the typical M-shape of the electrical current in a solenoid valve shown at position ① in Figure 6-3 and often cited in literature [Kryter90; Blakeman97].

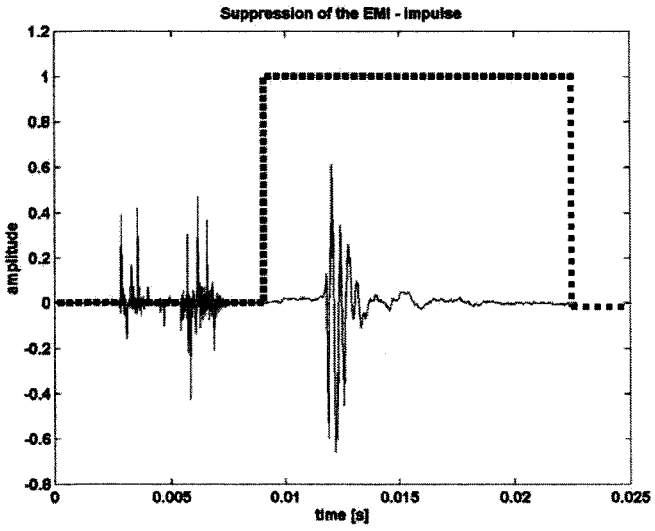

Figure 6-5: Suppression of the EMI-impulse

6.2 Conclusions

Both properties of the recorded pattern (nonstationarity and the EMI influence) make it necessary to preprocess the raw data. The EMI impulse was seen to be identified and suppressed easily as described above. The topic of nonstationarity is more difficult and more effort was spent to this task. Due to this interesting information was gathered about the signal and a new segmentation in the time- and frequency-domain was developed. This technique is considered to be of sufficient importance to merit its own chapter, which now follows.

7 Time-frequency segmentation

7.1 Introduction

An important and often performed step to emphasise hidden features with high discriminative power in a signal is to transform the signal from the time-domain into the frequency-domain. The Fourier-Transform (FT) is the most important technique for this step. Unfortunately, if the FT is applied to non-stationary signals the resulting spectrum will be an average over the occurring frequencies [Trethewey00, Ellwein01a, Bäni02]. To overcome this situation and similarly to transform non-stationary signals like speech, biomedical signals or transient impulses from switching valves time-frequency distributions (TFD) have been developed. These distributions isolate small segments in the time-signal and transform it by suitable means. The following section gives further details about this topic. Additional information can be found in literature [Chui92, Newland93, Rao98]. The rest of this chapter is organised as follows: in the next section 7.2 two very important distributions in the time-frequency-plane are presented: the Wavelet- and the Short-Time-Fourier-Transform. Because of some drawbacks of these techniques for the certain situation of this project a new segmentation technique is presented: the Source Based Segmentation (SBS) [Ellwein00b, Ellwein01a, Ellwein02b]. This method is explained in detail in the following sections 7.3 and 7.4. Afterwards the effect of this technique on the stationarity of the vibration signal is presented in section 7.5. The advantages of the new algorithm are summarised and explained in section 7.7 and finally the most important results of this chapter are reviewed in some conclusions in section 7.8.

7.2 Time-frequency distributions

This approach is to divide the overall non-stationary signal into short sequences, each with a higher degree of stationarity. It is often seen that the statistical parameters of the process vary rather slowly in time as compared to the frequency range of the sample functions themselves. For example, speech signals are mainly bound to a frequency band between 300Hz and 4kHz. It was seen that the stationarity of sequences with short duration (approximately 10ms) is substantially higher than the stationarity of the overall signal [Niemann90]. Generally, segmentation of speech signals is a complex topic and for detailed information it is referred to literature.

Segmentation into sub-series of the overall signal is also performed by estimation of time-frequency-distributions (TFD) of the data. There are several algorithms known to estimate TFDs, but two important ones are be the Short-Time-Fourier-Transform (STFT) and the Wavelet-Transform (WT). The STFT is a time-dependent version of the Fourier-Transform and the observed signal $x(t)$ is weighted with a window-function $w(t)$ which is vanishing at its ends and has a finite duration. The drawback of the STFT is that widths of the window is constant and its choice simultaneously affects both the frequency and time resolution: the window length has to be high for a good frequency resolution but on the other hand, the time resolution is worsened by a large window [Conforto99]. In Figure 7-1 the time-frequency-plane spanned by the STFT is shown.

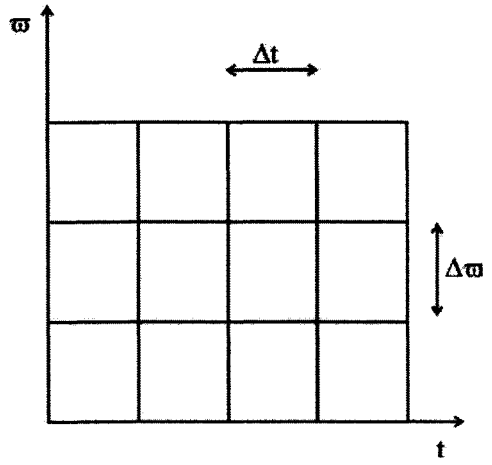

Figure 7-1 Time-Frequency plane of the STFT

The WT overcomes this drawback by using transient basis functions $\psi(t)$, so called wavelets, instead of the sinoids used in FT. The wavelets are square integrable and have finite energy. Because of their limited existence in time the WT "focuses" on sub-segments of the data signal $x(t)$. By means of dilatation (factor a in Figure 7-2) and translation a time-frequency-plane as shown in Figure 7-2 is analysed. An detailed introduction into WT is given in literature, for example [Chui92, Flandrin99].

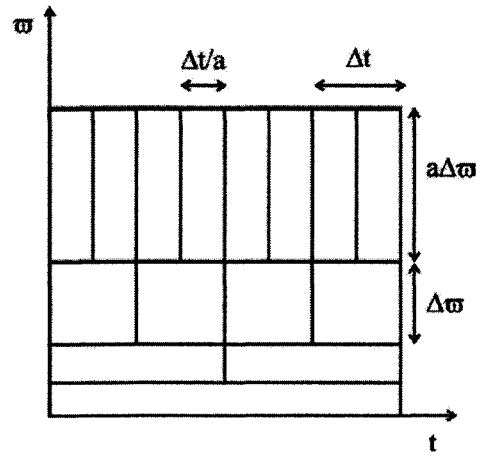

Figure 7-2 Time-Frequency plane of the WT

A new approach, the Source Based Segmentation (SBS), for segmenting a non-stationary signal is now presented for the vibration signals of solenoid valves [Ellwein02b]. The segmentation is based on isolation of different sources during the switching process. The vibration sub-patterns caused by these sources are more stationary than the overall vibration signal because each source has a certain statistical character. The individual degrees of stationarity for each source are higher than the overall degree of a mixture of these sources. This situation is not limited to the vibration pattern of solenoid valves but it is anticipated that this property can be found in many other reciprocating processes.

7.3 Segmentation in the time-domain

7.3.1 Mechanical processes during valve switching

An ON/OFF-valve switches between two stable positions when activated or deactivated. During the switching-on or switching-off process four different sub-processes happen and according to this also four different sources of vibration become active consecutively. The different steps of the switching event are distinct mechanical actions and they are explained in detail now.

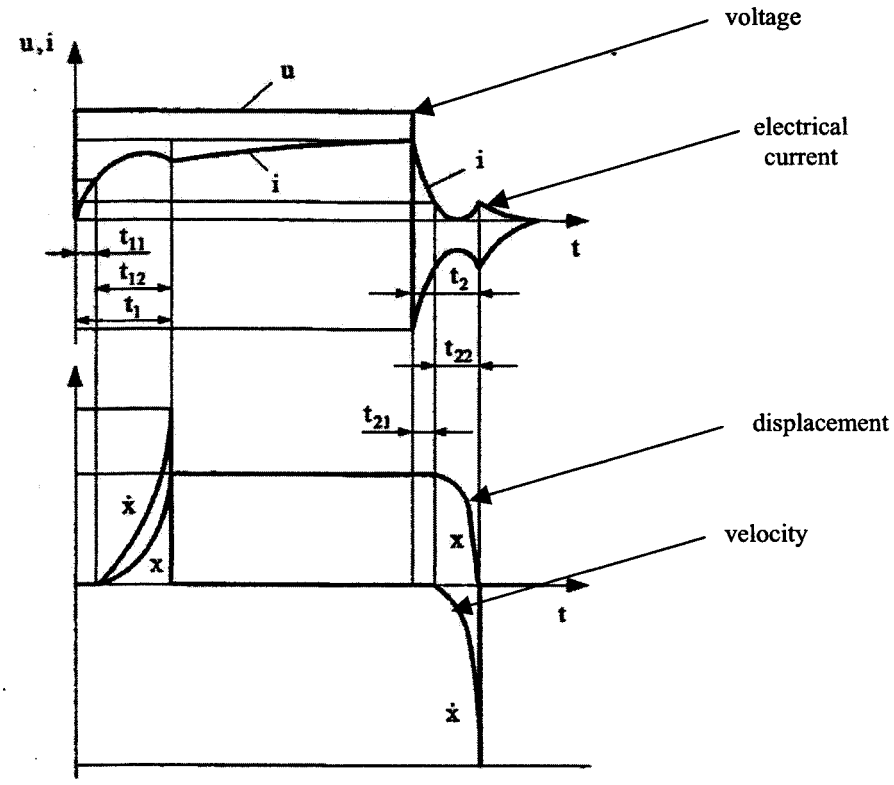

Figure 7-3 Switching-on and –off process of a solenoid valve

In Figure 7-3 the dynamic behaviour of a switching solenoid valve is shown [Kallenbach00]. Further details about the shape of the curves are given in section 6.1.2. The four curves are:

- *u*: the voltage applied to the solenoid coil. The valve is connected to a stable voltage source and thus the amplitude of the voltage switches between two distinct values. The negative peek at switching off is the reverse voltage of the inductance.
- *i*: the electrical current is dependent on the voltage *u*, the ohmic resistance *R* and the inductance *L* of the magnetic circuit. Because of the moving part of the valve being part of the magnetic circuit the inductance is time-dependent

and the shape of the electrical current has its characteristic shape [Blakeman97] (see also section 6.1.2 for further details).

- x: the displacement of the movable part in the valve is switched between two distinct positions (valve opened or closed).
- $\dot{x}$: the velocity is the derivative of x and it has peaks when the movable part hits its stable positions.
- t_1: switching-on time
- t_{11} and t_{21}: response times
- t_{12} and t_{22}: travelling times
- t_2: switching-off time

The absolute velocity has its maxima at the ends of both switching processes. Simultaneously the deviation of the electrical current has a second change in the sign.

Between two switching events there is usually a duration of minimum several hundred milliseconds. Due to this the movable part in the valve can get into static friction because the process of adhesion needs a certain amount of time for the reaction. If the level of the electrical voltage is switched four discrete steps happen during the switching process (Table 7-1). These steps influence also the vibration pattern because during each step a different source of vibration is generating vibrations. Thus the overall vibration signal can be partitioned into four segments which correspond to the mechanical processes. The time-diagram in Figure 7-4 shows the segments proposed in Table 7-1 in a graphical representation. In Figure 7-4 the energization, the escapement of the armature and binary operating cycle (valve open or closed) are shown in a

diagram schematically. When the device is energised (that is the voltage is applied to the coil), the response time gives the duration until the movable part starts movement. When the movement is starting the movable part is changing from static friction to sliding friction and the movable part accelerates. During the travelling time the movable part is altering velocity and displacement. This process is stopped when the movable part in the device hits the second stable position and the impact happens. The impact is significantly influenced by the material of the movable part and the second stable position in the device and the elasticity of the movable part. Further, it is common for the switching events, that the impact induces the whole device to vibrate and the energy of this vibration is decaying. Also most of the devices bounce after the first impact. That is, the movable part lifts from the stable position and reimpacts after a short duration. The time for all bounce to cease is called the operational bounce time.

Table 7-1 Different Segments in the vibration pattern

No	Section	Interpretation / included Information
1	**Lifting**	**This is the segment when the movable part changes from static to sliding friction.**
2	**Pre-impact**	**After this change to sliding friction the movable part in the valve is accelerated and moving to the second stable position. The vibration in this segment is influenced by friction during the motion. The length of this segment is determined by the travelling time of the movable part.**
3	**Impact**	**When the impact happens the velocity of the movable part has its maximum and is decreased rapidly. The vibration pattern in this segments is governed by the energy of the impact and the condition of the movable part.**
4	**Post-impact**	**After the impact the whole valve is excited by the hit. It is ringing at its natural frequencies. Due to this the condition of the whole vibrating device will influence this segment. Bouncing of the movable part in the device is also causing vibration and will be part of the vibration pattern in this segment.**

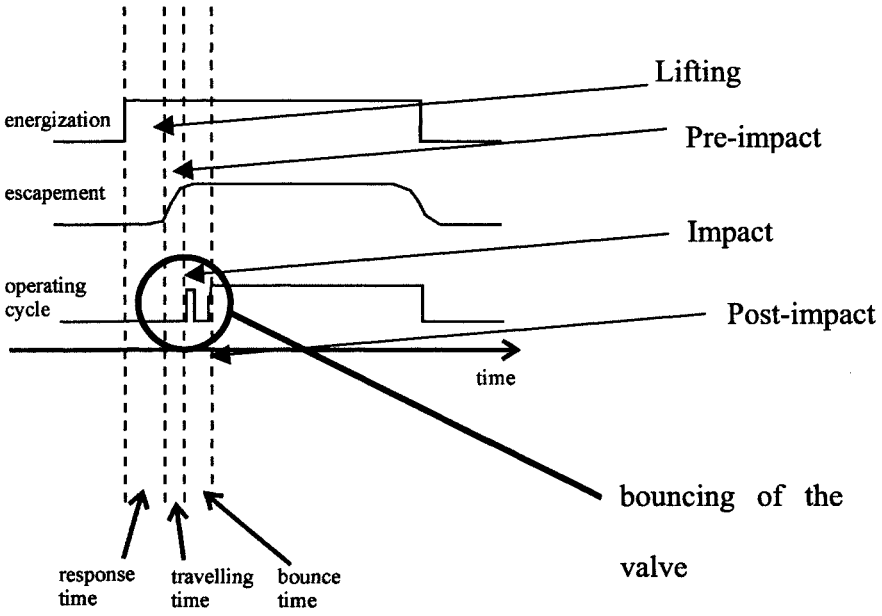

Figure 7-4 Temporal operation of a switching event

The four sources of vibration mentioned in Table 7-1 are different in nature and character. The different origins of the four sections cause the overall signal to be non-stationary and consequently it is not reasonable to analyse the entire signal as one large pattern. The sources are ordered consecutively in time and due to this it is possible to separate the different kinds of vibration by windowing the original signal with four different windows (i=1..4) and suppressing all but one source of vibration with each window.

The original signal has a highly non-stationary character because it is a combination of four different sources of vibration. The result of segmentation can be assessed by calculating the stationarity of each of the new segments.

7.3.2 Modified Hanning Window

Segmentation in the time-domain to improve the degree of stationarity for the measured vibration data is performed in this research project by a data derived technique which isolates the four different steps of operation during the switching process described above (Figure 7-4 and Table 7-1). To perform this segmentation a new window was proposed [Ellwein00, Ellwein01a] which is described in Equation (7-1).

$$W_i(t)=\begin{cases}0, & t \le b1_i \\ \frac{1}{2}\left[1-\cos\left(\frac{2\cdot\pi\cdot(t-b1_i)}{2\cdot b2_i}\right)\right] & b1_i < t \le b1_i+b2_i \\ 1, & b1_i+b2_i < t \le b1_i+b2_i+b3_i \\ \frac{1}{2}\left[1-\cos\left(\frac{2\cdot\pi\cdot(b1_i+b2_i+b3_i+b4_i-t)}{2\cdot b4_i}\right)\right], & b1_i+b2_i+b3_i < t \le b1_i+b2_i+b3_i+b4_i \\ 0, & b1_i+b2_i+b3_i+b4_i < t \le b1_i+b2_i+b3_i+b4_i+b5_i \end{cases} \quad (7\text{-}1)$$

Five sections (j=1..5) with arbitrary length ($b1_i..b5_i$) are used to describe the i^{th} window $W_i(t)$ (i=1..4). For sampled time signals with equidistant sampling intervals the parameters $b1_i$ - $b5_i$ are the number of data points for each section. The first section is a zero-valued part of length $b1_i$ and is used to suppress the part of the original time signal before the section of interest. The second part is a rising edge with Hanning characteristic [Oppenheim89]. The next part is the identity function to separate a section of the original time signal with an arbitrary length without perturbation. A decaying Hanning edge is the next section and at last the window equals zero again to suppress the right part of the original time signal. An example of a modified Hanning window was shown in Figure 7-5.

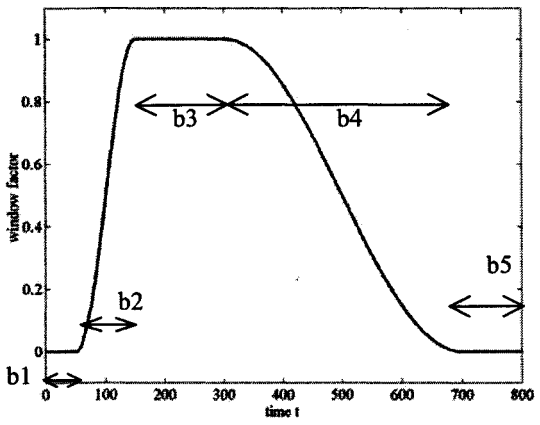

Figure 7-5 Example for a modified Hanning window

This new window has certain advantages over state of the art techniques: the four windows are not of equal length and shape as the windows usually used for time-frequency-distributions [Sun00] like the short-time Fourier transform (STFT) and the values for the b_{ji} can be computed from the envelope of the vibration signal. Both properties together give the possibility to

- isolate only the four interesting sources and not an arbitrary number of small segments which are in no correspondence with the sources of the overall signal as it is done with the STFT or Wavelet-Transform (WT).
- emphasise parts of the signal with a high amplitudes and higher signal-to-noise ratio (SNR). The noise of the data acquisition system can be assumed to be constant over the whole switching process. Because of the short time duration of the event (only some ten milliseconds) neither the internal noise of the sensor or the analog-digital converter nor the external noise of other disturbing vibration sources in vicinity to the monitored valve will change significantly. Hence, if the SNR is computed for

small segments of the overall vibration signal it will be highest around the impact where the maximum of vibration energy is found. The modified Hanning window enables a successive suppression of the decaying ends of the vibration signal which have a worse SNR and thus contain less reliable information for classification (see Figure 7-6).

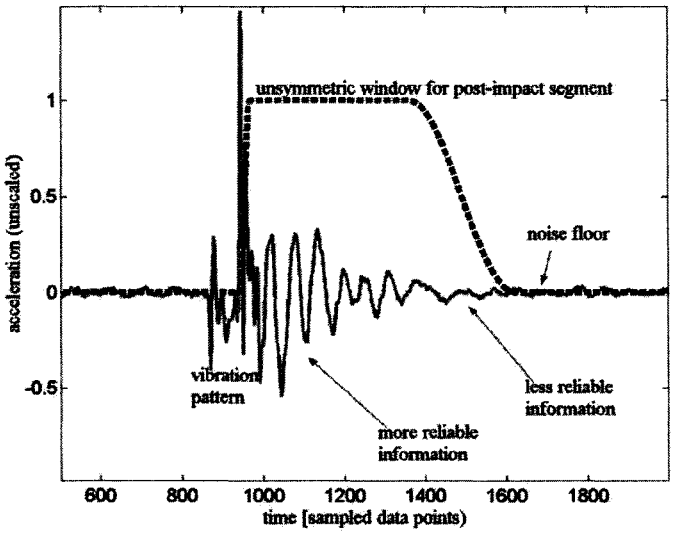

Figure 7-6 A modified Hanning window to isolate the post-impact signal

In Figure 7-7 the SNR of a typical vibration signal was computed over small segments of 50 data points (1.1ms).

$$SNR \ [dB] = 10 \cdot \log_{10} \frac{P_S}{P_N} \tag{7-2}$$

with

P_S : power of signal

P_N : power of noise

Because the signal itself is not accessible without noise an approximation was used to compute the SNR [Becker98]:

$$SNR\ [dB] \approx 10 \cdot \log_{10} \frac{P_S + P_N}{P_N} = 10 \cdot \log_{10} \left(\frac{P_S}{P_N} + 1 \right) \tag{7-3}$$

The vibration signal was displayed in the upper part of the Figure and the consecutive SNR values in the lower part. It can be seen, that the SNR is decreasing left and right hand of the impact. The aim of the modified Hanning window is to suppress less reliable parts of the vibration pattern and to emphasise segments of the vibration signal with high SNR.

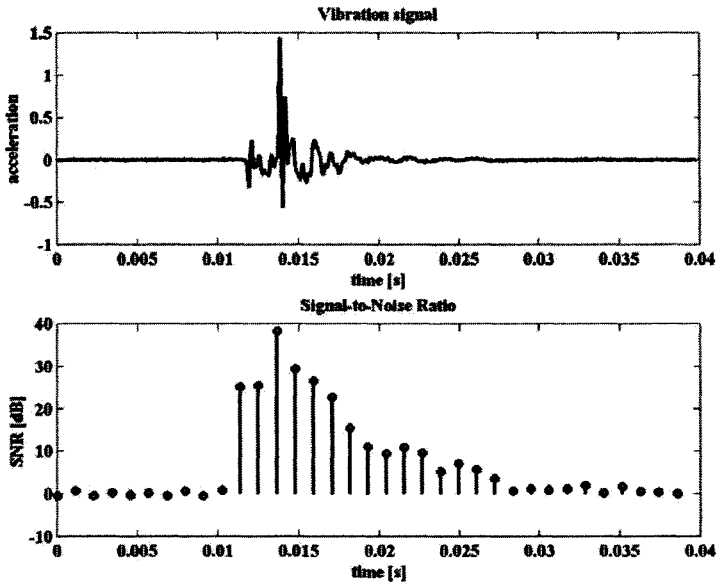

Figure 7-7 Time dependent SNR of a vibration signal

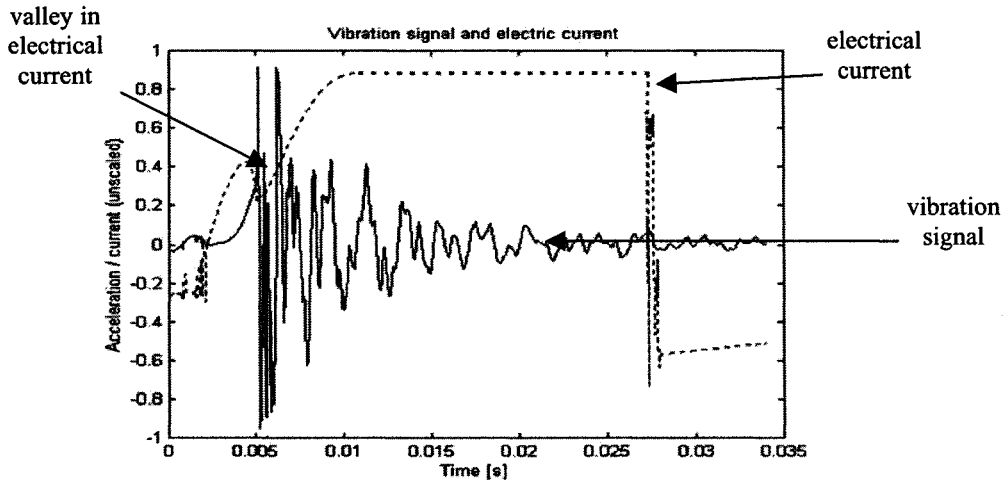

Figure 7-8 Vibration signal and electrical current

Table 7-2 Parameters for the modified Hanning window

	b1	b2	b3	b4	b5
Lifting	$\tau_i - 2.1 \cdot d_1$	$0.1 \cdot d_1$	d_1	d_1	$\dim(x) - (b1+b2+b3+b4)_{lifting}$
Pre-impact	$b_l+0.2 \cdot d_1$	$0.2 \cdot d_1$	$0.5 \cdot d_1$	$0.1 \cdot d_1$	$\dim(x) - (b1+b2+b3+b4)_{pre\text{-}impact}$
Impact	$\tau_i - \left(b2 - \frac{b3}{2}\right)_{impact}$	$0.05 \cdot d_1$	$0.05 \cdot (d_1 + d_2)$	$0.05 \cdot d_2$	$\dim(x) - (b1+b2+b3+b4)_{impact}$
Post-impact	$\tau_i - b2_{post\text{-}impact}$	$0.1 \cdot d_1$	$0.6 \cdot d_2$	$0.4 \cdot d_2$	$\dim(x) - (b1+b2+b3+b4)_{post\text{-}impact}$

with
τ_i : position of the impact
$d_1 = \tau - b_l$
$d_2 = b_r - \tau$

In Figure 7-9 and Table 7-2 the rules for adjusting the parameters *b1* to *b5* for the modified Hanning window are proposed. These settings are derived from the time-diagram of the switching process shown in Figure 7-4. The parameter *b3* is of capital importance for all four windows because it defines the part of the vibration signal which

influences the classification task most. *b3* is the length of the identity function in each modified Hanning window. Very important factors for definition of all parameters *b1* to *b5* are d_1 and d_2 which represent the duration of the vibration impulse left- and right-hand from the impact itself (see Figure 7-9). These factors d_1 and d_2 are determined by the time point of the impact τ_i and the left and right border of the transient vibration signal b_r and b_l. The impact of the movable part in the valve can be detected straightforward: it is indicated by the maximum absolute value in the vibration pattern. In Figure 7-8 a typical vibration signal (solid line) is shown together with the electric current (dashed line). The maximum of the vibration signal occurs when then current has a valley. It is verified that at this point the movement of the plunger in the valve stops and the impact happens. The shape of the current is determined by the closing of the magnetic circuit [Kryter90; Blakeman97]. If the air gap in the magnetic circuit is closed the inductance of the solenoid increases and so does also the impedance which causes the valley in the electrical current.

After closing the air gap the electrical current rises in an exponential way governed only by the self-induction voltage of the coil and time constant τ [Beuth88]:

$$\tau = \frac{L}{R} \tag{7-4}$$

where

L is the inductance of the coil

R is its ohmic resistance

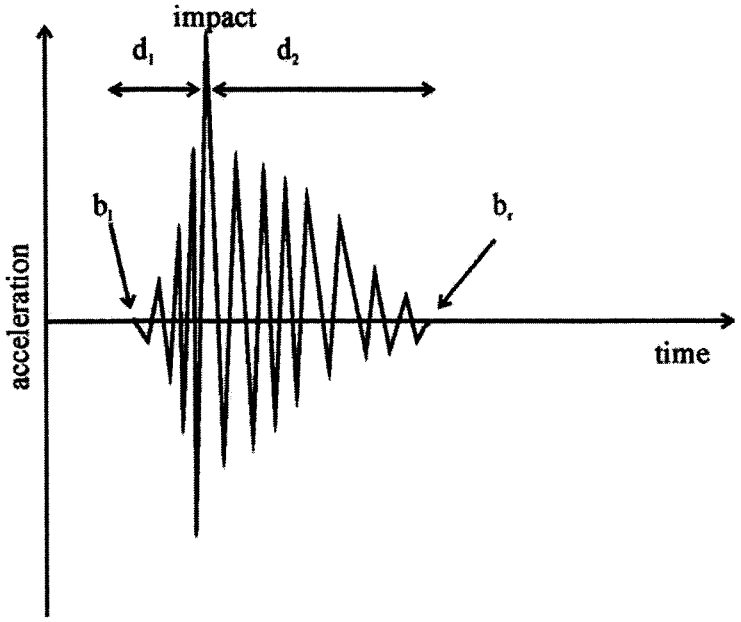

Figure 7-9 Factors *d1* and *d2* in an idealised vibration pattern

7.3.3 Application to different valves

The following Figures show that the proposed segmentation algorithm is adaptable to different sources (= valves) and patterns (= vibration signals). The time sequences are recorded from three different valves shown in Figure 7-13. In Figure 7-10 a vibration signal from the smallest of the three valves is shown together with the four windows. This valve 6011 was also used mainly during this project. The vibration signal of valve 6013 is shown in Figure 7-11 and valve 290 is presented in Figure 7-12. The last valve 290 is not only scaled version of the above mentioned types but it has a different mechanical design as shown in Figure 7-13.

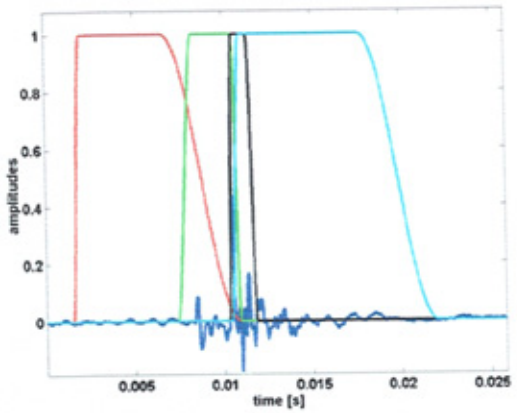

Figure 7-10 Segmentation of vibration signal from valve 6011

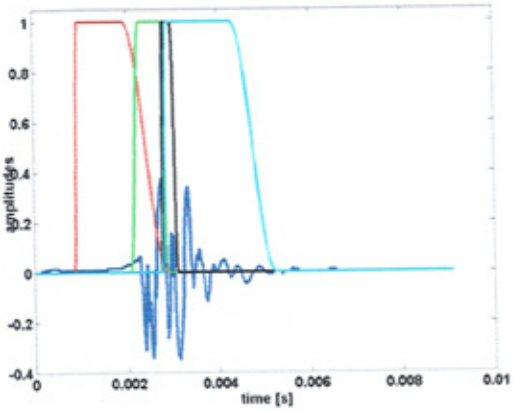

Figure 7-11 Segmentation of vibration signal from valve 6013

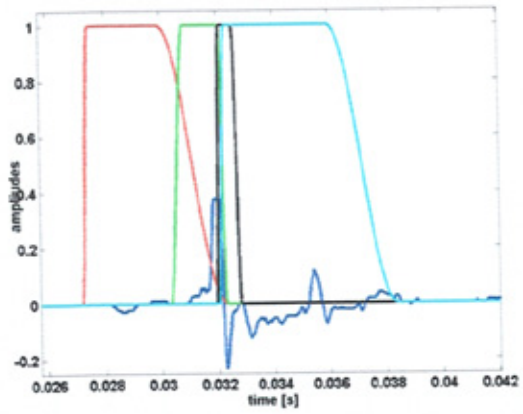

Figure 7-12 Segmentation of vibration signal from valve 290

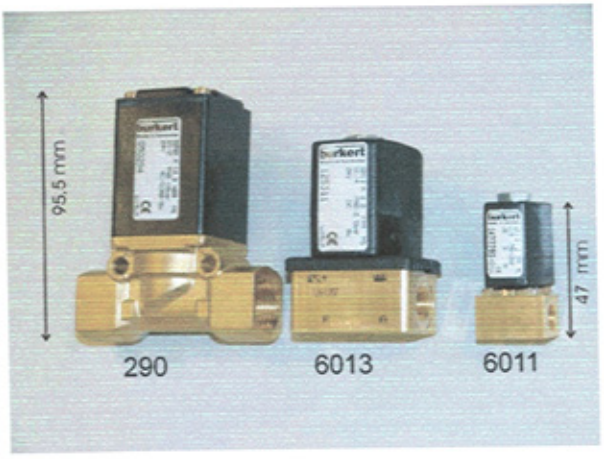

Figure 7-13 Three different solenoid valves

7.4 Segmentation in the frequency-domain

Motion of fluids cause random vibrations when the fluid encounters a throttling object (e.g. the seat of a valve) and creates downstream vortices. Mechanical friction also generates random vibration. On the other hand, if a mechanical structure is hit with a solid object (e.g. a hammer) it will ring at its natural frequencies and a superposition of individually damped sinusoids will be obtained. The resulting vibrations of such shock pulses are repetitive , but they die away due to damping [Wowk91]. Both sources can occur in a valve because the impact of the movable part is a similar excitation as a hit with a hammer and both, mechanical friction and fluid movement occur in a valve. For

a separation between both sources it is therefore necessary to isolated a damped repetitive process and a random process. A periodic process will be found in the frequency-domain as one or more peeks. A random process, on the other hand, has a more or less flat shape in the spectrum. Hence, a straightforward separation is to identify the main peek in the spectrum. This was done in this project and the frequency corresponding to the maximum amplitude of the FFT of a sub-sequence (see section 7.3) was used as bandwidth of two FIR-filters. The filters are a lowpass and a high-pass and both sources are separated by these filters. The following Figures show the effect of this processing step and validate the different character of both sources. In Figure 7-14 a typical unfiltered vibration signal of a valve switching event is shown. It can be assumed by visual inspection that there is a damped lower frequency part and a higher frequency noise signal.

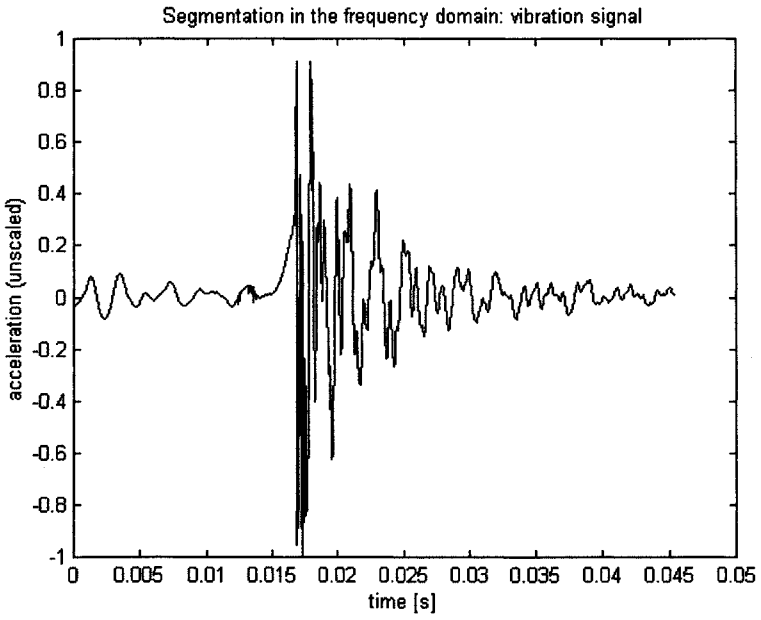

Figure 7-14 Unfiltered switching event

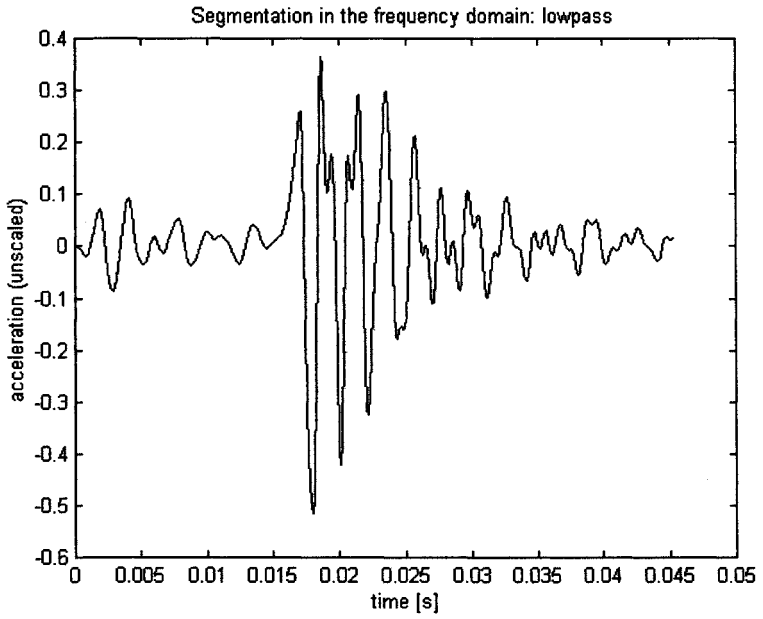

Figure 7-15 Low-frequency part of the vibration signal

The low-frequency part is isolated and presented in Figure 7-15 and the high-frequency segment is shown in Figure 7-16.

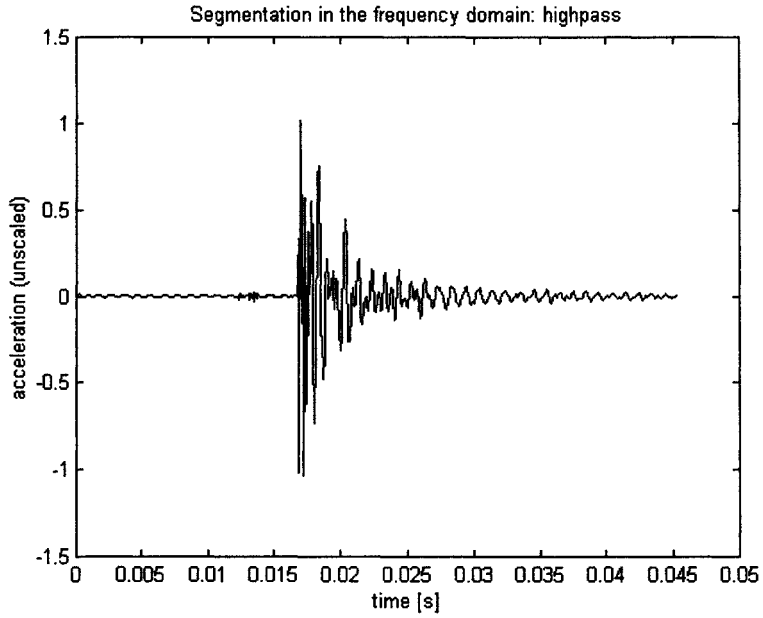

Figure 7-16 High-frequency part of the vibration signal

The different character of both segments with respect to their periodic or stochastic nature is validated by computing the autocorrelation sequence of both sub-sequences. A pure random signal has a single peek in the autocorrelation sequence at time-lag $\tau = 0$. On the other hand, the autocorrelation sequence of a periodic signal will be periodic with the same period as the original signal. Thus this test is suitable for identifying the different character of both sequences. Both autocorrelations are shown in Figure 7-17. The dashed graph is the autocorrelation sequence of the lower-frequency sequence and the solid line is the autocorrelation of the higher-frequency signal. It can be seen that the lower-frequent part in the vibration signal is more repetitive and less stochastic than the higher frequencies and thus both sub-sequences can be assumed to be generated by the different sources mentioned above.

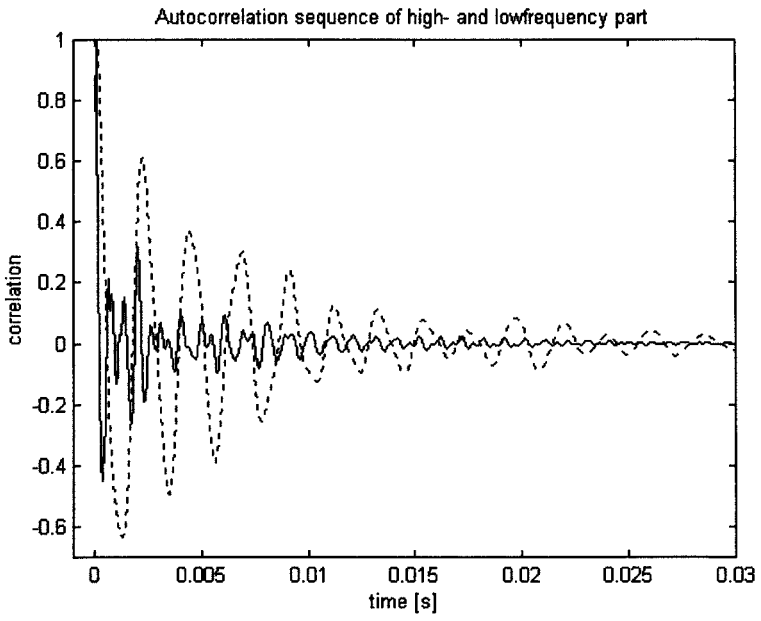

Figure 7-17 Autocorrelation functions of both sub-sequences

The time-frequency plane is segmented by the SBS as shown in Figure 7-18:

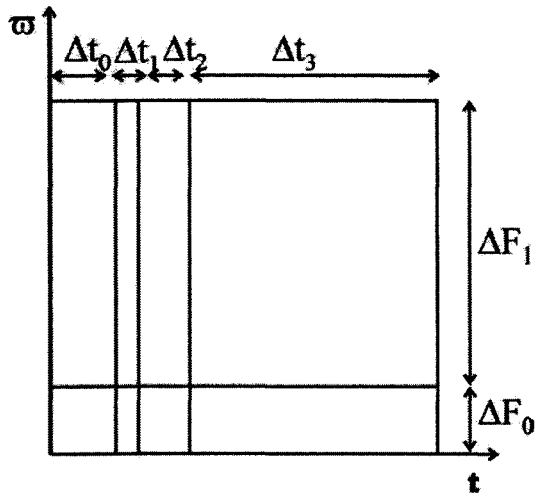

Figure 7-18 Segmentation by the SBS

Instead of the maximum of the FFT first a different approach based on the autocorrelation function of the measured data was investigated, the Muli-ACF method [Ellwein01b]. It was seen during the project that the results of both approaches were rather similar but the advantage of the FFT-method is that there is no need for a stop criterion as necessary in the Multi-ACF approach.

In Figure 7-19 the complete segmentation process is shown in a block diagram: at the left side the original measured signal is shown. This pattern is segmented into four sections in the time domain and each of these sections is divided into a high- and a low-frequency component. These eight segments are used for the further steps of feature extraction and classification.

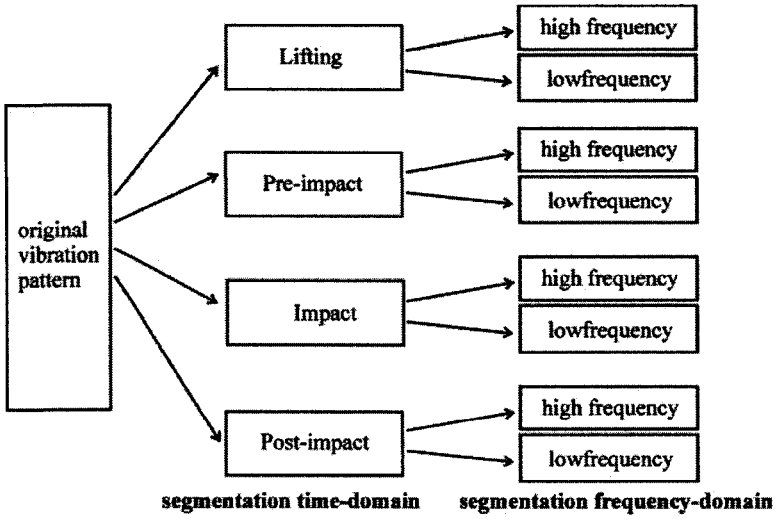

Figure 7-19 Segmentation of the Time-Frequency-Plane

7.5 Stationarity of the segments

The segmentation of the original transients in both time- and frequency-domain was performed to isolate sub-sequences with a higher degree of stationarity than the overall signal. The stationarity of the original signal and the segments was tested as described in [Bendat86]:

The tested data record is divided into N equal time intervals. The mean square value $\overline{x_i^2}$ (i=1...N) for each interval is computed and these sample values were aligned in time sequence, as follows: $\overline{x_1^2}, \overline{x_2^2}, \overline{x_3^2}, ..., \overline{x_N^2}$

The sequence of mean square values is tested for the presence of underlying trends or variations other than those due to expected sampling variations. This was done by means of the run-test.

The run-test formulates a null hypothesis H_0 that the tested data are distributed randomly and an alternative hypothesis H_1 that there is an underlying trend within the tested data. The analysed time sequence is transformed to a binary signal. One

possibility to do this is to compare each value with the mean of the sequence: the binary signal will become "1" if the current value is equal or higher than the mean of the sequence and it will become "0" else. So a 0-1-sequence of length N is obtained. A *run* is defined as a sequence of identical binary observations that is followed and preceded by a different observation or no observation at all:

$$\underbrace{1}_{1}\ \underbrace{1}_{2}\ \underbrace{0}_{3}\ \underbrace{1}_{4}\ \underbrace{0\ 0\ 0}_{5}\ \underbrace{1\ 1}_{6}\ \underbrace{0}_{7}\ \underbrace{1\ 1\ 1}_{8}\ \underbrace{0}$$

In this example there are $r = 8$ runs in the sequence of $N = 14$ observations. The number of runs in the binary sequence is an indicator if there is an underlying trend. There are tables available with the upper and lower limits for the number of runs for different lengths N and different levels of significance [Bendat86].

In the following Figures the results for a level of significance of $\alpha = 0{,}05$ are shown. The signal is stationary if the number of the runs lies within the borders of the run-test (solid lines in the Figures). These borders were derived from a table in [Bendat86] were the valid numbers of runs are compiled. The abscissa of the Figures represents the dimension of the different data vectors. That is the length of the sequences (original or segmented). It is obvious, that the original sequences consist of more data points and thus they are at the right side in the Figures and the shorter sub-sequences occur on the left side. At the ordinate of the Figures the number of runs are shown. Each Figure is segmented into three parts: two regions were non-stationary signals can be found and one corridor for the stationary sequences. As mentioned above a signal is expected to be stationary if the number of runs is between an upper and a lower limit which can be found in tables. These limits depend on the length of the tested sequence. Due to this the borders shown in the following Figure are a function of the dimension of the data

vectors. In each picture the results of a set of 135 switching events are shown. The unsegmented original signals are represented by the circles and the crosses represent the sub-segments. In each picture the unsegmented signals (circles) are compared with one of the eight sub-sequences proposed in Figure 7-19. Due to this the circles are identical in each of the following Figures and the crosses are different. Each circle or cross is the test of a certain switching event with or without segmentation. The segments are nearly stationary except the post-impact signal (Figure 7-24). But also the post-impact signal is more suitable for further processing because it contains mainly the influence of the ringing natural frequencies which are damped sinoids which makes it more deterministic than the overall signal. Thus the degree of stationarity was increased strongly by the segmentation in the frequency- and time-domain.

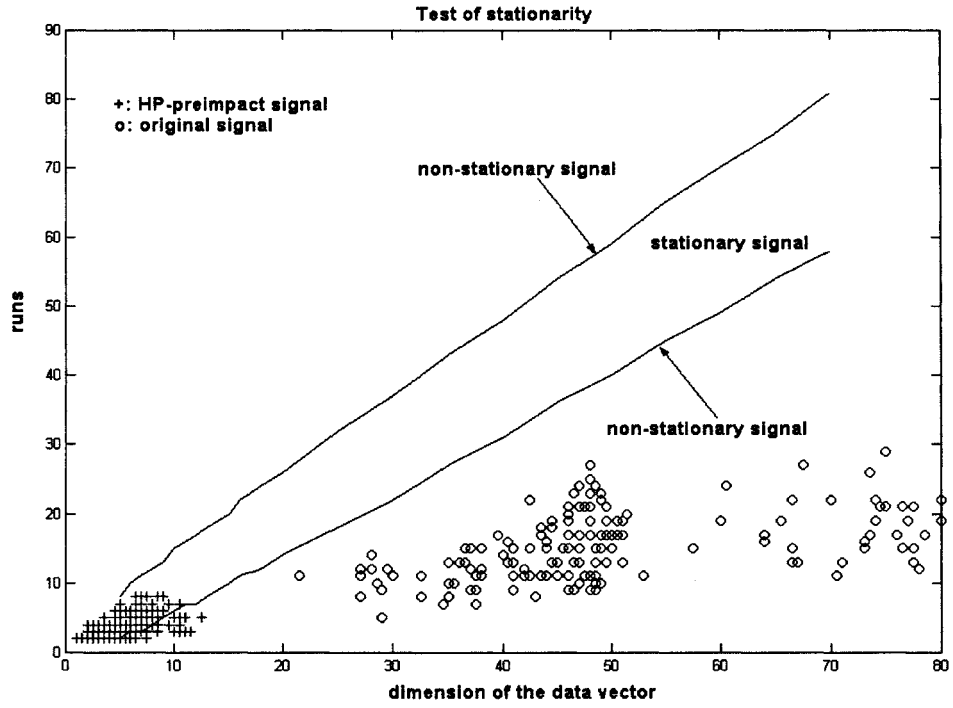

Figure 7-20 Stationarity of the high-pass pre-impact sub-sequence

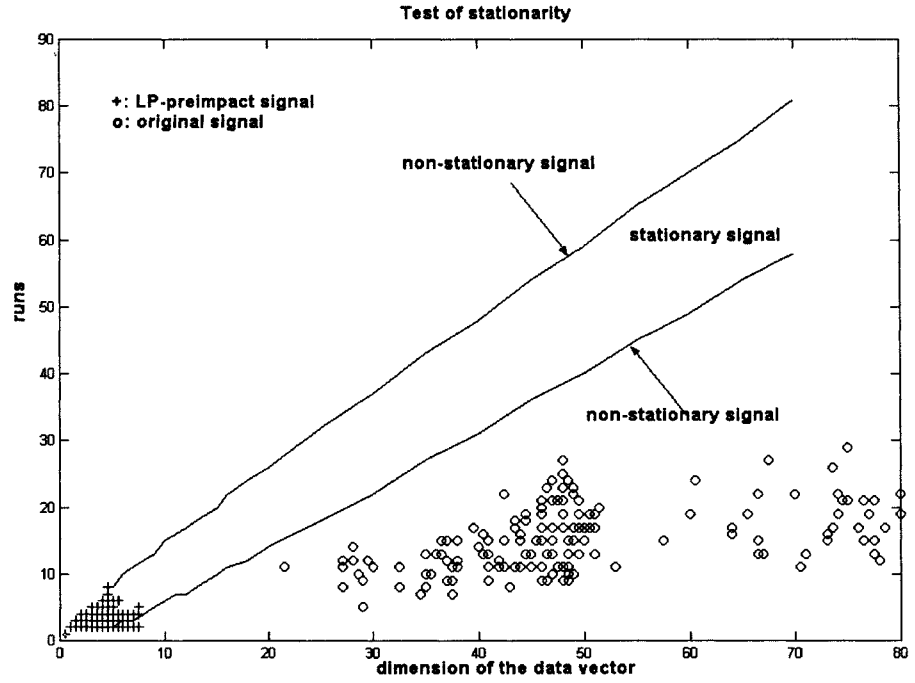

Figure 7-21 Stationarity of the low-pass pre-impact sub-sequence

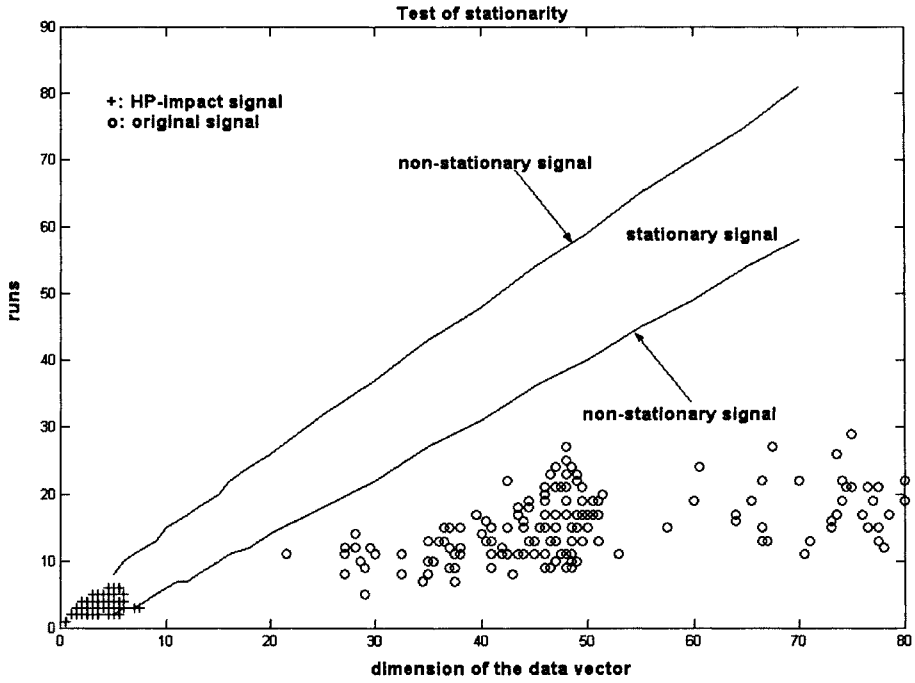

Figure 7-22 Stationarity of the high-pass impact sub-sequence

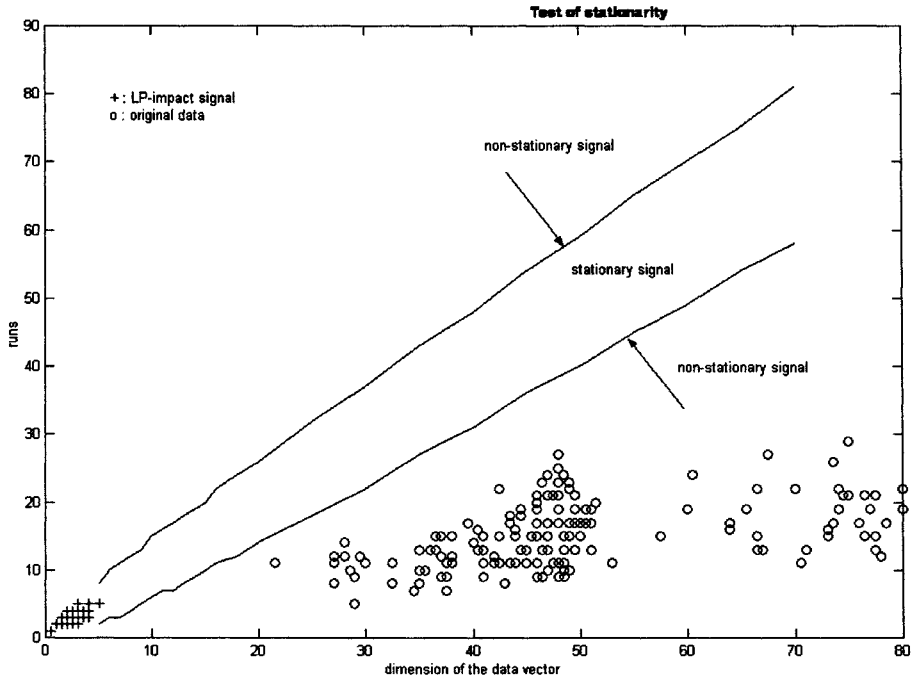

Figure 7-23 Stationarity of the low-pass impact sub-sequence

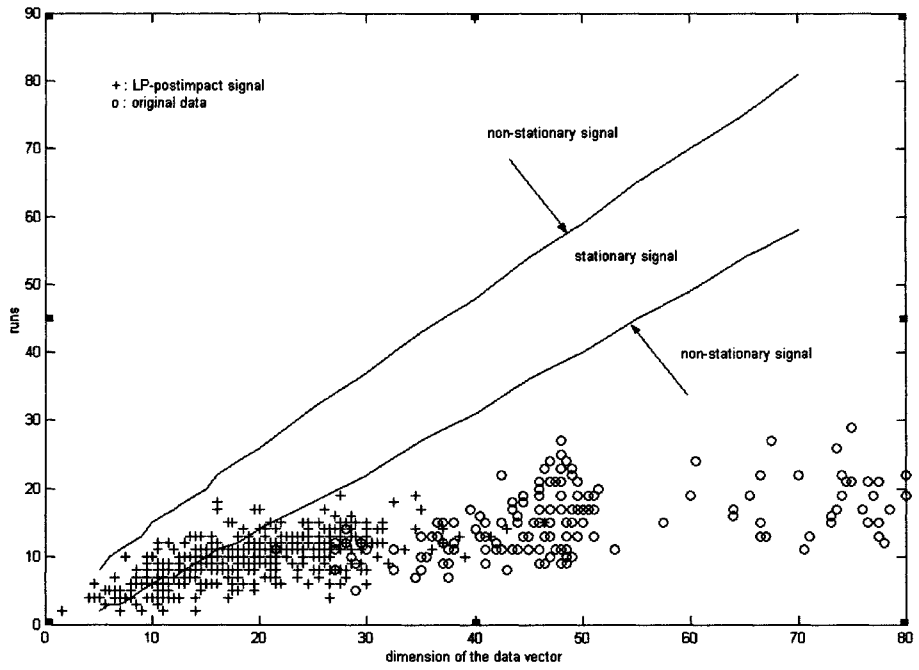

Figure 7-24 Stationarity of the low-pass post-impact sub-sequence

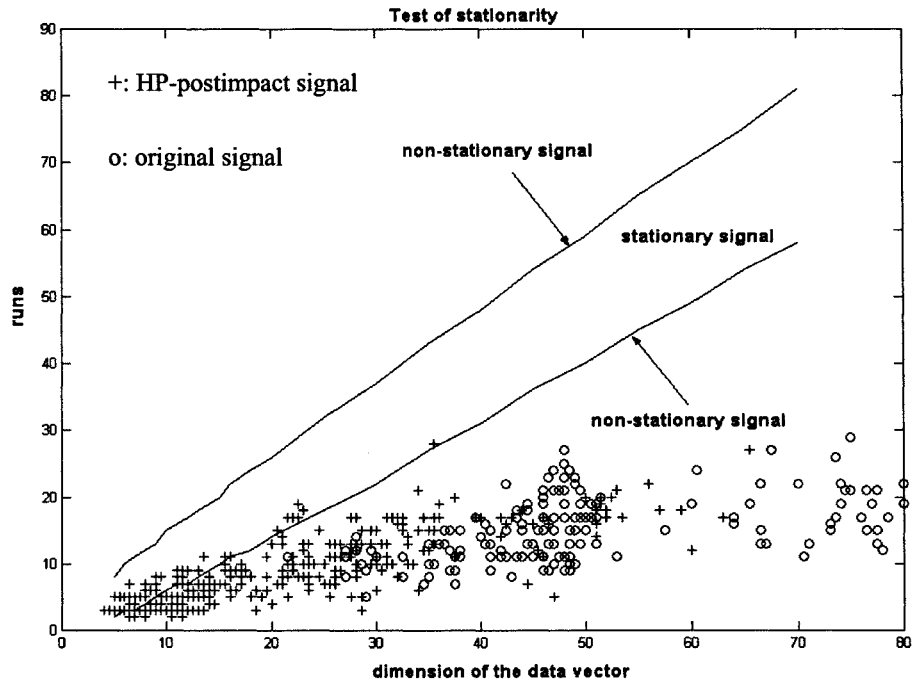

Figure 7-25 Stationarity of the high-pass post-impact sub-sequence

7.6 Stationarity of a train of switching events

In the previous paragraphs details about the stationarity of a single vibration impulse of a switching valve were presented. It was seen that these transient signals were originally non-stationary but that the degree of stationarity could be increased by segmentation in the time- and frequency-domain. This section is devoted the question how stationary a train of overall switching events is. The relation between both kinds of stationarity is shown in Figure 7-26. In the top of this Figure a single switching event is shown and the test of stationarity as described in section 7.5 is used for this situation. The stationarity of the single impulses is important because several algorithms in the field of digital signal processing are only applicable to stationary signals. A different question is shown in the bottom part of Figure 7-26: here the stationarity of a consecutive train of switching-on or switching-off impulses is tested. This test is important because non-

stationarity in this train of switching events indicates within-class-scatter which spreads the dispersion of the classes and makes classification more difficult.

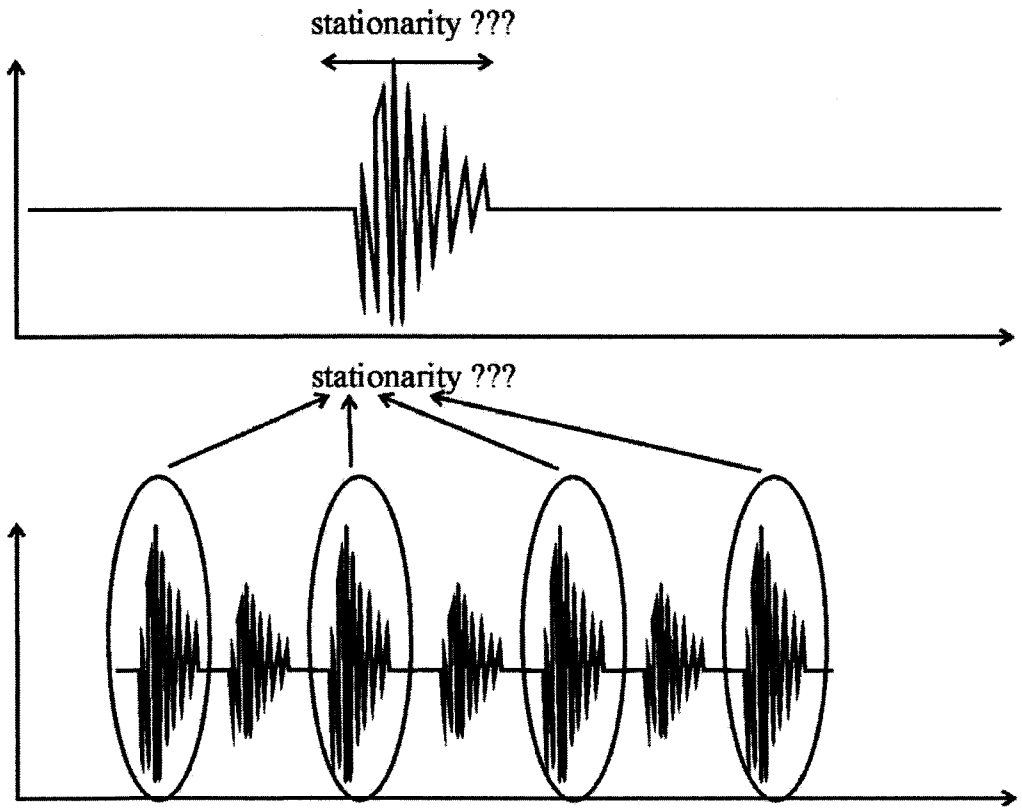

Figure 7-26 Stationarity of vibration impulses

For a train of 1090 switching-off events of unfaulty valves type 6011 (RMS value is shown in Figure 7-27) which were used as raw data for classification this second kind of stationarity was tested again with the run-test as described above for a single event. The square mean of each vibration pattern was analysed and $n_1 = 460$ events had higher energy than the average and $n_2 = 630$ lower energy. A null hypotheses H_0 was formulated that the energy was distributed without a trend and an alternative hypothesis H_1 that there is an underlying trend. For large data sets the number of valid runs is not listed in tables and has to be approximated by means of the normal distribution [Bendat86, Voß00]:

$$\mu_R = E(R) = \frac{2n_1 n_2}{n_1 + n_2} + 1 \tag{7-5}$$

$$\sigma_R^2 = V(R) = \frac{2n_1 n_2 (2n_1 n_2 - n_1 - n_2)}{(n_1 + n_2)^2 (n_1 + n_2 - 1)} \tag{7-6}$$

A number of r = 289 runs was found in this experiment. With a significance level of $\alpha = 0.05$ the number of runs had to be $507 < r < 559$. Hence, the null hypothesis was rejected and the train of switching events was expected to be non-stationary. This situation is also known for similar vibration signals excited from switching circuit breakers [Lang95].

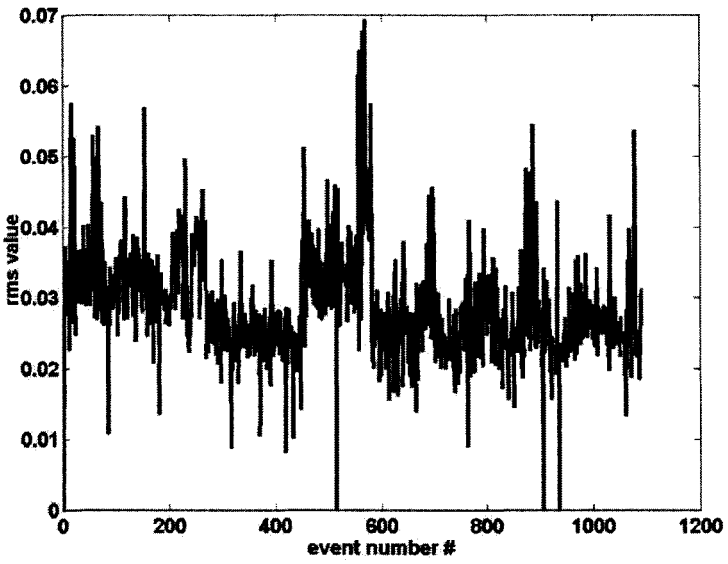

Figure 7-27 RMS of a train of switching events

7.7 Comparison with other TFDs

As mentioned above there is a large number of other distributions with segment the time-frequency-plane like STFT or WT. There are two major advantages of the new Source Based Distribution over the state of the art which are explained now in detail:

7.7.1 Automatic parameterisation

One important aspect of each algorithm is the way how it is adapted or parameterised to a certain problem. The above mentioned and well known techniques like STFT or WT have all several parameters which have to be adjusted for each problem. For example, the width and the shape of the window have to be set for the STFT or the mother wavelet has to be selected for the WT. In Figure 7-28 the Short Time Fourier Transform of a vibration pattern is shown with a window width of 16 and a Hanning window. Figure 7-29 displays the STFT of the identical time signal but with a window width of 512 and a triangular window. The significant difference between both images highlights the problem: a-priori knowledge has to be available or assumptions have to be made to parameterise the algorithm. The Source Based Separation has the aim to gather all important parameters from the signal itself and thus the algorithm is enabled to be self-adaptable to different types of valves.

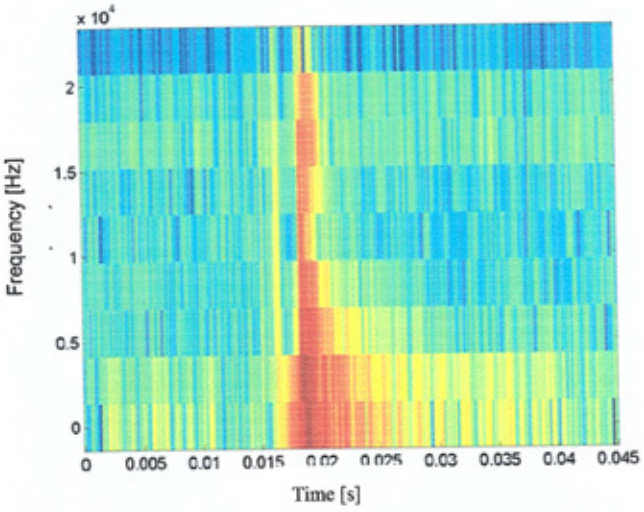

Figure 7-28 STFT of a vibration signal

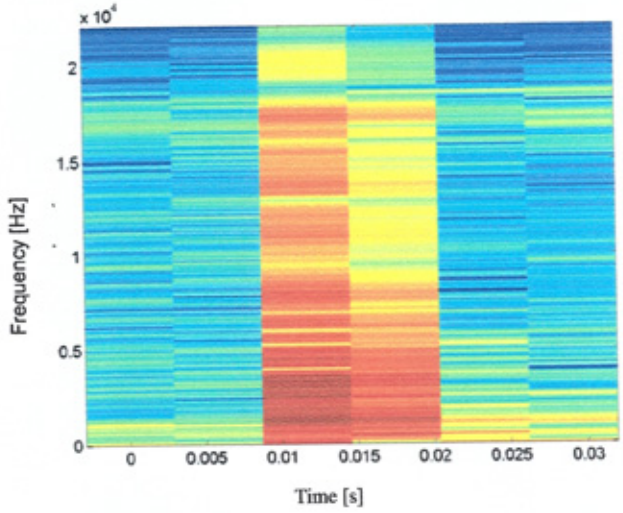

Figure 7-29 STFT of the same vibration signal but with different parameters

In Figure 7-30 and Figure 7-31 the same problem is shown for the Wavelet transformation: Figure 7-30 is the time-scale plane of a vibration signal with a mexican hat kernel and 128 analysed scales. In Figure 7-31 the same time-signal is transformed with the Daubechies wavelet order 2 and 32 analysed scales. The difference between both images is indicates that selecting the optimal (in sense of a minimal misclassification rate) parameters is both, important and difficult.

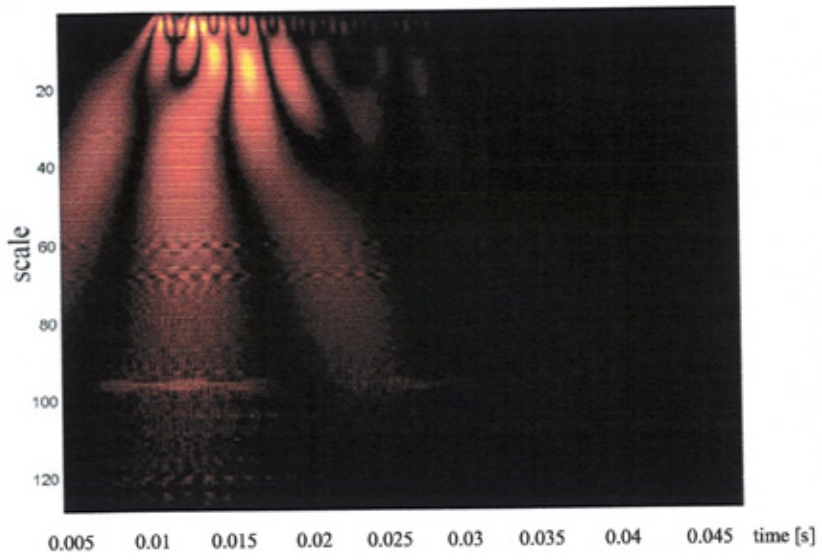

Figure 7-30 WT of a vibration signal

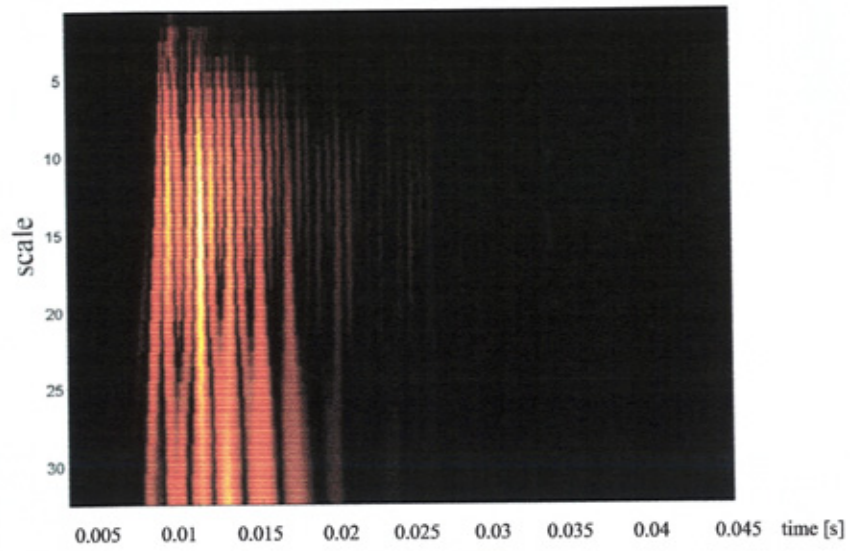

Figure 7-31 WT of the same signal but with different parameters

7.7.2 Identification of Regions of Interest

Switching of solenoid valves generates a train of vibration patterns which do not coincide exactly even if the valves under observation are of the same condition (e.g. faulty or one certain fault). This property of the vibration signals was shown in Figure 5-20 and Figure 5-24 by a set of sample data and also by the property of non-stationarity of a train of switching events as mentioned above. Due to mechanical tolerances or different environmental conditions like ambient temperature or orientation of the valve there are several influences which make the vibration signal be of stochastic character. The next step in the classification process is feature extraction and this step has to cope with the scattering nature of the original signals. Due to this the Spectral Analysis Matrix (SAM) was developed during this project which is explained in the next chapter. This matrix is used to detect regions of interest for feature extraction in a set of scattered spectra with random character. In this research project the SAM works with one-dimensional input data such as spectra. A similar approach for two-dimensional input data such as time-frequency- or time-scale-distributions will be much more difficult and could be part of another following research project. This was the second important advantage of the Source Based Segmentation over other algorithms like STFT or WT: the SBS has a set of one-dimensional spectra as output which could more easily be processed by the SAM.

7.8 Spectral representation

The result of the previous steps is a set of eight time sequences (see Figure 7-19): the original raw data were segmented into four time segments, each further divided into a high- and a low-frequency segment. These eight series are transformed into the frequency domain in the next step by means of an autoregressive-model (AR-model).

An AR-model based approach was chosen because these techniques are known to work very well with short data segments as they are found in this project [Maalej99; Quian00]. An autoregressive model of order q describes a value of a sequence as a linear combination of q previous samples plus an error term *e(n)* which is independent of past samples:

$$x(n) = -\sum_{k=1}^{q} \alpha_k \, x(n-k) + e(n) \quad n = 0,1...,N-1 \tag{7-7}$$

where

x(n) are the samples

α_k are coefficients of the model

N is the number of samples

The Akaike's information criterion (AIC) was used to determine the order q for the AR-models. This criterion is based on information theoretic concepts and was seen to be very useful in many applications [Priestley89; Maalej99; Pattichis99]. In Equation (7-8) the algorithm to compute the criterion for n observations and the estimate of the residual variance σ_ε^2 and model order q is shown [Priestley89].

$$\mathrm{AIC}(q) = n \log \sigma_\varepsilon^2 + 2q \tag{7-8}$$

The optimal model order q in the Akaike-sense is that which minimises the criterion AIC(q).

The following model orders were found by this means for the different sub-sequences extracted from the original raw data:

Table 7-3 Model order determined with AIC

segment	model order
LP lifting	**6**
HP lifting	**12**
LP pre-impact	**1**
HP pre-impact	**3**
LP impact	**2**
HP impact	**4**
LP post-impact	**13**
HP post-impact	**14**

The spectrum of the time-series can be estimated from the model by means of Equation (7-9) [Pattichis99]:

$$P_{AR}(\omega) = \frac{1}{\left|1 + \sum_{k=1}^{q} \alpha_k e^{j\omega k}\right|^2} \tag{7-9}$$

The Burg-algorithm was chosen for computation of the coefficients of the model because this method is specially suitable for short data sequences [MathWorks99a; Maalej99]. The algorithm is described in detail in literature [Kammeyer98].

7.9 Conclusions

In this chapter a new technique to isolate sub-segments of the original raw data with a higher degree of stationarity was presented. The resulting segments are interpretable in a mechanical or physical sense and the parameterisation of the method is fully derived from the input data. The resulting outputs can be processed suitable within the next steps of classification because they are one-dimensional. The next step of the classification scheme as presented in section 4.3 is feature extraction. This process will be explained in the following chapter with a special focus on the Spectral Analysis Matrix which was developed during this project to detect regions of interest for feature extraction.

8 Feature Extraction

8.1 Introduction

The result of all preliminary preprocessing steps was a set of sequences (Figure 7-19). These sequences were part of the time-domain signal or frequency-domain representation of the vibration signal. To classify the measured data it is necessary to extract features from these sequences. Features are statistical, geometrical or other properties of the sequences which emphasise the differences between the classes. Features are scalar numbers and all the extracted features are combined to the feature vector which is used as input vector for the classifier.

8.2 Features in the frequency domain

8.2.1 Introduction

For most analysis or classification tasks it is recommended to reduce the spectrum to as few parameters as possible. If too many parameters are used, the processing speed is usually decreased and the reliability of the result might become sub optimal, particularly if some of the parameters used do not assist in class separation. The aim is always to build a parsimonious analysing system using as few parameters as possible. It is therefore necessary to isolate smaller segments in the spectrum which carry information with a high discriminant power between classes. A segment or region of interest (ROI) can be a part of the spectrum with a lower frequency and an upper frequency border. After isolating the ROI further post-processing can be used to generate the features

actually used for classification. In addition these spectral ROI can be fused with other additional features for classification. These additional features can, for example, be statistical or geometrical parameters, or coefficients of a model based approximation.

To identify the ROI several methods are used. Some important ones are described in the next paragraphs.

8.2.1.1 Fixed border regions

A straightforward algorithm for segmenting a spectrum is to define a fixed number of frequency classes each with a lower and an upper frequency and equal length [Alguindigue93, Clark98]. The frequency classes may be overlapping or distinct. The spectrum can be separated in only two classes (low frequency and high frequency) or in three or more individual classes. It is important that the number of classes is chosen to be high enough to separate the sharpest occurring peaks. It is necessary therefore to have a priori knowledge about the spectrum and the observed process. If there are too few classes the parameters give only an average over many regions of interest. If the regions are too small and the number of regions is too high regions of interest in the spectrum are split into different segments and the extracted parameters may loose their power of discrimination because they do not represent a real ROI. Another drawback of this approach is that not all bins automatically contain discriminative and interesting information. There may be one or more regions without any discriminative power. These additional data may worsen following processing steps.

8.2.1.2 Neural networks for analysis of different classes

Another possibility to reduce the dimensionality of the spectrum and to find important features in the frequency domain is to process the frequency signal with a neural network. [Alguindigue91, Skitt93]. In this approach the spectrum is also divided in n_{seg}

different frequency segments and the average power in each segment is used as input for a neuron. The number of neurons in the input-layer of the net equals the number n_{seg} of bins in the spectrum. Further the net has one or more hidden-layers with fewer neurons than the input-layer. The number of neurons is expanded again in the output-layer to the same number as used in the input-layer. The neural network is trained to reproduce the input spectra and the number of neurons in the hidden layer minimised subject to match between the input and output being above some threshold i.e. –40dB. The hidden-layer represents a compressed version of the input-layer and the difference between the input- and output-layer represents the fitness of the representation. The trained net can be used as pre-processor for a classification task and the hidden neurons of this net can act as input vector for a classifier.

8.2.1.3 Selection of the important peaks

To segment the spectrum into a train of overlapping or non-overlapping bins is not the only way of building regions of interest. Another possibility is to recognise the peaks in the spectrum and isolate them. The main difference is that the bins generated by this approach are neither equidistant nor of the same length. A first attempt to find the peaks in the spectrum could be analysing the monitored process: often some frequencies can be determined which will be most interesting. This is a common approach for rotating machinery, gears, rolling element bearings [Zwingelstein90] and similar processes. Here the relation between the revolutions per minute and the spectrum is distinct. Sometimes it is even possible to find a deterministic equation for interesting frequency regions. Generally it is important not only to analyse the high peaks in the spectrum because some important features of the spectrum might also have low level [Alguindigue93]. In general whereas these three existing techniques are useful in

compressing the spectra into fewer parameters, there is no guarantee that these parameters will be useful for classification purposes. Features used as input vector for a classifier have to include significant discriminative power and this property can only be determined in mutual comparison of spectra of all classes which should be separated.

8.2.2 Segmentation with the Spectral Analysis Matrix

8.2.2.1 Introduction

A new approach for segmentation of the spectrum into ROI is the data derived Spectral Analysis Matrix (SAM) [Ellwein01d]. In its simplest form it is useful in the case where there are two distinct populations or classes and we wish to identify frequencies with high interclass discriminant ability. The discriminative power of a region in the spectrum is higher if the interclass distance between the means is higher and the scatter of the amplitudes is lower. A region of interest can not be identified by the spectrum of a single realisation of the observed process if the observed process has a random character which causes scatter in the frequency domain. This situation occurs in most "real-world" processes because of stochastic sources in the process itself, external noise sources which are also observed or internal noise sources in the measurement chain. Hence, very often it is necessary to observe a set of different realisations of the process at a train of successive time points to get a larger pool of time series which covers the important statistical properties of the process. The distribution of the spectral process can then be taken into account in the classification task. In the experimental setup of this research project this meant a set of 64 faulty solenoid valves and 10 unfaulty valves were switched on and off several times and the vibration of each switching event was recorded. Each of the switching off events was segmented in the time-frequency-plane (see chapter 7) and a set of eight sub-sequences with a higher degree of stationarity was

received after this operation (see Figure 7-19). After transforming these sub-sequences to the frequency domain a new matrix called Spectral Analysis Matrix (SAM) was generated for each of the sub-sequences with the same number of columns c_{SAM} as distinct frequencies in the spectrum and as many rows r_{SAM} as the absolute integer amplitude range of the spectrum. If, for instance, the spectrum has an amplitude range from 0dB to –200dB the SAM has 201 rows. For a spectrum of the range [0; 1kHz] with a resolution of 10Hz the SAM will have 101 columns. In other words, the original spectrum, which is discrete or continuos in frequency and continuous in amplitude is threshold to a grid of discrete bins in both axes. The elements of the SAM are initialised with a starting value (e.g. zero). For estimating the distribution of the spectra the set of time series data is transformed to the frequency domain and the amplitudes of the resulting spectra are truncated to integer values. As many spectra were received as time series were recorded earlier. Each distinct point of these spectra corresponds to an element s_{ij} of the SAM. This element is located by the discrete frequency and the truncated amplitude of each point in the spectrum. For a two-class-separation the value of this element in the SAM is increased if the corresponding spectrum belongs to class 1 and decreased if the spectrum belongs to class 2. The result is a matrix where regions of class 1 are indicated by values larger than the starting value and regions of class 2 have elements with lower values than the starting value. For example, let the first ten data points of the spectral representation of a certain time-series be given in Table 8-1.

Table 8-1 Example for the generation of the SAM

Frequency [Hz]	1	2	3	4	5	6	7	8	9	10
PSD [dB]	-30	-33	-33	-35	-36	-33	-40	-42	-45	-40

The amplitudes of the original spectrum are truncated to integer values in Table 8-1. Each column in Table 8-1 corresponds to one element in the Spectral Analysis Matrix: the first column is the first point in the spectrum (-30dB at 1Hz) and so on. This column corresponds to the 30th row and the 1st column of the Spectral Analysis Matrix **S**. Now, the elements $s_{30,1}$ $s_{33,2}$ $s_{33,3}$ ... $s_{40,10}$ are increased by one if the time-series belongs to class 1. If the time-series would belong to class 2 then the mentioned elements of the SAM would be decreased by one.

The lower the scatter in a given frequency bin, the higher the absolute values are because the increase or decrease will be concentrated within a smaller region. This approach is very similar to the histogram method for estimating a probability density function [Webb99]. In this approach the probability density function (PDF) of a random process is estimated by computing the amplitude histogram of the process. The histogram was seen as a rough and truncated estimation of the PDF. The SAM is a similar approach where the distribution of the spectra is estimated. Important differences are that two different processes are used to generate the SAM and algorithms of the field of image processing are used for further processing to identify the ROI.

The SAM can be interpreted as an image where the different values of the elements cause different colours or grey scales in the image. In the following the generation and the analysis of a SAM is shown. The later Figures 8-1 to 8-7 show consecutive processing steps which are necessary to identify the ROI in the SAM. They are all performed on the same original data shown in Figure 8-1 where the SAM was generated from 808 individual spectra and was printed as an image with the MatLab command `imagesc`. It is important to use the almost same number of spectra from

each class to generate the SAM to equal the influence of increasing and decreasing patterns. Due to this 404 spectra of each class were used for this example of the SAM. The brighter a pixel in the image is the higher is the corresponding the value in the SAM and vice versa dark pixels in the image are caused by low values in the SAM.

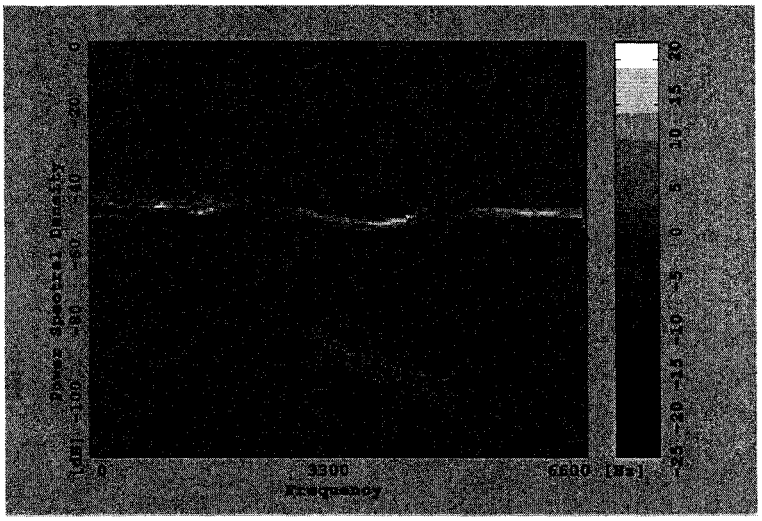

Figure 8-1 The Spectral Analysis Matrix (SAM)

The challenge is now to identify the regions of interest (ROI) within this matrix. This is done by applying algorithms from the field of digital image processing and pattern recognition to the SAM. These algorithms were chosen because it is often possible for humans to identify the ROI by visually inspecting the image. The identification of the ROI is done in several steps which are described in the following paragraphs:

8.2.2.2 Eliminating regions with high overlapping

If in a certain column of the SAM (that is for a certain frequency of the spectra) the overlapping of both regions is too high this column was not suitable for classification. Let n be the number of switching events which are used to build the SAM and r_{SAM} the number of rows in the SAM (that is the integer range of the amplitudes). If s_{ij} is the

element of the i^{th} row and the j^{th} column of the SAM then Equation (8-1) holds if there's no overlapping at all.

$$s_{column} = \sum_{i=1}^{r_{SAM}} \left| s_{ij} \right| = n \tag{8-1}$$

Usually there will be overlapping of the two classes and s_{column} will be smaller than n. The degree of overlapping can be found by Equation (8-2):

$$overlapping = \frac{s_{column}}{n} \tag{8-2}$$

If for a certain column the degree of overlapping is smaller than a threshold ε_1 this column is not suitable for classification because of the overlapping and this column will be eliminated by filling all elements of this column with the starting value of the SAM (in the image representation of the SAM this column will be filled with the background colour; see ① in Figure 8-2). threshold ε_1 is set the less frequency bins were accepted to be interesting. If ε_1 is too high no regions of interest can be found in the SAM. This effect was used to adjust ε_1: the desired number of ROI is determined by the available computational power for classification because training the classifier slows down significantly with an increasing number of inputs. ε_1 was adjusted to a value that a reasonable number of ROI (typically below 20) were detected. The ROI-detection in the

SAM is performed in a way that always the most powerful ROI are returned. If some parameters of the ROI-detecting steps are altered in a way which will reduce the number of returned ROI (for example if ε_1 is increased) then only the less powerful regions are suppressed. In this experimental setup ε_1 was set to 0.3.

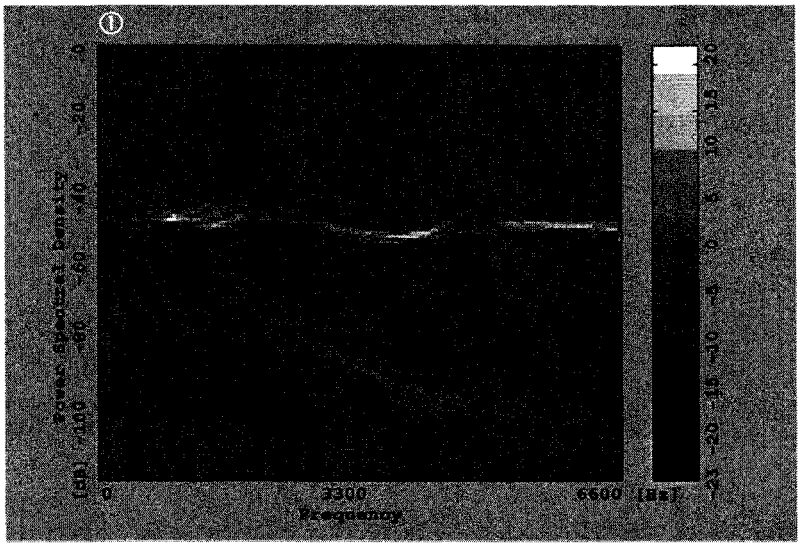

Figure 8-2 SAM without highly overlapping regions

8.2.2.3 Thresholding

To emphasise frequency regions in the image where the power for spectra of each class are condensed into to a small amplitude range two thresholds t_1 and t_2 were applied to the SAM. These regions with highly localised classes are indicted by high absolute values in the SAM. If the spectrum is spread widely or overlapping happens the absolute values of the elements will be around the starting value. The thresholds cause that only three values occur in the SAM (±1 and 0). The following Figures displaying different processing steps of the SAM are in this three colours: value 1 is indicated by white colour, zero corresponds with grey and value –1 with black.

$$s_{ij} = \begin{cases} +1, \text{ if } s_{ij} > t_1 \\ -1, \text{ if } s_{ij} < t_2 \\ 0, \text{ else} \end{cases} \tag{8-3}$$

t_1 is larger than the starting value and t_2 is smaller than the starting value. To adjust t_1 and t_2 it is recommendable to perform three steps:

1. The maximum value s_{max} of the SAM is detected
2. The minimum value s_{min} of the SAM is detected
3. $t_1 = factor \cdot s_{\max}$ $\quad t_2 = factor \cdot s_{\min}$

   typical values for *factor* are 0,1 to 0,5.

The setting of t_1 and t_2 is evaluated again by the criterion proposed above: the number of final ROI should depend on the computational power and enough ROI should be taken into account to reach a desired misclassification rate.

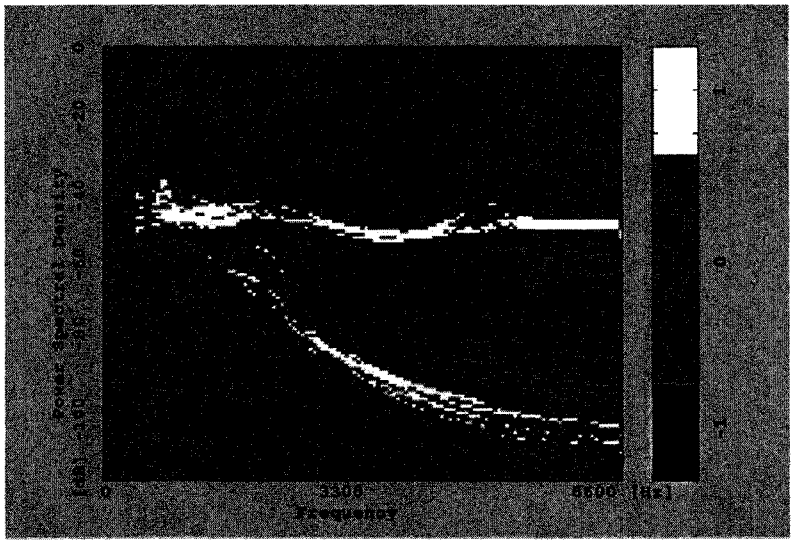

Figure 8-3 Thresholded version of the SAM

8.2.2.4 Median filtering

Usually there are some small isolated points in the SAM, caused by noise in the spectra which causes consequential noiselike regions in the image. These points have no valid information for the identification of the ROI and they should be suppressed. This is done by applying a median filter to the SAM. This morphological operation effectuates after filtering only larger regions of both classes remaining in the image. The kernel of the median filter depends on the dimensions of the SAM and the influence of noise. Good results were achieved with a 3 x 3 – kernel.

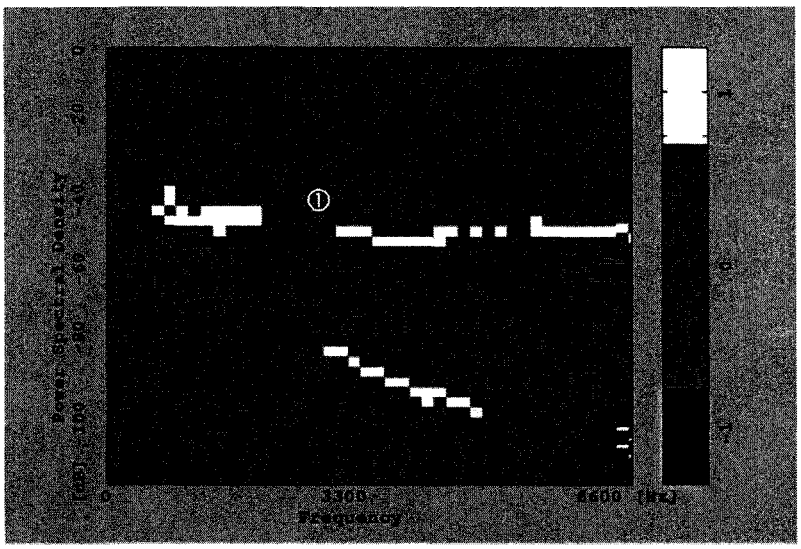

Figure 8-4 SAM after median filtering

8.2.2.5 Eliminating single class regions

It can happen that in certain columns (frequencies in the spectrum) only values larger or lower than the starting value appear. This means in these columns are only regions of class 1 or class 2, respectively (see ① in Figure 8-4). Due to filtering and thresholding the matrix these columns can appear. They are not suitable for classification because information about both classes in necessary to perform a separation. These columns are also filled with zero which is the new "background colour".

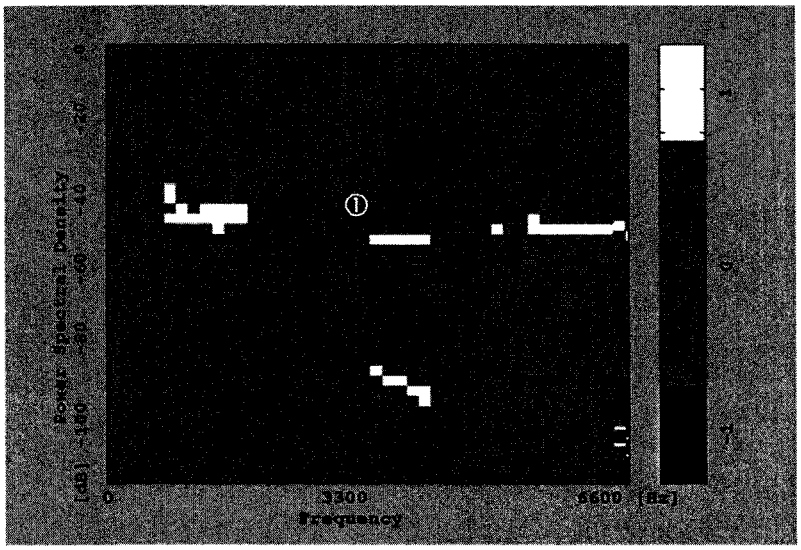

Figure 8-5 SAM without single class regions

8.2.2.6 Eliminate direct connections

If the two classes are too near in the spectral domain at a certain frequency, these columns will similarly not be useful as they have a low discriminant power (see ① in Figure 8-5). To find these frequencies a difference filter is applied to the columns of the (see Equation(8-4):

$$s'_{ij} = s_{ij} - s_{i+1j} \qquad i = 1...r-1 \tag{8-4}$$

If a region of class 1 is connected directly to a region of class 2 than a ±2 step occurs in the filtered signal because a region with value one connects to a region with value minus one in the SAM. If such a step occurs in a column of the SAM than these column is also filled with zero.

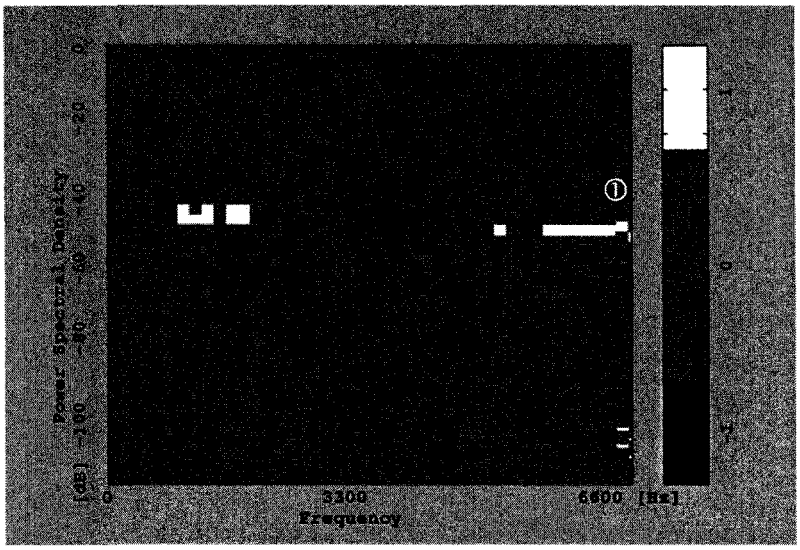

Figure 8-6 SAM without direct connected regions

8.2.2.7 Eliminate enclosed regions

In the case study used to demonstrate this algorithm, a classification between faulty and unfaulty solenoid valves, a two-cluster-classification was performed. However in this case the "faulty" class consisted of many failure sub-classes and obviously one class of unfaulty valves. All the different failure classes were mapped to one cluster because failure identification is not necessary (the faulty devices were replaced and not repaired). The different failures which should be detected by this classification are presented in Table 2-1 (page 15). All these sub-classes should be separated from another class, the unfaulty valves. Consequentially the number of decision borders can be reduced. Due to this it may happen that two regions of the class of faulty valves occur with higher and lower amplitudes than that of the unfaulty class (see ① in Figure 8-6). Thus the unfaulty region may be enclosed by two or more subclasses from the faulty spectra. These frequencies are more difficult to classify and thus they are eliminated (see Figure 8-7).

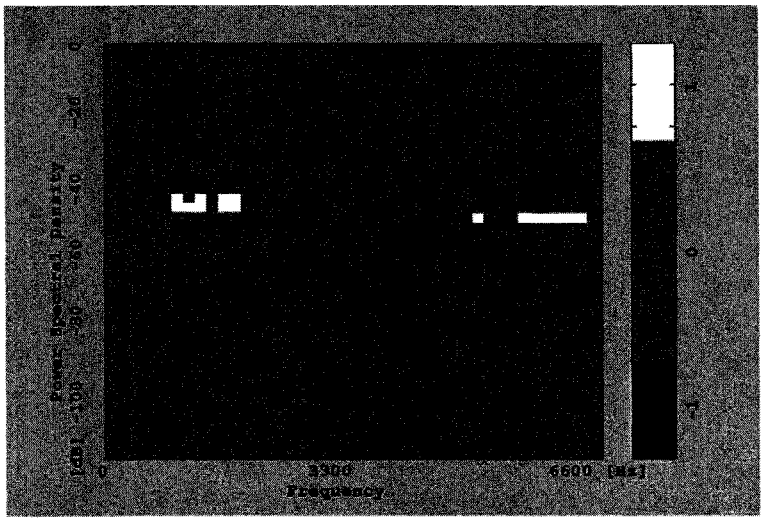

Figure 8-7 SAM without enclosed regions

8.2.2.8 Calculating the discriminant ability

A new vector **q** with dimension c_{SAM} (=number of columns in the SAM) which represents the discriminant ability of each distinct frequency is now computed. The quality is computed by Equation (8-5):

$$q(j) = \sum_{i=1}^{r_{SAM}} |s_{ij}| \quad j = 1 \ldots \; c_{SAM} \tag{8-5}$$

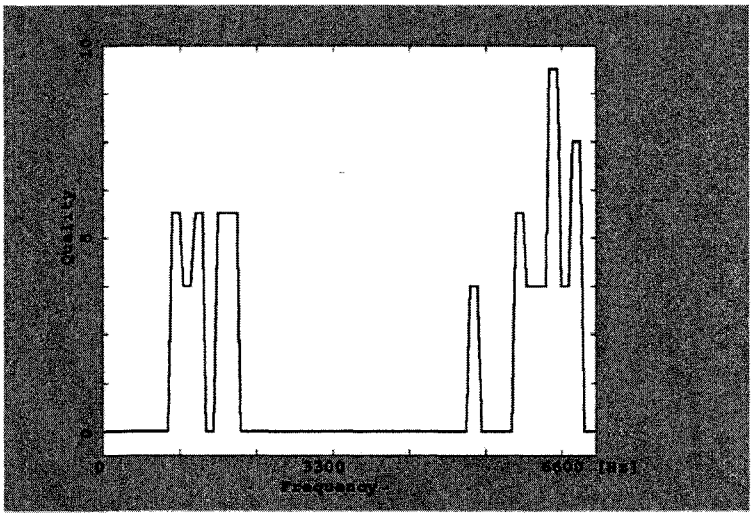

Figure 8-8 Discriminant ability of the spectrum

In Figure 8-8 the discriminant ability of each frequency bin in shown. All bins with a corresponding value *q(j)* higher than zero can be used as a region of interest for classification.

8.3 Comparison of the SAM-method with other techniques

This new algorithm was developed because of important drawback of the current algorithms mentioned above: to perform a segmentation into bins with a fixed width it is necessary to have a-priori knowledge about the observed process but this is not always available. In this research project the aim was to develop a monitoring system for a large set of valves (different sizes, different materials) and the spectral densities are different from valve type to valve type. Thus it is not feasible to gather detailed information manually for each valve. The advantage of this new algorithm is the ability to derive the borders for the segments in the spectrum directly from the measured data without human expert knowledge. By this means the parameters of a monitoring system can be adapted easily to a new situation.

It can also be seen in this chapter that the regions of interest for the presented situation are not always the peaks of the spectrum (compare the ROI in Figure 8-8 with the original spectra in Figure 8-1). This result led to the conclusion that identifying peaks in a spectrum is not necessarily the most suitable feature extractor for a classification. Important and powerful features can also be hidden between the peaks of the spectrum. This new algorithm is capable to identify ROI in both, the peaks and the segments between the peaks.

To compare the discriminative power of the ROI detected with the new SAM method with a traditional segmentation of the spectrum into regions with fixed width both

segmentation techniques were implemented in a classification system: the time-series of switching valve vibrations were segmented to improve the stationarity of the signals as described in the previous chapter. Thus eight subsequences were the final result of this step and each of the new series was transformed to the frequency domain with an AR-model based approach (Burg's method [MathWorks99a]). The resulting spectra have a length of 129 data points.

The SAM method returned eleven regions of interest in the all eight power density spectra. With traditional segmentation technique each of the eight spectra was segmented into eight overlapping segments with a width of 20 data points. The following features were computed from in each region of interest in both approaches:

- the gradient of the linear trend of the region
- the sum of the data points in the region
- the 2-norm of the data vector in the region
- the sum of the linear trend of the region

Additionally some features are computed directly from the time-series but these features were not changed in this comparison[2]. An overall of 68 features were extracted from each raw vibration pattern with the SAM method and 216 features were gathered with the fixed border method for each vibration signal. A principal component analysis was performed to reduce linear dependability between the features and afterwards a set of 29 new variables were received for the SAM method and 34 new variables for the fixed border algorithm. These new variables were used as input vector for the neural network

[2] The topic "feature extraction" in this research project is explained in detail in paragraph 8.4 and 8.5

classifier. The neural network was a Feedforward Multi-Layer-Perceptron Neural Network and had two hidden layers with 28 and 8 neurons, respectively. The Levenberg-Marquardt training algorithm was used with Bayesian regularisation [Demuth98, Foresee97]. A separate test set was used to verify the performance of the classifier. The misclassification rates were presented in Table 8-2:

Table 8-2 Misclassification rates

	false accept [%]	false reject [%]
SAM method	**2,75**	**2,39**
Fixed border method	**2,06**	**9,85**

It can be seen that the SAM algorithm has a much better overall result. The false accept rate is rather similar but the false reject rate is about four time worse for the fixed border technique.

The presented technique of identifying regions of interest with the SAM is a typical "blind" technique, not using any model. No assumptions about the analysed signals are made and thus is it expected that this technique can be used in many applications and tasks. Important is to take into account that the approach is limited to separation of two classes. Further work has to be done to expand this technique to a multi-class analysis. This limitation is not severe for a vast number of classification tasks, because the separation between faulty and unfaulty, correct and incorrect and so on is a very often performed task. As shown in this case study it is also often possible to combine sub-classes to one single cluster.

8.4 Features extracted from the ROI

After identifying the ROI it is necessary to extract features from these spectral sequences which contain the discriminative power of the ROI.

8.4.1 Linear trend

The whole estimated spectrum of a real world time series or segments of the spectrum have often an underlying linear trend. It often impairs the analysis of properties in the spectrum which are not due to this trend. Thus it is recommended to isolate the linear trend and to analyse both parts of the spectrum individual [Grieser97]. A very important feature to describe the linear trend is its gradient which was extracted as a first feature from the spectra.

8.4.2 Energy

A second important feature of the spectral segments is the energy in the segment. It is computed by

$$E_{seg} = \sum_{n=0}^{m-1} x_n^2 \tag{8-6}$$

for a segment **x** of length m.

8.4.3 Kurtosis

The kurtosis was extracted from the sequence and used as a third feature. The kurtosis is a measure how outlier-prone a distribution is and it is often used as feature extracted from vibration signals [Pachaud97; Jossa99]. The kurtosis is defined by Equation (8-7) [MathWorks99b]

$$k = \frac{E(x-\mu)^4}{\sigma^4} \tag{8-7}$$

where

μ is the mean of the investigated sequence

$E(x)$ is the expected value of x

σ is the standard deviation

8.4.4 Skewness

A last feature which was computed from the frequency domain was the skewness of the sequence which is a measure of the asymmetry of the distribution. The skewness is also often used for feature extraction [Jossa99] and is defined by

$$s = \frac{E(x-\mu)^3}{\sigma^3} \tag{8-8}$$

8.5 Time-domain features

Important features for classification are often not only hidden in the spectral representation of a signal but also in the time domain. Thus additional features are extracted from the eight segments proposed in chapter 7. The features gained from these sequences are described in the following.

8.5.1 Length of the segment

The length of the segment depends on the raw data and can thus be used as feature. The length of the segment is the number of data points in the vector extracted from the original vibration pattern by segmentation.

8.5.2 Energy

The energy of the sequence is computed similar to section 8.4.2 from the time series.

8.5.3 Kurtosis

The kurtosis of the sequence is computed similar to section 8.4.3 from the time series.

8.5.4 Skewness

The skewness of the sequence is computed similar to section 8.5.4 from the time series.

8.6 Conclusions

In this chapter the Spectral Analysis Matrix was introduced and described in detail. This new development of this research project is a very powerful tool to identify regions of interest in spectra without a priori knowledge. It is very important for a reliable classification to extract features from regions in spectra which contribute to classification. An important advantage of the SAM is that regions with lower discriminative power are suppressed automatically.

Features are extracted from these regions and also described in this chapter. All features together build the feature vector. The next step in the classification scheme proposed in chapter 4.3 is now to apply this feature vector to a classifier. The feature vector is normalised and redundancy within the vector is reduced by a Principal Component Analysis. The new variables are applied to a Neural Network for classification. These steps are described in detail in the next chapter.

9 Classification results

9.1 Introduction

In this chapter the classifier and the results of the classification are presented. A vast number of different classifiers have been developed during the last decades and some details about the theory has been presented in chapter 4. Several constraints led to the decision to use a Neural Network as classifier, which were summarised in and explained in this chapter. Some other classifiers have also been tested and they are discussed briefly within the next sections. This chapter is organised as follows: first, preprocessing of the feature matrix is described and after that the reasons for the selection of the classifier are explained in section 9.3. Some minimum distance classifiers are discussed in section 9.4. Two different Neural Networks are presented in section 9.5 and the reasons for choosing a MLP are described. The chapter ends with some conclusions in section 9.6.

9.2 Preprocessing of the feature matrix

The three feature matrices for training, validation and testing each consist of 44 rows (different features). The number of columns (number of observations) is 1328 for training and validation and 2125 for the test data set. Each column represents a different variable with different units because of the different features extracted from the time- and frequency-domain (as described in chapter 8). For using the different variables later in one classifier each one is normalised to zero mean and unit standard deviation as recommended in [Niemann90]. After that a Principal Component Analysis (PCA) is performed to eliminate mutually linear dependencies between the variables. By means

of this the number of variables could be reduced to 23 in the training-, validation- and test-set.

9.3 Selection of a classifier

The selection of a classifier for a certain pattern recognition problem is a rather difficult task because of the vast number of different algorithms and classification techniques available. In this research project the main focus of investigation was set to preprocessing of the vibration data because it is much easier to classify data when features with a high discriminative power are available. The selection of a classifier was marked out by two reasons or considerations: first, an intensive survey of literature was performed to find previous projects and investigations where similar data were classified. There is a large number of papers and publications which present results of vibration analysis projects and the experience brought together by this literature survey was very valuable in this PhD-project. Secondly, a rough study of different families of classifiers was performed to identify techniques which might be suitable and others which seem to be inadequate. The results of this analysis are presented in Table 9-1. The results of these considerations were proved by practical implementation of several different classifiers. Of course, it is not feasible to investigate all classifiers and all techniques with the same intensity. Therefor, the goal which should be reached by this project was not to find the classifier which is globally optimal in a certain sense (e.g. which has the lowest misclassification rate) but to find a classifier which is suitable for a condition monitoring system for solenoid valves. The most important requirements are:

- the misclassification rate (false accept + false reject) should be below 5% (this number was defined according to the experience and advice of Bürkert engineers)
- the classifier should be trainable with data gathered form new valves which were not used in this research project

In Table 9-1 four important properties of different families of classifiers were compared. This comparison is rather crude because each family contains a large number of classifiers and algorithms which differ in their properties but a first assessment can be retrieved by this investigation. Hence, only two values were assigned to each property in the Table: " + " indicates, that a family of classifiers is mainly suitable for a certain task and the symbol " - " shows that there might be problems and a family is mainly not suitable. The four families which are compared were suggested in [Jain00]: *Template Matching* are straightforward approaches which compare the similarity between two entities of the same type. A template or prototype of each class (e.g. the shape of a vibration signal for faulty and unfaulty valves) is compared with the pattern which are to be recognised by a kind of distance measurement. Some of these classifiers were realised in this project and tested later on in section 9.4. *Statistical Approaches* determine the decision boundaries by the probability distributions of patterns belonging to each class. *Syntactic Approaches* try to compose complex patterns of simple subpatterns. These approaches are of a hierarchical nature. A complex pattern is decomposed to a set of subpatterns which might again be decomposed to simple subpatterns. These primitives can be syllables or alphabetic characters for speech recognition. *Neural Networks* were already introduced in chapter 4.6.2. They can be viewed as massively parallel computing systems consisting of interconnected simple processing units.

Table 9-1 Investigation of different families of classifiers

	Template Matching	Statistical Approach	Syntactic Approach	Neural Networks
Ability to be trained with new data	+	+	-	+
Use of probability density function	+	-	+	+
Ability to classify noisy data	-	+	+	+
Training time	+	-	-	-

Table 9-1 indicates that Neural Networks were seen to be rather suitable except of the training time. Training is often a rather time consuming process for Neural Networks because it is a heuristic technique and no analytical techniques are knows to adjust the weights in a Neural Net directly. Nevertheless, this drawback is not very severe because the classifier has usually to be trained only once for each family of valves and solenoid valves are often used for many years. Due to this the ratio of training time to the average lifetime of a valve is rather small and thus this is not a problem. All approaches based on the class conditional probability density function are not suitable for this task because this function is different for each final application of the valves because it depends on parameters like the operated medium, the temperature and pressure of the medium or the switching frequency. Hence, it is not possible to estimate this function with reasonable cost because this estimation has to be done for each individual valve (see also sections 4.6.1 and 4.7). Syntactic approaches are also not usable because it would be necessary to define a set of primitives which cover the differences between

the classes. One challenge in this project was that even the vibration pattern of a distinct class (unfaulty or one of the faults mentioned in Table 2-1, page 15) were not stationary. This situation was described in detail in section 7.6. Due to this it would be very difficult to define a suitable set of primitives which covers both, the between-class variability and also the within-class scatter. Template Matching Algorithms were implemented and tested during this project but is was seen that the ability of these rather simple algorithms to separate the different classes was not high enough.

In the literature a large number of projects were presented where similar vibration pattern were classified using Neural Networks with a reasonable accuracy [Yamashina90; Alguindigue93; Uhrig93; McCormick96]. These previous results and the above presented reasons led to the decision to use a neural networks as classifier. This selection was also validated by the low misclassification rates which could be achieved with a Neural Network.

9.4 Minimum Distance Classifiers

Two well-known minimum distance classifiers were applied to the feature vector to separate the faulty and the unfaulty valves in a first attempt. Minimum distance classifiers measure the proximity of test patterns with learned templates. The templates for the classifiers used in this work were the median and mean values of the variables in the training set.

9.4.1 Correlation coefficient

The first classifier tested with the data was a cross-correlation measurement between the computed template vectors and each new feature vector [Fukunaga90]. This classifier is described by Equation (9-1)

$$d_c = \mathbf{t}^T \mathbf{x} \tag{9-1}$$

where the vector **t** is the template extracted from the training data and **X** is a single vibration pattern from the test data set.

The correlation coefficient was mentioned in [Britt93] to be not very effective. The results were not convincing at all in this work, too. The misclassification rates were shown in Table 9-2:

Table 9-2 Classification results with correlation coefficient based classification

	mean based template	median based template
false accept	**22.8 %**	**17.99 %**
false reject	**1.87 %**	**2.08 %**

9.4.2 Euclidean distance

The Euclidean distance was the next distance measure used in this work. The Euclidean distance d_e between the feature vector **x** and the template vector **t** was calculated by means of Equation (9-2):

$$d_e = \sum_{k=1}^{p} \sqrt{(x_k - t_k)^2} \tag{9-2}$$

A feature vector **x** was assigned to the class of the template vector with the smaller distance d_e. The results are presented in Table 9-3:

Table 9-3 Classification results with Euclidean distance based classification

	mean based template	median based template
false accept	**17.81 %**	**14.35 %**
false reject	**2.5 %**	**3.33 %**

The result for both minimum distance classifiers was that the results are not convincing and the classifiers are not useful to perform that classification task because the misclassification rates are rather high.

9.5 Neural Network Classifiers

9.5.1 Introduction

Neural Networks are very famous classifiers used for pattern recognition and system identification in a wide field of applications [Kubat00]. A great advantage of neural networks is their ability to learn a classification rule from a set of pre-classified training data. They are capable to perform non-linear decision hyperplanes and to classify high dimensional spaces. Neural Networks also became very popular because they need no assumption of the statistical distribution of the data, whereas techniques such as the maximum likelihood algorithm assume that data has a known statistical distribution. This is an important reason why a Neural Network was chosen as classifier: the probability distribution of the different classes can only be estimated for the data sets used for training (training-, validation- and test-data-set). It is important to mention that this is *not* the probability distribution of the classes for further valves which will be monitored with the trained classifier. If the accomplished and trained monitoring system is applied to a new valve and the device is observed through its lifetime the probability density for the classes is individual for each application and each valve. The probability that a certain failure occurs depends on the particular situation that means the ambient temperature, the medium pressure and the type of medium which is switched, the voltage applied to the coil and other parameters. This individual probability cannot be estimated and due to this an assumption-free approach was chosen.

Neural Networks are also very suitable classifiers if the input signals used for classification are of different nature and units. In [Peters96] Neural Nets are suggested for those application when a set of unequal input variables are combined to one input vector for classification. By visual inspection of the raw data and estimated power spectra it was seen very early in this project that both, the time- and the frequency-domain representation of the data contain discriminative power and may contribute to classification. This was another important reason for choosing a Neural Network as classifier in this project.

9.5.2 Architecture

A Multilayer Perceptron (MLP) was tested as classifier in this project because this architecture was used in several application of vibration analysis successfully [Uhrig93; Yamashina90]. To avoid overfitting and to increase the ability of the network to generalise early stopping was chosen as recommended in [Mathworks98]. Two hidden layers were implemented in the net because it is known that a Network of this architecture is capable to approximate any non-linear function to any arbitrary accuracy [McCoormick96, Cichocki93]. The network has 23 input neurons because 23 new variables were found by the Principal Component Analysis. Two output neurons represent both classes: faulty and unfaulty. The number of neurons in both hidden layers was varied over a wide range and the optimal number was found be 30 neurons in each hidden layer. The tangent sigmoid function was chosen as transfer function for both hidden layers and the output layer has a linear transfer function. To increase the speed of convergence backpropagation with variable learning rate and momentum was used as training algorithm (MatLab training algorithm *traingdx*).

In Figure 9-1 the total number of neurons in both hidden layers is shown for different architectures. This first investigation was performed to estimate the need of "computational power". This global minimum was found with a network consisting of 60 neurons. If there are fewer neurons the network is not able to suitable approximate the patterns. If the number of neurons is too high, the ability to generalise is lost and the network tends to overfit the training data. The ordinate in

Figure 9-1 shows the overall misclassification rate which is the sum of false accept and false reject. Each misclassification number shown in

Figure 9-1 (and also the following graphs) was the best result of 10 training cycles of the neural net. Because the initial values of the weights in the net were chosen randomly the results were different for each iteration. The best results were identified automatically and presented in this thesis.

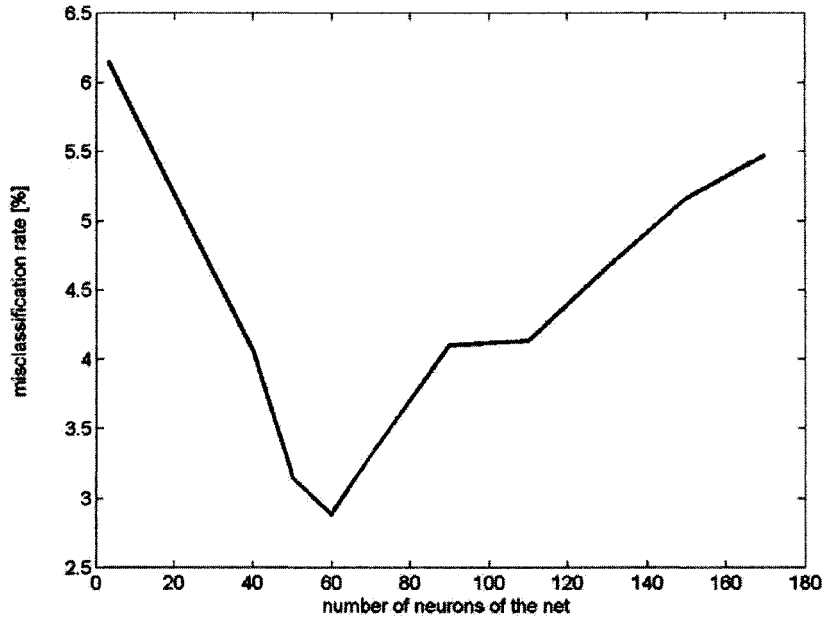

Figure 9-1 Number of neurons used in the Neural Network

To find an optimal architecture in the sense of the lowest misclassification rate also different architectures of nets with 60 neurons were tested. The number of neurons in the first and the second hidden layer was varied and only the sum of the neurons in both hidden layers was held constant. The results of this investigation are presented in Figure 9-2 and due to these experiments the number of neurons in both hidden layers was set to 30.

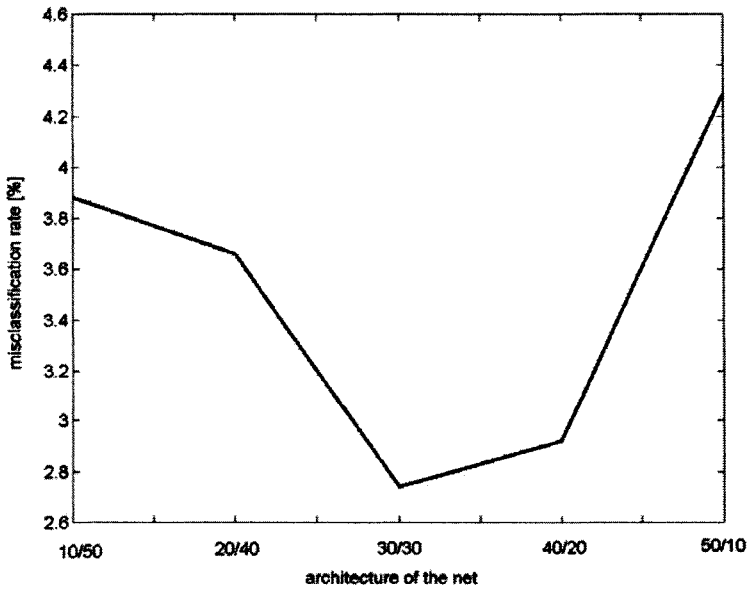

Figure 9-2 Architecture of the Neural Network

Table 9-4 Classification results with MLP

	Backpropagation with variable training rate and momentum	Scaled Conjugate Gradient training algorithm
false accept	**2.74 %**	**4.37 %**
false reject	**0 %**	**2.57 %**

Two different training algorithms were tested: firstly, variable training rate and momentum (MatLab command *traingdx*) and secondly, the Scaled Conjugate Gradient training algorithm (MatLab command *trainscg*) were implemented. As shown in Table 9-4 the results of the first algorithm were much better. The misclassification rates presented in Table 9-4 are also the best result of a train of ten training cycles. The neural net was trained ten times with randomly chosen initial weights until it converges. The best results are presented here in the thesis. The Scaled Conjugate Gradient algorithm is not a steepest descent algorithm such as the first one. In the conjugate gradient algorithms a search is performed along conjugate gradients and often a faster convergence is performed by this class of training algorithms [Mathworks98].

A Learning Vector Quantization Network (LVQ) architecture was also tested. In these networks a first hidden competitive layer classifies the input data into classes which depend on the distance between the different input vectors. A second layer with linear transfer functions is used in this network to transform the competitive layer's classes into target classes defined by the user [MathWorks98]. The number of hidden neurons which were used in the competitive layer was again varied and two output neurons represent the final classes. The misclassification rate was significantly higher than for the MLP in this research project:

Table 9-5 Misclassification of a LVQ network

number of hidden neurons	10	20	50	100	200	500
misclassification rate [%]	19.7	21.2	21.1	21.7	19.6	19.7

9.6 Conclusions

Several classifiers were investigated in this chapter. It was seen that the Multi-Layer-Perceptron had the lowest misclassification rate and due to this network is proposed as

classifier for this research project. Neural Networks were seen to be very suitable for this task because the are not based on assumptions about the probability distribution of the different classes. This distribution is not known because it differs for each valve depending on the final application of the valve and the system where the valve is mounted. It is also very important that Neural Networks can be trained by sample data. Thus it is possible to take the non-stationary nature of the switching events into account. Most of the effort in this research project was spent on the topics pre-processing of the raw-data and feature extraction. Powerful and reliable feature were found and thus the classifier itself could be designed with less effort.

10 Conclusion and Recommendations

10.1 Conclusions

Supervision of small solenoid valves which are used in automation and control is an important step to increase the reliability of the overall system in which valves are used. There are several techniques known for observation of larger valves which are part of nuclear power stations. These state of the art methods use process signals such as pressure, flow or temperature as well as electrical parameters such as voltage and current or the vibration patterns of switching valves. One common drawback of these techniques is that the effort which has to be taken is rather high. Especially the number of sensors is often greater than one single transducer and the financial expense will often outweigh the advantages made by supervision if the observed devices become rather small and cheap.

Vibration analysis was seen to be very suitable for failure detection for solenoid valves because the most important failures of these devices are of mechanical nature and will influence the vibration signal. Other applications and fields of research where vibration analysis is used very successfully are, for example, observation of artificial heart valves or circuit breakers, the detection and prediction of earthquakes or the inspection of combustion engines.

There are two main challenges which had to be solved during this project: first, the measured vibration pattern is highly non-stationary and it was necessary to segment the time-frequency-plane to smaller and higher stationary sub-sequences. Additionally, the

parameterisation of this segmentation should be self-adaptive to many different valves because the number of slightly different valves of this small and cheap type is very high. The estimated results of commonly used Time-Frequency-Distributions are very dependent on the chosen parameters. To overcome this drawback the Source Based Segmentation was developed during this project which can be adapted to a certain observation task by deriving the necessary parameters directly from the measured signal. This approach returns a set of sub-sequences with a higher degree of stationarity than the raw-data.

The second challenge was the scatter within a train of switching events. It was seen that also vibration patterns within a set of consecutive switching on- or off-events gathered from the same valve with a constant degree of deterioration do not coincide perfectly. Not only the vibration pattern of a single switching event is non-stationary but also the train of consecutive events. Due to this a new technique, the Spectral Analysis Matrix, was developed to detect regions of interest within the distributed spectra which cover the discriminative power. The Spectral Analysis Matrix is also a completely automatic algorithm which needs no a-priori knowledge. Thus both new techniques together give the ability to extract powerful and robust features from the measurements.

10.2 Recommendations for further work

10.2.1 Extended Spectral Analysis Matrix

The Spectral Analysis Matrix as presented in this work is capable to detect regions of interest within one-dimensional spectra. Because Time-Frequency-Distributions like STFT or WT, which are used very often, may be more desirable for other applications and signals it is recommended to expand the Spectral Analysis Matrix to two- or three-

dimensional input data. This is part of the ongoing master project of Petré Sora (University of Applied Science at Heilbronn) which is supervised by Christian Ellwein.

10.2.2 Observation of similar devices

There are several devices which have a similar reciprocating mode of operation such as valves, for example relays or cylinders. There could also be the need to observe these devices and detect failures. There are also some important differences between valves and these systems: relays have a movable part (the electrical contact) which has a resilient nature. Thus it differs significantly from the solid movable part of a solenoid valve. Due to this the Source Based Segmentation technique has to be modified to correspond to the different mechanical processes. Nevertheless, these other devices also generate the transient and non-stationary vibration pattern and also the mechanical processes during movement are partly similar. Thus a expansion of the developed techniques to further application seems to be feasible.

Appendix A: Author's publications

This appendix reprints the publications in which I am one of the authors.

In section A.1, the paper introduces the segmentation in the time- and frequency-domain and the modified Hanning window.

The paper in section A.2 reports some difficulties and challenges when non-stationary signals are to be processed by means of digital signal processing. The theoretic results were illustrated by the vibration signals of switching valves.

The paper in section A.3 shows the gain of stationarity which was received by segmenting the non-stationary vibration pattern in time- and frequency-domain. Instead of the Multi-ACF algorithm proposed in this paper the FFT was used for segmentation in the frequency-domain because both techniques had nearly similar results but the detection of the threshold is easier using the FFT.

The paper in section A.4 shows the differences between a capacitive accelerometer and a piecoelectric accelerometer as it was used by the Fraunhofer Instiute in the collaboration. Special attention was paid to the influence of the electromagnetic inference (EMI).

In section A.5 the paper gives a review over important classifiers and the classification scheme with feature extraction and classification.

In section A.6 the paper is a description of the Spectral Analysis Matrix and the advantages of this new tool for feature extraction.

The paper in section A.7 is a reviewed and accepted paper which will be presented at the 4th international conference on quality, reliability and maintenance in march 2002 in Oxford, England. The paper presents the Source Based Segmentation algorithm.

Finally, the paper in section A.8 is a reviewed paper which is already accepted by Academic Press and which will be published within 2002 in the Mechanical Systems and Signal Processing journal. It describes the Spectral Analysis Matrix and its application in detail.

List of papers

A.1 Ellwein, C.; Danaher, S.; Jäger, U.: *A Vibration Signal Family of Impact Events*; Proceedings of the European Symposium on Intelligent Techniques; 14.-15.9 2000 Aachen, Germany; 2000

A.2 Ellwein, C.; Jäger U.: *Processing of Time-Invariant Signals*; [in German]; Elektronik; vol. 50; no. 4; pp. 86-91; 2001

A.3 Ellwein, C.; Danaher, S.; Jäger, U.: *Condition Monitoring for Reciprocating Devices*; Proceedings of the TEST2001; Nürnberg, Germany; 8.-10.05.2001

A.4 Ellwein, C.; Jäger, U.; Hentschel, D.; Haupt, L.; Frankenstein, B.: *Sensorik zur Schwingungsüberwachung von Ventilen*; 13. Kolloquium Schallemission; University of Jena, Germany; 27.-28.9.2001

A.5 Ellwein, C.; Jäger, U.: *Klassifikation – die Grundlagen*; [in German]; Elektronik; vol. 51; no. 2; pp. 68 – 75; 2002

A.6 Ellwein, C.; Jäger, U.; Hentschel, D.; Frankenstein, B.: *Merkmalsextraktion aus Spektren zur Klassifikation*; Technisches Messen; vol. 68; no. 12; pp. 564-569; 2001

A.7 Ellwein, C.; Danaher, S.; Jäger, U.: *Data derived time-frequency segmentation of non-stationary vibration signals*; 4th ORM International Conference on Quality, Reliability and Maintenance; 21st – 22nd March 2002; Oxford

A.8 Ellwein, C.; Danaher, S.; Jäger, U.: *Identifying Regions of Interest in Spectra for Classification Purposes*; Mechanical Systems and Signal Processing; the paper is accepted and will be published within the year 2002

Appendix B: Author's lectures

This appendix presents a list of lectures, which I have presented during the official image processing seminar at the University of Applied Science, Heilbronn. The lectures had an approximate length of about 20 minutes. The purpose of these lectures was to present to a student auditorium extended knowledge about digital signal processing and report new trends in signal processing applications and technologies.

B.1 Introduction to Soft Computing

B.2 Statistics and Classification

B.3 Signal Processing with MatLab

B.4 Data acquisition

B.5 Vibration Analysis – Applications and related topics

B.6 Accelerometers and Vibration Analysis

B.7 Autoregressive Models

B.8 Online Fault Detection for Electromagnetically Switched Devices

B.9 Neural Networks / part 1: Architectures

B.10 Neural Networks / part 2: Training and Learning

B.11 Neural Networks / part 3: Further Topics

B.12 Modern Information Retrieval using the Internet

B.13 Preprocessing of Vibration Signals of Reciprocating Devices

B.14 Cluster-Analysis

B.15 Spectral Analysis with MatLab

Appendix C: Related studies

During this PhD-project the author has undertaken an intensive programme of related studies which is described briefly in this appendix. The author has attended a lecture about digital filters at the University of Applied Science at Heilbronn (level 4, first year postgraduate) and he has given lectures in the image processing, microelectronics and related subjects seminary, also at Heilbronn University (see Appendix B). He has also joined several relevant conferences (EUFIT 1999, Aachen; ESIT 2000, Aachen; TEST 2001, Nürnberg; 13th Colloquium Acoustic Emission 2001, Jena). These conferences were mainly about Neural Networks, Soft Computing and Nondestructive Testing. During the project also some related books were read which gave a deeper insight to the field of pattern recognition and digital signal processing. Especially important books were *Pattern Analysis and Understanding* [Niemann90] and *Applied Pattern Recognition* [Paulus01]. Further literature, both books and papers, which influenced the project were cited within this thesis.

References

Alguindigue91 Alguindigue, I.; Uhrig, R.E.; *Compression of Spectral Signatures Using Recirculation Neural Networks*; Scientific Computing & Automation vol. 43; pp. 43-50; 1991

Alguindigue93 Alguindigue, I.; Loskiewicz-Buczak, A.; Uhrig, R. E.: *Monitoring and Diagnosis of Rolling Element Bearings Using Artificial Neural Networks*; IEEE Transactions on Industrial Electronics; Vol. 40; No. 2; pp. 209-217; 1993

Analog99 Analog Devices Inc.: *ADXL105 Data Sheet*; 1999

Appel83 Appel, U.; Brandt, A. v.: *Adaptive Segmentation of Piecewise Stationary Time Series*; Information Sciences; vol. 29; pp. 27-56; 1983

Aurud91 Aurud, T.; Hegerberg, R.; Runde, M.: *Acoustic and electric diagnostic method for evaluation of contact wear in high voltage circuit breakers*; 7th International Symposium on High Voltage Engineering; 26-30 August, 1991, Dresden, Germany; pp 201- 204,1991

Au-Yang91 Au-Yang, M.K.; Ataman, V.T.; Key, M.W.: *A non-intrusive check valve monitoring systeem using ultrasonic and acoustic techniques*; International Power Generation Conference; Octobert 6-10 1991; San Diego, CA, USA; 1991

Azzoni95 Azzoni, P.; Marseguerra, M.: Assessment of the potential of a Wiener-Hilbert filter for automatic diagnosis of spark ignition engine faults; Mechanical Systems and Signal Processing; vol. 9; no. 2; pp. 119-128; 1995

Bäni02 Bäni, W.: *Wavelets*; München: Oldenbourg; 2002

Basak98 Basak, J.; De, R. K.; Pal, S., K.: *Unsupervised feature selection using a neuro-fuzzy approach*; Pattern Recognition Letters; Vol. 19; No. 11; pp. 997-1006; 1998

Basseville93 Basseville, M.; Nikiforov, I. V.: *Detection of Abrupt Changes: Theory and Application*; Englewood Cliffs: Prentice Hall Inc.; 1993

Beck94 Beck, K.: *Simulink model of solenoid valve*; Bürkert Fluid Control Systems; 1994

Becker98 Becker, W.-J.; Bonfig, K.W.; Hoing, K.: *Handbuch elektrische Meßtechnik*; Heidelberg: Hüthig Verlag; 1998

Béliveau99 Béliveau, A.; Spencer G.; Thomas, K.A.; Roberson, S.L.: *Evaluation of MEMS Capacitive Accelerometers*; IEEE Design & Test of Computers; vol. 16; no. 4; pp. 48-56; 1999

Bendat86 Bendat, J. S.; Piersol, A. G.: *Random Data*; New York: John Wiley & Sons; 1986

Beuth88 Beuth, K.: *Elektronik 2 - Bauelemente*; Würzburg: Vogel-Verlag; 1988

Biegner99 — Biegner, A.: Zur Schallemission der selbsttätigen Ventile oszillierender Verdrängerpumpen; PhD thesis; University of Erlangen, Germany; 1999

Bissessur99 — Bissessur, Y.; Martin, E.B.; Morris, A.J.: *Monitoring the performance of the paper making process*; Control Engineering Practice; vol. 7; no. 11; pp. 1357-1368; 1999

Blakeman97 — Blakeman, E.D.; Kryter, R.C.: *Noninvasive testing of solenoid-operated valves using transient current signature analysis*; International Conference on Maintenance and Reliability – MARCON 1997, Knoxville, Tennessee, USA;1997

Britt93 — Britt, B.S.: *Cluster Analysis*; London: Arnold; 1993

Bürkert00 — Private conversation with engineers at Bürkert Werke, Germany; 2000

Candy95 — Candy, J.V.; Jones, H.E.: *Processing of prosthetic heart valve sounds for single leg separation classification*; Journal of the Acoustic Society of America; Vol 97; No. 6; pp. 3663-3673; 1995

Cann92 — Cann R.G.: *New diagnostic procedures for locating faults in diesel engines*; Diesel & Gas Turbine Worldwide; vol. 24; no. 6; pp. 52-55; 1992

Casada96 — Casada, D. A.; McElhaney, K.L.: Condition Monitoring and Testing for Operability of Check Valves and Pumps; Water Reactor Safety Meeting;

Chui92 — Chui, C.K.: *An Introduction to Wavelets*; Boston: Academic Press; 1992

Cichocki93 — Cichocki, A.; Unbehauen, R: *Neural Networks for Optimization and Signal Processing*; Toronto: Wiley; 1993

Clark98 — Clark, C.; Clark, A.F.: *Spectral identification by singular value decomposition*; International Journal of Remote Sensing; vol. 19, pp. 2317-2329; 1998

Conforto99 — Conforto, S.; D'Alessio, T.: *Spectral Analysis for Non-Stationary Signals from Mechanical Measurements: a Parametric Approach*; Mechanical Systems and Signal Processing; vol. 13; no. 3; pp. 395-411; 1999

Conte96 — Conte, J.; P. Peng, B. F.: An explicit closed-form solution for linear systems subjected to non-stationary random excitation; Probabilistic Engineering Mechanics; vol. 11; pp. 37-50; 1996

Danaher92 — Danaher, S.: *Singular Value Decomposition in Multispectral Radiometry*; International Journal of Remote Sensing; vol. 13; no. 9; pp. 1771-1777; 1992

Darrell98 — Darrell, L. A.: Development of an NDT method to characterise flaws based on multiple eddy current sensor integration and data fusion; Ph.D Thesis; School of Engineering, Leeds Metropolitan University; 1998

Deller93 — Deller, J. R.; Proakis, J.G.; Hansen, J.H.L.: *Discrete-Time Processing of Speech Signals*; New York: Mcmillan Publishing Company; 1993

Demuth98 Demuth, H.; Beale, M.: *Neuroal Networks Toolbox 3.0*; The Mathworks Inc. 1998

Dimmick86 Dimmick, J. G.; Cobb, J. M.: *Ultrasonic leak detection cuts valve maintenance costs*; Power Engineering; vol. 90; no. 8; pp. 35-38; 1986

Dobrinski93 Dobrinski, P: *Physik für Ingenieure*; Stuttgart: Teubner; 1993

Eberhardt97 Eberhardt, E.; Stead, D.; Stimpson, B.; Read, R.S.: *Changes in acoustic event properties with progressive fracture damage*; Int. J. Rock Mech. & Min. Sci.; vol. 34; no. 3-4; 1997

Ellwein99 Ellwein, C.: Einsatz der Schwingungsanalyse in der Endprüfung von Magnetventilen; Diploma thesis at the University of Applied Sciences at Heilbronn, Germany; Department of Electronic Engineering; 1999

Ellwein00a Ellwein, C.; Jäger, U.: *Use of personal computer sound cards for digitising measuring data*; [in German]; Elektronik; vol. 49; no. 11; pp. 60-65; 2000

Ellwein00b Ellwein, C.; Danaher, S.; Jäger, U.: *A Vibration Signal Family of Impact Events*; Proceedings of the European Symposium on Intelligent Techniques; 14.-15.9 2000 Aachen, Germany; 2000

Ellwein01a Ellwein, C.; Jäger U.: *Processing of time-invariant signals*; [in German]; Elektronik; vol. 50; no. 4; pp. 86-91; 2001

Ellwein01b Ellwein, C.; Danaher, S.; Jäger, U.: *Condition monitoring for reciprocating devices*; Proceedings of the TEST2001; Nürnberg, Germany; 8.-10.05.2001

Ellwein01c Ellwein, C.; Jäger, U.; Hentschel, D.; Haupt, L.; Frankenstein, B.: *Sensorik zur Schwingungsüberwachung von Ventilen*; 13. Kolloquium Schallemission; University of Jena, Germany; 27.-28.9.2001

Ellwein01d Ellwein, C.; Jäger, U.; Hentschel, D.; Fröhlich, K.J..; Frankenstein, B.: Feature extraction from spectra for classification [in German]; Technisches Messen; vol. 68; no. 12; pp. 564-569

Ellwein02a Ellwein, C.; Jäger, U.: Klassifikation – Die Grundlagen; Elektronik; vol. 51; no. 2; pp. 68 – 75; 2002

Ellwein02b Ellwein, C.; Danaher, S.; Jäger, U.: *Data derived time-frequency segmentation of non-stationary vibration signals*; 4th ORM International Conference on Quality, Reliability and Maintenance; 21st – 22nd March 2002; Oxford

Flandrin99 Flandrin, P.: *Time-Frequency / Time-Scale Analysis*; London: Academic Press; 1999

Foresee97 Foresee, F.D.; Hagan, M.T.: *Gauss-Newton approximation of Bayesian learning*; Proceedings of the 1997 International Joint Conference on Neural Networks; pp. 1930 – 1935; 1997

Fukunaga90 Fukunaga, K.: *Introduction to Statistical Pattern Recognition*; San Diego: Academic Press; 1990

Gallier97 Gallier, S.C.: *Valve and Motor Diagnostic Products & Services*; Framatome Technologies Inc., Lynchburg, VA, USA; December 31,1997

Golub96 Golub, G. H.; Van Loan, C. F.: *Matrix Computations*; Baltimore: The John Hopkins University Press; 1996

Gordon81 Gordon, A.D.: *Classification*; London: Chapman and Hall Ltd.; 1981

Grieser97 Grieser, J.: *Spektralanalysen*; http://www.rz.uni-frankfurt.de/~grieser/spek/spek.html; 1997

Gupta00 Gupta, I.D.; Trifunac, M.D.: *A note on nonstationarity of seismic response of structures*; Engineering Structures; vol. 23; pp. 1567-1577; 2000

Hänsler97 Hänsler, E.: *Statistische Signale*; Berlin: Springer; 1997

Hascher96 Hascher, W.: *Die Meß-Minis*; Elektronik; vol. 45; no. 18; pp. 666; 1996

Hebb49 Hebb, D.: *Organisation of Behaviour*; New York: Wiley; 1949

Hellendoorn97 Hellendoorn, H.; Driankov, D.: *Fuzzy Model Identification*; Berlin Heidelberg: Springer; 1997

Hinton86 Hinton, G. E.; Rumelhart, D. E.; Williams, R. J.: *Learning representations by backpropagation errors*; Nature; vol. 323; pp. 533 – 536; 1986

Isermann92 Isermann, R.: *Identifikation dynamischer Systeme 1*; Berlin Heidelberg: Springer; 1992

Jain00 Jain, Anil, K.; Duin, Robert P.W.; Mao, Jianchang: *Statistical pattern recognition: a review*; IEEE Transactions on Pattern Analysis and Machine Intelligence; vol. 22; no. 1; pp. 4 – 36; 2000

Jansen81 Jansen, B. H.; Hasman, A.; Lenten, R.: *Piecewise Analysis of EEGs Using AR-Modeling and Clustering*; Computers and Biomedical Research; Vol. 14; pp. 168-178; 1981

Jonuscheit98 Jonuscheit, H.; Wagner, J.; Groppe, H.: *Vollautomatische Qualitätskontrolle von Dachziegeln*; Ziegelindustrie International; no. 11; pp. 741-751

Jossa99 Jossa, I; Marschner, U.; Wittkopf, H.; Fischer, W.-J.: *Signal-Based Feature Extraction in a Vibration Monitoring Microsystem*; Proceedings of the European Congress on Intelligent Techniques and Soft Computing (EUFIT) 13.-16.9.1999; Aachen, Germany

Kalix93 Kalix, D.A.: *Predicting valve maintenance vital*; InTech; vol. 40; no. 5; pp. 37-39; 1993

Kallenbach00 Kallenbach, E.: Dimensioning and Optimisation of Solenoids; 13.-14.7.2000: Bürkert Fluid Control Systems and Technical University of Ilmenau, Germany

Kammeyer98 Kammeyer, K. D.; Kroschel, K.: *Digitale Signalverarbeitung*; Stuttgart: Teubner; 1998

Kiesbauer00 Kiesbauer, J.; Hoffmann, H.: *Detektion der inneren Leckage von Stellgeräten*; Automatisierungstechnische Praxis; vol. 42; no11; pp. 50-53; 2000

Kinnebrock94 Kinnebrock, W.: *Neuronale Netze*; München: Oldenbourg; 1994

Kocur00 Kocur, D.; Stanko, R.: *Order Bispectrum: A new tool for reciprocated machine condition monitoring*; Mechanical Systems and Signal Processing; vol. 14; no. 6; pp. 871-890

Kryter90 Kryter, R. C.: Nonintrusive Methods for monitoring the operational readiness of solenoid-operated valves; Nuclear Engineering and Design; vol. 118; No. 3; pp. 409-417; 1990

Kubat00 Kubat, M.: *Designing neural network architectures for pattern recognition*; The Knowledge Engineering Review; vol. 15; no. 2; pp. 151-170; 2000

Lai98 Lai, M. L. et al.: *Mechanical Failure Detection of circuit breakers*; IEEE Transactions on Power delivery; vol. 3; no. 4; pp. 1724-1731; 1998

Lang95 Lang, J. Q.; Stokes A. D.: *Analysis of Circcuit-Breaker Mechanical Signature using Matrix Pencil*; Proceedings of the International Power Conference, Singapore, 27.2 – 1.3.1995

Lehmann97 Lehmann, P.: *Fast time-frequency analysis based on the short time Fourier transform* [in Germany]; Technisches Messen; vol. 64; no. 6; pp. 247 – 258; 1997

Li95 Li, C.J.; Yu, X.: *High pressure air compressor valve fault diagnosis using feedforward neural networks*; Mechanical Systems and Signal Processing; vol. 9; no. 5; pp. 527-536; 1995

Lindner99 Lindner, D. K.: *Introduction to Signals and Systems*; WCB McGraw-Hill; 1999

Lowther85 Lowther, D.A.; Silvester, P.P.: *Computer-Aided Design in Magnetics*; Berlin: Springer; 1985

Lyon87 Lyon, R.: Machinery Noise and Diagnostics; Boston, Mass.: Butterworths; 1987

Maalej99 Maalej, M.; Karasaridis, A.; Hatzinakos, D.; Pantazopoulou, S.J.: *Spectral analysis of sensor data in civil engineering structures*; Computers and Structures; vol. 70; pp. 675 - 689; 1999

Mannhardt00 Mannhardt M.: *Feature Extraction in Vibration Signals*; MSc project report; University of Northumbria at Newcastle; 2000

Mathworks98 The Mathworks Inc.: *Neural Network Toolbox User's Version Guide 3.0*; 1998

MathWorks99a The Mathworks Inc.: *Signal Processing Toolbox User's Guide Version 4.2*; 1999

MathWorks99b The Mathworks Inc.: *Statistics Toolbox User's Guide Version 2.0*; 1999

McCormick96 McCormick A.C.; Nandi, A.K.: *Rotating machine condition classification using artificial neural networks*; Proceedings of COMADEM; University of Sheffield; 16th – 18th July 1996

McCulloch43 McCulloch, W.S.; Pitts, W.: *A logical calculus of the ideas immanent in nervous activity*; Bull. Math. Biophys.; vol. 5; pp. 115-133; 1943

Menon98 Menon, A.K.; Boutaghou, Z-E.: *Time-frequency analysis of tribological systems – part 1: implementation and interpretation*; Tribology International; vol. 31; no. 9; pp. 501-510; 1998

Minski69 Minski, M.; Papert, S.: *Perceptrons*; Cambridge, Massachusets: MIT Press; 1969

Newland93 Newland, D.E.: An Introduction to Random Vibrations, Spectral & Wavelet Analysis; Essex: Prentice Hall; 1993

Niemann90 Niemann, H.: *Pattern Analysis and Understanding*; Berlin: Springer Verlag; 1990

Oppenheim89 Oppenheim, A.V.; R.W. Schafer: *Discrete-Time Signal Processing*; Englewood Cliffs, NJ; 1989

Pachaud97 Pachaud, C.: *Crest Factor and Kurtosis Contributions to identify defects inducing periodical impulsive forces*; Mechanical Systems and Signal Processing; vol. 11; no. 6; pp. 903 – 916; 1997

Pandya96 Pandya, A. S.; Macy R. B.: *Pattern Recognition with Neural Networks in C++*; Boca Raton: CRC Press; 1996

Papargyris01 Papargyris, A.D.; Papargyri, S.A.: *Acoustic emission characterization of kaolin-based clay ceramics*; Applied Clay Science; vol. 18; pp. 191-204; 2001

Park90 Park, S.Y. et al: *Measurements for noninvasive mechanical diagnostics of power circuit breakers*; Electric Power Systems Research; vol. 19; pp. 1 – 10; 1990

Patel92 Patel, H.:*Silicon that moves towards the smart sensor*; IEE Review; vol. 38; no. 7-8; pp. 268-269; 1992

Pattichis99 Pattichis C. S.; Elia, A. G.: *Autoregressive and cepstral analyses of motor unit action potentials*; Medical Engineering & Physics; vol. 21; pp. 405 – 419; 1999

Paulus01 Paulus, D.W.R.; Hornegger, J.: *Applied Pattern Recognition*; Braunschweig: Vieweg; 2001

PCB Piezotronics99 PCB Piezotronics: *Accelerometer mounting considerations*; Shock and Vibration Sensor Catalog 1999

Peters96 Peters, H.: *Anwendung künstlicher neuronaler Netze in Überwachungssystemen;* Automatisierungstechnische Praxis; vol. 38; no. 11; pp. 37 – 48; 1996

Pham01 Pham, D. T.; Sagiroglu, S.: *Training multilayeres perceptrons for pattern recognition: a comparative study of four training algorithms*; International Journal of Machine Tools & Manufacture; vol. 41; pp- 419 – 430; 2001

Plemons95 Plemons T. D.; Hovenga M.: *Acoustic classification of the state of artificial heart valves*; Journal of the Acoustic Society of America; vol. 97; no. 4; pp. 2326-2333; 1995

Pohl56 Pohl, E.J.: Über die Sicherung und Überwachung des Betriebszustandes von maschinellen Anlagen mit einem Beitrag über den Stand der Überwachung der Spiele und des mechanischen Laufes von Turbogeneratoren; Der Maschinenschaden 5/6 1956; pp. 61-70; 1956

Priestley89 Priestley, M. B.: *Spectral Analysis and Time Series*; San Diego, CA: Academic Press; 1989

Putnam96 Putnam, W.; Knapp, R.B.: *Input/Data Acquisition System Design for Human Computer Interfacing*; Mus252/CS377A: Human Computer Interface Design; Stanford University Center for Computer Research in Music and Acoustics; 1996

Quian00 Qian, S: *Frequenzanalyse, basierend auf Modellen*; Elektronik vol. 49; no. 2; pp. 91-96; 2000

Rao98 Rao, R. M.; Ajit, S. B.: *Wavelet transforms: introduction to theory and applications*; Harlow: Addison Wesley Longman; 1998

Riley96 Riley, W. F.; Sturges, L. D.: *Engineering Mechanics: Dynamics*; New York: John Wiley & Sons; 1996

Runde96 Runde, M.; Ottesen, G.E.; Skyberg, B.: *Vibration analysis for diagnostic testing of circuit-breakers*; IEEE Transactions on Power Delivery; vol. 11; no. 4; pp. 1816-1823; 1996

Schubert95 Schubert, D.: *Beschleunigungssensoren in Silizium-Techniken*; Technisches Messen; vol. 65; no. 11; 1995

Scruby87 Seruby, C.B.: *An introduction to acoustic emission*; Journal of Physics – E; vol. 20; no. 8; pp. 946-953; 1987

Shieh01 Shieh, J.; Huber, J.E.; Fleck, N.A.; Ashby, M.F.: *The selection of sensors*; Progress in Materials Science; vol. 46; no. 3-4; pp. 461-504; 2001

Shigeishi01 Shigeishi, M. et al.: *Acoustic emission to assess and monitor the integrity of bridges*; Construction and Building Materials; vol. 15; pp. 35-49; 2001

Shiotani01 Shiotani, T.; Ohtsu, M.; Ikeda, K: *Detection and evaluation of AE waves dur to rock deformation*; Construction and Building Materials; vol. 15; pp. 235-246; 2001

Skitt93 Skitt, P.J.C.; Javed, M.A.; Sanders, S.A.; Higginson, A.M.: *Process monitoring using auto-associative, feed-forward artificial neural networks*; Journal of Intelligent Manufacturing; vol. 4; no. 1; pp. 79-94; 1993

Smith99 Smith, S.W.: *The Scientist and Engineer's Guide to Digital Signal Processing*; California Technical Publishing; 1999

Srinivasa01 Srinivasa, P.; Nagabhushana, T.N.; Ramakrishna Rao, P.K.: *Tool wear estimation using resource allocation network*; International Journal of Machine Tools & Manufacture; vol. 41; pp. 673-685; 2001

Sun00 Sun, M.; Scheuer, M. L.; Sclabassi, R. J.: *Decomposition of biomedical signals for enhancement of their time-frequency distribution*; Journal of the Franklin Intitute; vol. 337; pp. 453-467; 2000

Thompson97 Thompson, G.; Zolkiewsky, G.: An experimental investigation into the detection of internal leakage of gases through valves by vibration analysis; Proceedings of the Institution of Mechanical Engineers Part E; vol. 211; pp. 195-207; 1997

Tietze93 Tietze, U.; Schenk, C.: *Halbleiter-Schaltungstechnik*; Berlin: Springer; 1993

Trepel99 Trepel, M.: *Neuroanatomie Struktur und Funktion*; München: Urban & Fischer; 1999

Trethewey00 Trethewey, M.W.: *Window and overlap processing effects on power estimates from spectra*; Mechanical Systems and Signal Processing; vol. 14; no. 2; 2000

Uhrig93 Uhrig, R. E.; Tsoukalas, L.H.; Ikonomopoulos, A.: *Using Neural Networks to Monitor the Operability of Check Valves*; Preoceedings of The Conference on expert System Applications for the Electric Power Industry Phoenix, Arizona, USA; 1993

Verplaetse95 Verplaetse, C.: Can a pen remember what it has written using inertial navigation ?: An evaluation of current accelerometer technology; http://xenia.media.mit.edu/~verp/projects/smartpen/ruff_drapht.html; 1995

Voß00 Voß, W.: *Taschenbuch der Statistik*; München: Fachbuchverlag Leipzig; 2000

Wang01 Wang, Z.; Willett, P.; DeAguiar, P. R.; Webster, J.: *Neural network detection of grinding burn from acoustic emission*; Int. J. of Machine Tools & Manufacture; vol. 41; pp. 283-309; 2001

Webb99 Webb, A.: *Statistical Pattern Recognition*; London: Arnold; 1999

Wilson99 Wilson, J.: A practical approach to vibration detection and measurement part 1: Physical Principles and Detection Techniques; Sensors; vol. 16; no. 2; pp. 12, 14-27

Wowk91 Wowk, Victor: *Machinery Vibration*; Boston: McGraw-Hill; 1991

Yamashina90 Yamashina, H. et al.: *Failure diagnosis of a servovalve by neural networks with new learning algorithm and structure analysis*; International Journal of Production Research; vol. 28; no. 6; pp 1009-1021; 1990

Young74 Young, T. Y.; Calvert, T. W.: *Classification, Estimation and Pattern Recognition*; New York: Elsevier; 1974

Zimmermann95 Zimmermann, L. et al: Airbag application: a microsystem including a silicon capacitive accelerometer, CMOS switched capacitor electronics and true self-test capability; Sensors and Acctuators A; vol. 46; no. 1-3; pp. 190-195; 1995

Zwingelstein90 Zwingelstein, G.; Hamon L.: *EDF studies on condition monitoring of rolling element bearings*; Proceedings of the 4th Incipient Failure Detection Conference, Philadelphia, PA; 1990